

**WATER-SOLUBLE, ANIONIC
POLYCHLORAMIDE
DISINFECTANTS**

WATER-SOLUBLE, ANIONIC POLYCHLORAMIDE DISINFECTANTS

By

GAOYIN HE, B.Sc. M.Sc.

A Thesis Submitted to the School of Graduate Studies

in Partial Fulfilment of the Requirements

for the Degree of Doctor of Philosophy

McMaster University

© Copyright by Gaoyin He, June 2023

DOCTOR OF PHILOSOPHY (2023)

McMaster University

(Chemical Engineering)

Hamilton, Ontario

TITLE: Water-soluble, Anionic Polychloramide
Disinfectants

AUTHOR: Gaoyin He

B.Sc. (China University of Petroleum
(East China), China)

M.Sc. (China University of Petroleum
(East China), China)

SUPERVISOR: Dr. Robert H. Pelton

NUMBER OF PAGES: VIII, 133

Lay Abstract

The persistence of various microbes on high-touch surfaces has emphasized the importance of long-lasting surface disinfectants. Dilute bleach has been widely used to clean contaminated surfaces. However, dilute bleach can not provide residual antimicrobial activity after drying on the surfaces. The core objective of this research is to explore the novel film-forming polymer platform, which extends the non-infectious time of bleach-cleaned surfaces.

Novel water-soluble, anionic polychloramides were specifically designed with the reaction of maleic anhydride groups and primary amines. I identified water-soluble and anionic polychloramides could display residual antimicrobial properties. I illustrated the linkages between polymer structures and biocidal activities. In addition, I demonstrated the antimicrobial efficacy of anionic polymers over cationic counterparts in a highly soiled environment. Finally, I proposed a new approach to enhancing the biocidal activity of anionic polymers.

Abstract

Antimicrobial N-halamine polymers can continuously protect the surfaces by actively killing microbes on the surfaces. The proposed work is aimed at exploring factors influencing the antimicrobial efficacy of water-soluble, anionic polychloramides. There are four themes covered in this dissertation:

In the first theme, water-soluble, anionic polychloramides (PC3Cl) were reported by first reacting poly(ethylene-alt-maleic anhydride) with primary amines and then chlorination with bleach. It was observed that anionic, water-soluble polychloramide was an effective, antimicrobial biocide. In addition, the flexible anionic polyamides can be grafted onto cellulose filter paper in the catalyst and reagent-free conditions, and after chlorination, the PC3-treated paper has biocidal activity.

The second theme is to identify the polychloramide's structure – biocidal activity relationships. The contributions of polychloramide molecular weight (MW), configuration, and the overlap concentration, C^* in solution were evaluated. The polymer-modified Chick–Watson (PCW) model indicated that lower MW polymers and more compressed configurations of polymers in solution were more effective biocides. Experimental results supported the conclusions.

In the third theme, environmental nonmicrobial soils may degrade the performance of polymer biocides. Single component model soil was employed to evaluate the biocidal activity of anionic polymers, cationic polychloramides, and cationic poly(quaternary ammonium) biocides in non-microbial chemicals. The results demonstrated that negatively charged polyacrylic acid (PAA) and cellulose nanocrystals (CNCs) inhibited cationic biocides by sequestration but did not influence anionic polychloramides. Glycine and bovine serum albumin (BSA) lowered the biocidal activity of the anionic and cationic polychloramides by extracting oxidative chlorine. Anionic antimicrobial polymers could have advantages over cationic counterparts in highly soiled applications.

In the fourth theme, to enhance the antimicrobial activity of anionic polychloramide, an imide shuttle approach was proposed. Three low molecular weight imide model compounds, including 1-(hydroxymethyl)-5,5-dimethylhydantoin (HDMH), 5,5-dimethylhydantoin (DMH), and succinimide (SI), were employed to evaluate the biocidal influence of water-soluble, anionic polychloramides. The results demonstrated that small imides shuttled oxidative chlorine from soluble, anionic polychloramides to bacteria, thus increasing the biocidal activity.

Acknowledgments

Studying at McMaster University has been a challenging and rewarding experience in my life. I have learned a lot from many people. Here I would like to express my deepest thanks to all the people who helped me on the way to becoming a Ph.D.

First and foremost, I would like to express my sincere thanks to my supervisor, Dr. Robert Pelton for allowing me to study in a fascinating field. For my research, Dr. Pelton has given me invaluable guidance, thoughtful feedback, and courage whenever I was in trouble. He has inspired me with his passion and dedication to scientific research. During the research, He taught me how to find scientific questions, explore mechanisms, and demonstrate the findings from a specific view. I am very fortunate to have had the privilege to work with him for my Ph.D. studies. In addition, he taught me how to present my work to various audiences from industrial and academic backgrounds. Also, I appreciate his patience and kindness in life. Especially during the Covid pandemic, Dr. Pelton cared a lot about me and supported my life in Canada.

I would like to thank my supervisory committee members, Prof. Todd Hoare and Prof. Michael Brook. Their specific questions and valuable advice provided me with a better understanding of this project. I enjoyed the chance to work with them. Additionally, I appreciate the help of Prof. Zeinab Hosseinidoust, Prof. Jose Moran-Mirabal, Prof. Carlos Filipe from McMaster, Dr. Michael Fefer, Jun Liu both from Suncor, and Prof. Bin Shi from China University of Petroleum (East China).

Furthermore, I would like to thank our laboratory manager Mr. Doug Keller, instrumentation technologist Michael Clarke, research technician Tim Stephens, mechanical technologist Paul Gatt, and administrative secretary Sally Watson. Also, I thank the Natural Sciences and Engineering Research Council of Canada (NSERC) and Suncor Energy for their financial support.

I would like to thank all my colleagues in the McMaster Interfacial Technologies Group for their support and friendship. Many thanks to Dr. Emil Gustafsson, Dr. Ayodele Fatona, Dr. Dong Yang, Dr. Lei Tian, Dr. Fengyan Wang, and Mr. Eduardo González Martínez for their training and advice. Thanks to Mr. Zhen Hu and Mr. Chaochen Song for their important contributions to this project as summer students. Also, I would like to thank my colleagues Dr. Hongfeng Zhang, Mr. Xiao Wu, and Mr. Abdollah Karami for their support in our group.

I cannot express enough thanks to my parents and my sisters for all their love and support. They always support and encourage me in my long study journey. Without their full support and patience, I cannot be who I am today.

Last but not least, I would like to express my deepest love and warmest gratitude to my wife Yaqiong Huang. Over the last 10 years, we experienced all the happiness and hardship together. I would be lost in my life without you. Hope to learn together, grow together, evolve together for our future.

Table of Contents

Lay Abstract	iii
Abstract	iv
Acknowledgments	v
Table of Contents	vi
List of Abbreviations and Symbols	viii
Chapter 1.....	1
Introduction and Objectives	1
1.1 Surface Disinfection	2
1.2 N-Halamine Compounds	4
1.3 Introduction of Microbial Surface Components.....	8
1.4 Oxidative Chlorine Transport to Microbes	10
1.5 Antimicrobial Mechanisms of N-Halamines.....	12
1.6 Factors Influencing Antimicrobial Activity of N-Halamines.....	13
1.7 Examples of Antimicrobial Polymeric N-Halamine Coatings	15
1.8 Objectives.....	19
1.9 Outline	19
References	21
Chapter 2.....	33
Water-soluble Anionic Polychloramide Biocides Based on Maleic Anhydride Copolymers	33
Supporting Information	54
Chapter 3.....	61
Modeling the Impact of Polychloramide Solution Properties on Bacterial Disinfection Kinetics.....	61
Chapter 4.....	84
Impacts of Non-microbial Soils on Polychloramides Disinfectants	84
Supporting Information	101

Chapter 5	107
Low Molecular Weight Imide Shuttle Molecules Enhance Polychloramide Antimicrobial Activity	107
Supporting Information	121
Chapter 6	133
My Contributions	133

List of Abbreviations and Symbols

ADP	adenosine diphosphate
A_{es}	The projected area of the equivalent sphere encasing a polymer chain (m^2).
AM_{cl}	The atomic mass of chlorine (Da)
APA-1	poly[(6-morpholino-s-triazine-2,4-diyl)-N-chloro-[2,2,6,6-tetramethyl-4-piperidyl]imino]-hexamethylene[(2,2,6,6-4-piperidyl)imino]]
ARDS	acute respiratory distress syndrome
ATP	adenosine triphosphate
B_o	The initial viable bacteria concentration (m^{-3})
BC	bactericidal Concentration
BSA	bovine serum albumin
C^*	The polymer overlap concentration (g/dL)
Cl_{coil}	The chlorine atom concentration in an equivalent sphere (mol/L)
Cl_{mf}	The mass fraction of chlorine in the dry polymer
Cl_T	The total mol oxidative chlorine atoms divided by the total volume (mol/L)
CNCs	cellulose nanocrystals
Cys	cysteine
DMF	N, N-Dimethylformamide anhydrous
DMH	5,5-dimethylhydantoin
DTNB	5,5'-dithiobis(2-nitrobenzoic acid)
f_{ps}	The Poisson stamping function
HAIs	healthcare-associated infections
HTS	High-touch surfaces
HOCl or OCl ⁻	hypochlorous acid or hypochlorite ion
HDMH	1-(hydroxymethyl)-5,5-dimethylhydantoin
HMW	High molecular weight polychloramide (400 kDa)
k_{cw}	The Chick-Watson rate constant ($m^3/mol.s$)
k_{col}	The rate constant for polymer bacteria impacts (m^3/s)
k_{pcw}	The combined constants in the PCW model ($m^6/(kg.s.mol)$)
K_{mh}	The Mark-Houwink prefactor ($8.5 \times 10^{-5} m^3/kg$)
k_{smol}	The Smoluchowski collision rate constant ($1.23 \times 10^{-17} m^3/s$)
k_{tr}	The non-collision contribution to the rate constant for the PCW model (m^3/mol)
LbL	layer-by-layer
LB	Luria-Bertani
LMW	Low molecular weight polychloramide (40 kDa)
$logSR$	The log survival ratio (B_t/B_o)
IN_A	The number of polymer bacteria impacts per bacteria area (m^{-2})
IN_V	The number of polymer bacteria impacts per volume of solution (m^{-3})

<i>MBC</i>	The minimum biocide concentration (g/dL)
MC	1-chloro-2,2,5,5- tetramethylimidazolidin-4-one
MH	The Mark-Houwink equation
<i>MW</i>	Polymer molecular weight (Da)
<i>n</i>	The biocide concentration exponent in the Chick-Watson model
NaDCC	sodium dichloroisocyanurate
NaOCl	sodium hypochlorite
NaOH	Sodium hydroxide
NCS	N-chlorosuccinimide
Na ₂ S ₂ O ₃	sodium thiosulfate
P	phosphate
PAA	polyacrylic acid
PBS	phosphate-buffered saline
PC3	isopropylamine modified poly(ethylene-alt-maleic acid)
<i>pc</i>	The polychloramide concentration (g/dL)
<i>PC_{coil}</i>	The number concentration of polymer chains (m ⁻³)
PC3Cl	polychloramide based on PC3
PCW	The polymer-modified Chick-Watson Equation
PDA	polydopamine
PEI	polyethylenimine
PEMA	poly (ethylene-alt-maleic anhydride)
PEMs	Polyelectrolyte multilayers
PLGA	poly (lactic-co-glycolic acid)
PMMA	poly (methacrylic acid)
PSC3	isopropylamine modified poly(styrene-alt-maleic acid)
PSCl	polychloramide based on PSC3
PSMA	poly (styrene-alt-maleic anhydride)
PU	polyurethane
PVA	polyvinyl alcohol
<i>q</i>	Poisson intensity factor, an integer >0
<i>r_b</i>	The equivalent spherical bacteria radius (m)
R-SH	thiol-containing compounds and
R-S-S-R'	disulfides
R-SO ₃ H	sulfonic acids
SEM	Scanning electron microscope
SI	succinimide
TCCA	trichloroisocyanuric acid
TMP	2,2,6,6-tetramethyl-4-piperidinol
TNB	5-thio-2-nitrobenzoic acid
UV	Ultraviolet
<i>V_{coil}</i>	The volume occupied by a polymer chain in dilution solution
<i>α</i>	The MH exponent
<i>β</i>	The dimensionless collision frequency rate constant

$[\eta]$ The intrinsic viscosity of polymer (dL/g)
 λ_{ps} The Poisson stamping lambda function

Chapter 1

Introduction and Objectives

Hospital-acquired infections are significant public health issues all over the world. Microbe-contaminated surfaces may cause disease infections in healthcare settings. Surface disinfection is one practical strategy to prevent microbe infections on surfaces. Chlorine was firstly discovered by the Swedish chemist, C. W. Scheele in 1774. [1] During World War I, Dakin introduced around 0.5% bleach solution ($\text{NaOCl} + \text{NaOH}$) to disinfect open and infected wounds. [2] Thereafter, cost-effective dilute bleach was widely used to clean contaminated surfaces and reduce the cross-transmission of microbes. [3] Disinfectant bleach confers a broad-spectrum antimicrobial activity and rapid biocidal action. To date, the use of dilute bleach to clean surfaces increased dramatically during the Covid pandemic.

However, the treatment of dilute bleach leaves an unprotected surface with little residual antimicrobial activity after drying on the surfaces. N-halamines, acting as a chlorine reservoir, can stabilize oxidative chlorine in the long term, and can be recharged with chlorine. N-halamine compounds can continuously protect the surface by actively killing microbes on the surfaces.

In this chapter, the structures and stability properties of N-halamines are introduced. Then, the oxidative chlorine transport process from N-halamines to microbes and their antimicrobial activity were discussed. Thereafter, some examples of poly N-halamines surface coating applications are addressed. Lastly, the goal of this project and an outline of this thesis are provided.

1.1 Surface Disinfection

Healthcare-associated infections (HAIs) pose a serious threat to modern medicine, resulting in significant morbidity with an economic burden. [4] These infections may occur in hospitals, long-term care facilities, and ambulatory settings, and even after discharge. The European Centre for Disease Prevention and Control estimated a mean prevalence of 7.1% in healthcare-associated infections (HAIs). [5] Furthermore, an increasing occurrence of multidrug-resistant pathogens has also been regarded as a serious threat. [6] Healthcare-associated infections (HAIs) are caused by various types of microorganisms, including bacteria, viruses, and other microbes. [7] However, bacteria are the most common cause of healthcare-associated infections (HAIs), accounting for about 80% of all HAIs. [8] The most common bacterial pathogens responsible for HAIs are gram-positive bacteria, including *Staphylococci*, *Streptococcus*, and *Enterococcus species*, and gram-negative bacteria such as *Pseudomonas aeruginosa*, *Acinetobacter baumannii*, and *Enterobacteriaceae family* (e.g. *Escherichia coli*, *Proteus mirabilis*). [9, 10] Apart from bacterial infections, viral infections have gained significant attention due to the ongoing pandemic. [11]

Numerous studies have demonstrated that healthcare-associated pathogens can contaminate public surfaces. For example, studies have shown that inanimate surfaces within an aircraft cabin can become contaminated within 2-3 hours. [12] Pathogens can initially deposit onto environmental surfaces or objects, after which they can be transferred to a person's hands upon contact, causing microbe infection. [13] According to Weber et al. [14], hospital surfaces can serve as a reservoir for pathogens such as norovirus, *Clostridium difficile*, and *Acinetobacter* species. Such pathogens can survive for extended periods on surfaces, and their transmission can occur through direct contact with these surfaces or by indirect contact through contaminated hands of healthcare workers or patients. Moreover, the Covid pandemic has emphasized the need for surface disinfection technologies in both public and private spaces. [15] This is particularly important because people can be infected with SARS-CoV-2 through contaminated surfaces. [16] In healthcare settings, contaminated surfaces account for 20%-40% of nosocomial infections, [17] posing a significant challenge in preventing the spread of infections.

The classification of inanimate surfaces was divided into three general categories (e.g., critical, semi-critical, non-critical) by Spaulding in 1972. [18] For devices or instruments, the classifications can be used: critical surfaces contact with normally sterile areas of the body; semi-critical surfaces touch mucous membranes; and non-critical surfaces, touch the skin or come into indirect contact with people. In 1991, the Centers for Disease Control and Prevention suggested that environmental surfaces, including floors, walls, and other housekeeping surfaces that do not directly come into contact with a person's skin, be included as an additional category. [19]

High-touch surfaces (HTS) may be classified as non-critical items or environmental surfaces, which are likely to be contaminated by harmful microbes. HTS can be external

solid-water interfaces such as shower caps, taps, drains, or solid-gas interfaces such as door handles, clothes, curtains, floors, or walls. [14, 20] In addition, high-touch surfaces in residential settings such as care homes, hotels, and leisure facilities also pose a risk for the transmission of harmful microbes due to the presence of multiple individuals. [21]

Dilute chlorine bleach ($\text{NaOCl} + \text{NaOH}$) has been widely used to clean contaminated HTS as both a cleaner and a disinfectant because bleach is inexpensive and effective. [22, 23] Sodium hypochlorite (NaOCl) is commonly known as household bleach product. Chlorine was first discovered by C. W. Scheele in 1774. [1] Afterwards, bleach product was applied to disinfect infected wounds and clean surfaces. [2] In an aqueous bleach solution, chlorine exists in the forms of Cl_2 , hypochlorous acid (HOCl), and hypochlorite ion (OCl^-) in equilibrium due to pH-dependent aqueous chemistry (See **Figure 1-1**). **Figure 1-1** gives the species distribution of Cl_2 , HOCl , and ClO^- as a function of pH at 25 °C. HOCl is the predominant species and Cl_2 is negligible at pH 3-6. The main species are HOCl and ClO^- at pH 7-8. In the typical high pH, ClO^- is the major component of the solution. The term “free chlorine” refers to the content of HOCl and ClO^- in an aqueous solution.

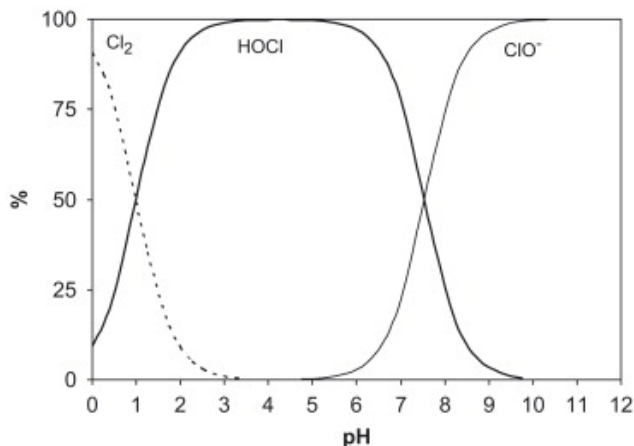


Figure 1-1 Relative distribution of main aqueous chlorine species as a function of pH at 25 °C and for a chloride concentration of 5×10^{-3} M. Figure reprinted from ref [24].

However, the treatment of bleach leaves the unprotected surfaces with little residual antimicrobial activity after drying on the surfaces. This is because HOCl is more volatile than water and leads to oxidant chlorine loss during the drying process in the air. [25] Preventing microbial colonization on high-touch surfaces is significant to limiting the spread of infection. An alternate approach is using N-halamines that continuously protect the surfaces by actively killing microbes on the surfaces. [14, 26] N-Halamines have been reported with powerful, broad-spectrum, antimicrobial activity for bacteria and viruses. [27]

This section attempts to summarize N-halamine compounds, and antimicrobial mechanisms of N-halamines. Then, factors influencing the biocidal activity of N-halamines are discussed. Finally, the examples of N-halamine coatings and commercial surface coatings are outlined in terms of extending the non-infectious lifetime of bleach-cleaned surfaces.

1.2 N-Halamine Compounds

Introduction of N-halamine compounds. In 1969, Kovacic and co-workers [28] proposed the early chemistry of N-halamines. After that, Worley et al. [29, 30] focused on the synthesis and antimicrobial applications of N-halamine compounds. An N-halamine compound contains one or two halogen atoms (chlorine, bromine, or iodine) covalently bonded to nitrogen. [27, 31] N-halamines can effectively stabilize and store halogen atoms in N-X covalent bonds, where the halogen atom is in a highly oxidative state (+1). Chlorine is the most used halogen in N-halamine compounds. The general N-halamines include inorganic groups (e.g., phosphate, sulfate) [27] and organic groups (e.g., alkyl group, carbonyl group). Organic cyclic and acyclic N-halamines are classified into three main types: chloramines (RR'-NCl), chloramides (-C(O)-NCl-R), and chlorimides (-C(O)-NCl-C(O)-). R is an organic group and R' refers to an organic group or H. In general, cyclic N-halamines have primarily five- or six-membered rings with one or more N-X bonds, such as hydantoin [32], succinimide [33, 34], 4-piperidinol [35], barbituric acid [36-38], or cyanuric acid [39]. On the other hand, some examples of acyclic N-halamines include amine N-halamines, amino acids, and aromatic N-halamines. [40-42]

The formation of N-halamines. N-halamines with N-Cl could be synthesized from the chlorination of N-H bond-containing compounds. The chlorination reaction is the transfer of chlorine atoms from the chlorinating agent to the N-containing compounds. Common chlorinating agents include sodium hypochlorite [43], sodium dichloroisocyanurate (NaDCC) [44], and trichloroisocyanuric acid (TCCA) [45].

The mechanism of chlorination reaction depends on the nature of chlorinating agents and the N-containing compounds. Primary and secondary amines can undergo chlorination reaction in bleach solution. Although OCl^- and HOCl are reactive in the chlorination reaction, hypochlorous acid (HOCl) is the dominant reactive species with aliphatic amines and reaction is fast. [46] Due to their acid-base properties of amines, there are neutral and protonated amines in the solution and the neutral amines were significant species to react with HOCl . [47] Water-assisted mechanism was proposed to assist the chlorine transfer reaction. (**Figure 1-2A**) In this process, the apparent second-order rate constant related to pH is typically observed for aliphatic amines and aqueous chlorine. Chlorine transfer reaction from HOCl molecule to a free amino group is the elementary step and the rate constants of primary amines are higher than secondary amines. [46]

When using N-chlorosuccinimide (NCS) as chlorinating agent, Antelo's group evaluated the chlorination reaction kinetics of chlorinate organic amine (e.g., dimethylamine, diethylamine, and methylethanolamine). Authors proposed two hypothetical chlorine

transfer mechanisms from NCS to amines. One is the direct exchange of positive chlorine from the N-chlorosuccinimide to the amines and this step is the rate-controlling step, as shown in **Figure 1-2B**. [48] Another one is the slow hydrolysis of the chlorinating agent NCS and then the fast chlorination of HOCl with R'RNH (see **Figure 1-2C**). In the presence of excess amines, the overall reaction rate is the hydrolytic step, which is independent of the concentration or nature of R'RNH. However, authors reported the rate constant increased with the concentration of amine and the substituents of amines. This supports the conclusion that the direct exchange of positive chlorine between NCS and the amine is a rate-controlling step.

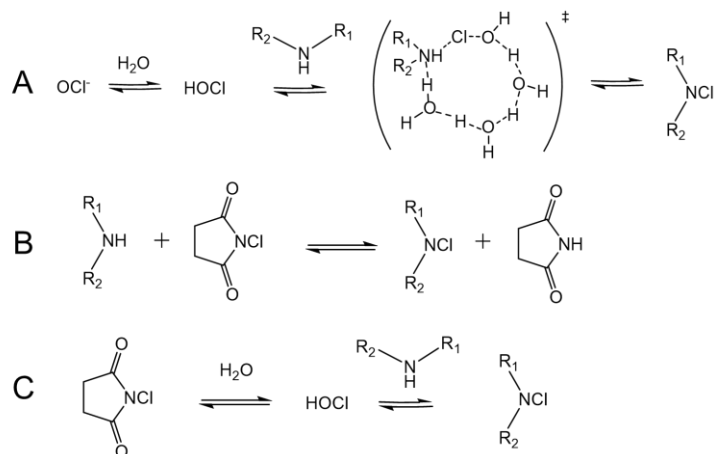


Figure 1-2 General chlorination reaction equation of organic primary and secondary amines with bleach (A), direct chlorine transfer from N-chlorosuccinimide (NCS) (B), and the hydrolysis of NCS. R₁ and R₂ refer to the aliphatic groups.

Similarly, the amide chlorination mechanism in hypochlorite ion (ClO^-) is via Cl^+ transfer from chlorine to the nitrogen atom. Hardy and Robson proposed the chlorination mechanism of N-methylbenzamides with bleach. [49] The first step of the amide reaction was the formation of an O-chlorinated intermediate in hypochlorite ion (ClO^-), and then followed by chlorine rearrangements to the stable N-chlorinated products. The research reported the substituent groups on amides affected the chlorination reactivity and the higher electron density of the amide N facilitates the up-take of positive chlorine. [50] On the other hand, a smaller chlorine reactivity with amide functions was commonly observed, compared to amine functions. This is due to the electron-withdrawing character of the carbonyl function. [24] Furthermore, Pastoriza et al., [51] found that the reactivity order of chlorinating agent hypochlorous acid (HOCl) is higher than NCS in the chlorination reactions of 2-oxazolidinone.

The chlorine contents of poly N-halamines can be controlled by adjusting the concentration of the chlorinating agent [52], reaction time [53, 54], reaction temperature [55], and environmental pH [56, 57]. For example, the oxidative chlorine contents of natural polysaccharides such as chitin [58], hyaluronic acid [52], or modified chitosan

[59] can be controlled by chlorination conditions (see **Figure 1-3**). In addition, Liu et al., [56] concluded that the control of pH can facilitate chlorination and suppress the hydrolysis reaction of grafted acrylamide structures on cellulose. The slightly basic condition (pH = 8) and addition of NaCl were able to improve the chlorination of polyacrylamide and less than 10% hydrolysis occurred. Therefore, optimization of the reaction conditions is necessary to achieve the desired level of chlorination and antimicrobial activity.

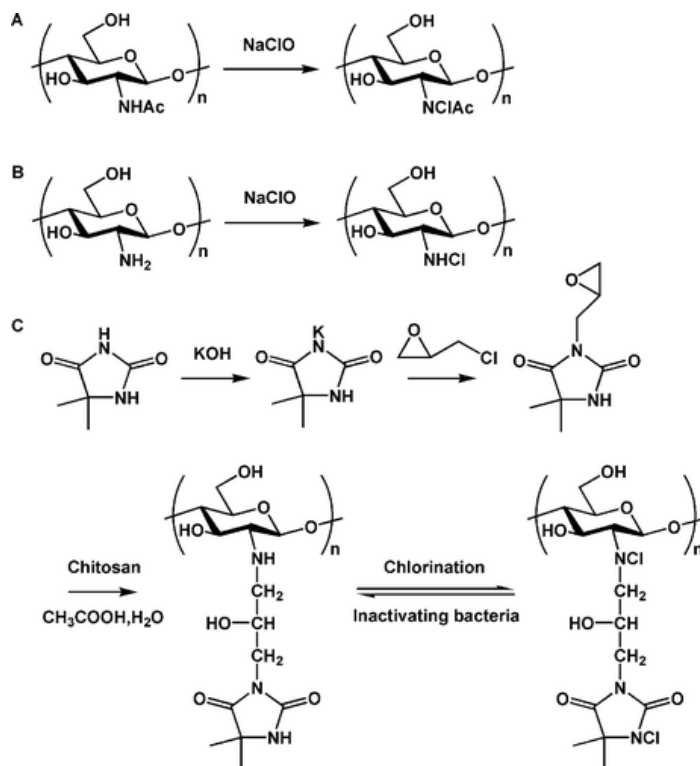


Figure 1-3 Chlorination reaction of chitin (A), chitosan (B), and chitosan-3-glycidyl-5,5-dimethylhydantoin (C). Picture adapted from ref [60].

Stability of poly N-halamines. Poly N-halamines are regarded as a reservoir to store oxidative chlorine. In this regard, the stability of poly N-halamines is a critical factor in their antibacterial applications. Their storage stability is significantly influenced by structure, light, and water. The stability of N-halamines toward the release of free chlorine follows the sequence: chloramines > chloramides > chlorimides because of the effects of electron withdrawal and donation. [27] Also, Akdag et al. [61] found the imide N–Cl bond to be more labile than the amide one in the theoretical calculations. Furthermore, the chlorimide N–Cl bond was more ionic and showed a more rapid dissociation rate by hydrolysis. Another structural effect is the aramid groups of Kevlar and Nomex. Results demonstrated p-diaminophenylene part of Kelvar decomposed over

time in a bleach solution. However, Nomex can be treated in bleach without any significant decomposition. [62]

In addition to structural influence, environmental factor such as UV light affects the storage stability of N-halamines. To date, N-halamines are sensitive to UV light in practical applications and **Table 1-1** summarized the chlorine stability of poly N-halamine. Upon exposure to UV light, UV light might break the N-Cl bond of N-halamines and N-halamines then tend to degrade in the hour's range. Kocer et al., [63] found only 13% of oxidative chlorine on hydantoin derivative polymer remained within 24 h of exposure to UV light. Also, variation of alkyl substitution at position 5 on the hydantoin ring has been applied to understand the UV light stability and concluded that the alkyl substituent group was not the determining factor for UV exposure. [64]

In terms of the oxidative chlorine loss mechanism, a type of intramolecular rearrangement reaction (e.g., Hoffmann-Loeffler rearrangement) is used to explain the chlorine loss on N-Cl moieties under UV light. Petterson et al. [65] reported the chlorine rearrangement from the N-Cl to the acyl chain N-chlorimide or N-chloramide. Furthermore, Kocer et al. [66] investigated the UV stability of N-halamine siloxanes within UV exposure and decomposition products. At the beginning stage, the chlorine might migrate onto the alkyl chain at C-8 (1,6-hydrogen atom transfer) or C-7 (1,5-hydrogen atom transfer) with exposure to UV light (see **Figure 1-4A**). Then, the cleavage of the alkyl group on the siloxane coatings and the loss of hydantoin moieties occur (see **Figure 1-4B**).

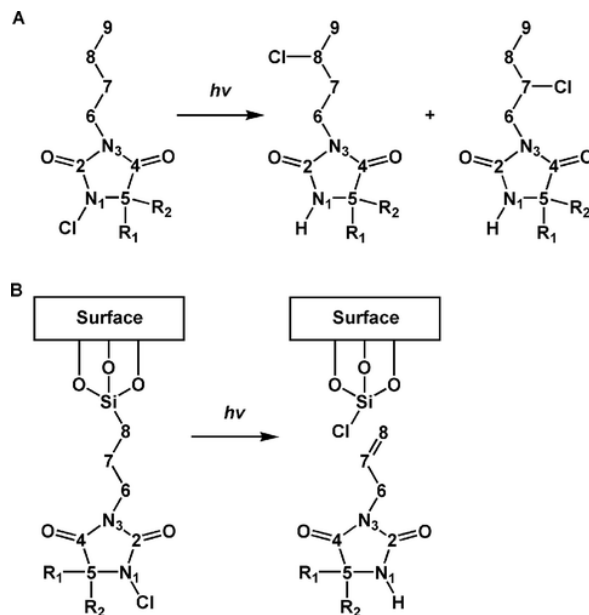


Figure 1-4 (A) Photolytic rearrangements for 3-butyl-1-chlorohydantoin. (B) Proposed degradation of an N-chlorohydantoinylsiloxane. Picture adapted from ref [66].

Table 1-1 Chlorine stability on poly N-halamine with light and dry storage.

material	chlorine contents (%)	storage condition	light and time	remaining chlorine (%)	ref.
hydantoin derivative polymer on cellulose fibers	0.15	air-dry	UV (Type A, 315–400 nm) chamber, contact time 24 h	13	[63]
hydantoin based polymer on polyester fibers	0.19	air-dry	UV (Type A, 315–400 nm) chamber, contact time 24 h	47	[67]
hydantoin based polymer on cotton	0.26	air-dry	UV light (Type A, 315–400 nm, 0.89 W/m ² , 60 °C), contact time 8 h	1.5	[68]
hydantoin based polymer with paint	0.46	air-dry	UV (Type A, 315–400 nm) chamber, contact time 14 days	28	[69]

Water is another important medium for the stability of N-halamines because of the hydrolysis process of N-halamines. In general, the stability of N-halamines in water is closely related to their dissociation constants in an aqueous solution. Tsao et al.[70] measured equilibrium constants for the hydrolysis reaction of N-halamines and concluded N,N'-dihalo-4-imidazolidinones have long stability in direct sunlight. The dissociation constants for various N-halamines in water follow amine (10^{-12}) > amide (10^{-9}) > imide (10^{-4}). [31] On the other hand, the hydrolysis product of N-halamines may result in a possible polymer chain scission. [71] Wienk et al. [72] proposed that polymer scission in bleach was initiated by free radical-induced hydrogen abstraction of the proton alpha to the carbonyl. In addition, a decarboxylation and a deamination reaction of α -amino acids (amine) occur after the initial chlorination and form ammonia and a nitrile. [73, 74]

1.3 Introduction of Microbial Surface Components

The surface properties of bacteria or viruses influence the activity of biocides. Bacterial cell envelope encompasses the cytoplasm of the cell, which determines its shape and interaction with its surroundings. The bacterial cells are complex multilayered structures that can be classified as either Gram-positive or Gram-negative. [75]

Peptidoglycan, also known as mucopeptide or murein, constitutes the cell wall in almost all prokaryotes. [76] Macromolecular peptidoglycan is a heteropolymer with polysaccharide chains cross-linked through short peptides. Gram-positive bacteria, such as *Staphylococcus*, lack an outer lipid membrane and are surrounded by multilayered and thick peptidoglycan embedded with teichoic acid polymers (above 20 nm) (see **Figure 1-5**). Porous peptidoglycan strands allow the penetration of molecules through their mesh. However, gram-negative bacteria, such as *Pseudomonas*, are surrounded by a lipopolysaccharide-rich outer membrane and a phospholipid-rich inner layer. The length or diameter of bacteria is approximately 1 μm , and their shapes are determined by various types of cytoskeletal proteins. Spiral-shaped bacteria, called spirilla, can range from gently curved to corkscrew spirals. The length of rod-shaped bacteria can be anywhere between 2 and 100 μm . In addition, bacterial cells present a net negative surface charge at physiological pH values. Negative charges of bacteria come from the ionized phosphoryl and carboxylate substituents groups of lipopolysaccharides on the outer membrane. [77]

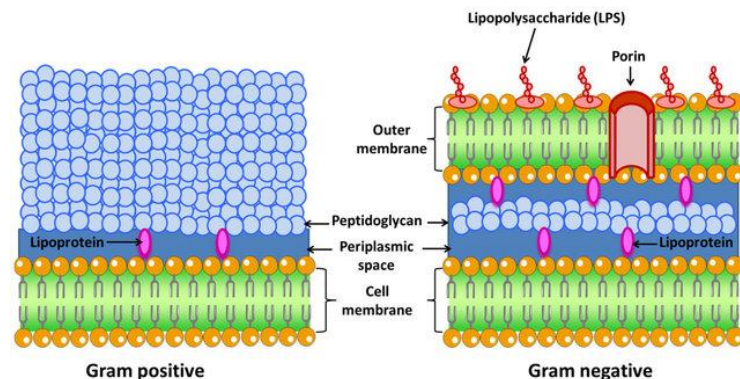


Figure 1-5 Illustration of the cell surfaces of gram-positive and gram-negative bacteria. Picture adapted from [78].

Viruses are commonly surrounded by a protective protein coat (e.g., capsid) and have a core with biological entities of DNA or RNA (see **Figure 1-6**). The sizes of infectious viruses in humans typically range from 20 to 260 nm, although a few classes of viruses can grow much larger. [79] Some viruses (such as influenza and coronavirus), are wrapped with an additional protective lipid bilayer-envelope. [79] The envelope not only gives a protective ability during budding out from the cell but also offers structure flexibility. [80] Coronavirus is an example of a virus that causes a broad range of clinical manifestations, from mild symptoms to acute respiratory distress syndrome (ARDS) and mortality. [81] The virus structure is made up of membrane glycoproteins, spike proteins, hemagglutinin ester dimer proteins, nucleocapsid proteins, and envelope proteins.

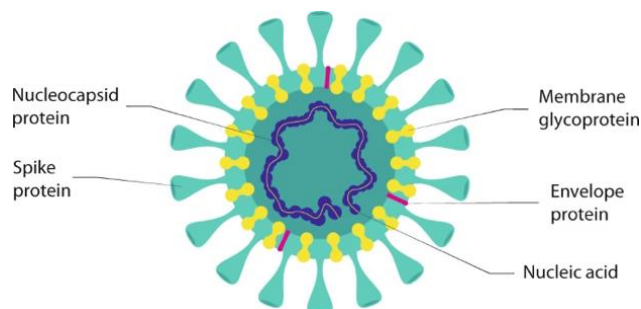


Figure 1-6 Virus structure based on coronavirus. The nucleic acid is wrapped by a protein capsid. The protein capsid contains envelope proteins, glycoproteins, and a spike protein. Picture adapted from ref [82].

1.4 Oxidative Chlorine Transport to Microbes

The antimicrobial properties of N-Cl in N-halamine moieties are based on chlorine transfer to microbes. Considered now are the transport mechanisms whereby oxidative chlorine moves from the chlorine source to the bacteria surfaces. There are three chlorine transfer mechanisms, direct transfer, hydrolytic transfer, and shuttle transfer (see **Figure 1-7**). (1) “Direct transfer”, oxidative chlorine from an N-halamine molecule moves to the bacterial surface directly; (2) “hydrolytic transfer”, the N-halamine molecule reacts with water to release HOCl which diffuses to the bacteria; (3) “shuttle transfer, oxidative chlorine of an N-halamine molecule moves to a shuttle chemical which then moves to the bacteria. The shuttle mechanism is demonstrated in Chapters 4 and 5.

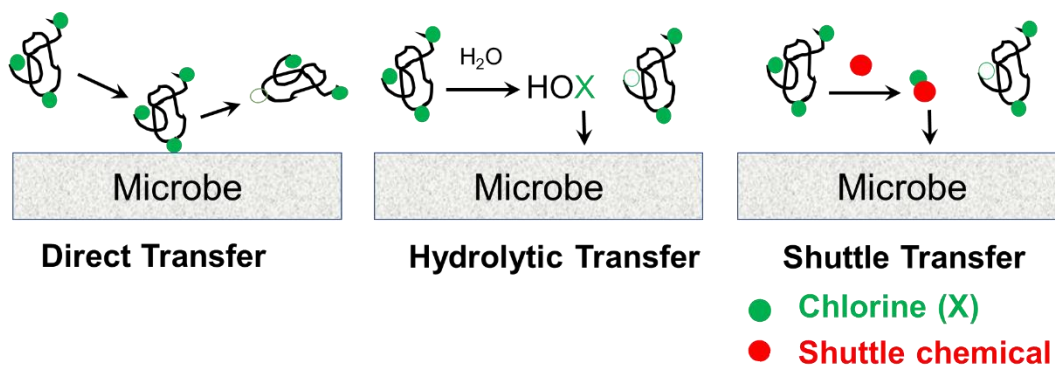


Figure 1-7 A model illustrating the oxidative chlorine transfer mechanisms of N-halamines to microbes, including direct transfer, hydrolytic transfer, and shuttle transfer.

N-Halamines with stable N–X bonds prefer direct transfer of oxidative chlorine. For example, Worley’s group[83] demonstrated the direct chlorine transfer from 3-chloro-4,4-dimethyl-2-oxazolidinone (compound 1) to bacteria, rather than the limited amount of

free chlorine in hydrolysis equilibrium of compound 1. Similarly, Luo et al.[84] found poly[(6-morpholino-s-triazine-2,4-diyl)-N-chloro-[2,2,6,6-tetramethyl-4-piperidyl]imino]-hexamethylene[(2,2,6,6-tetramethyl-4-piperidyl) imino]] (APA-1), as an additive into polyurethane killed the bacteria via direct chlorine transfer without leaching out of the polyurethane samples. Moreover, there is no inhibition region around the APA-1 samples in the inhibition zone test, suggesting that the biocidal activity of APA-1 is not by releasing oxidative chlorine.

Hydrolytic transfer is verified by the inhibition zone test and chlorine release kinetics. In one example, Li et al.[85] prepared amine N-halamine-labeled silica nanoparticles based on 2,2,6,6-tetramethyl-4-piperidinol (TMP) and placed N-halamine nanoparticle disk onto bacteria-containing LB agar disk (see **Figure 1-8**). Results showed N-halamine nanoparticle disk gave an inhibition ring, demonstrating the oxidative chlorine from the disassociation of N-halamines. For chlorine release of N-halamines in an aqueous solution, Liu et al.[57] found continuous chlorine release of inorganic-based N-halamine nanofibrous membranes into the water through hydrolysis reaction in acidic or basic conditions. Furthermore, the hydrolysis equilibrium constants in an aqueous solution follow the order chlorimide>chloramide>chloramine. [86]

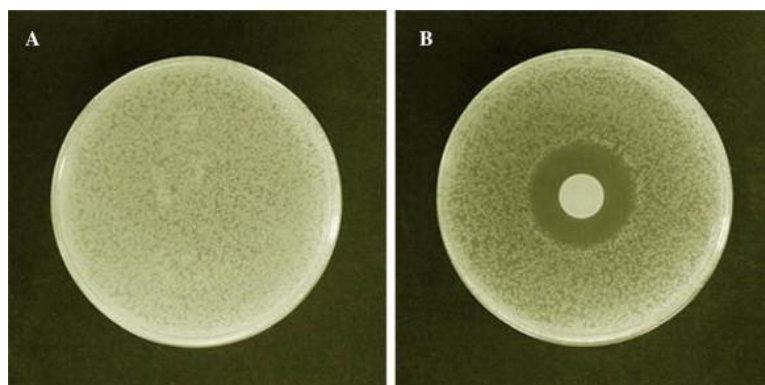


Figure 1-8 Optical images of the inhibition zone against *Escherichia coli* (ATCC 25922): (A) Untreated *Escherichia coli*; (B) *Escherichia coli* treated with 4-piperidinol-containing N-halamines. Picture reproduced from ref [85].

Halogen shuttle transfer from N-halamine to a microbe is another chlorine transfer process. The chlorine shuttle transfer refers to the chlorine transfer between nitrogen-containing components. The chlorine shuttle transfer was generally demonstrated by the nutrient broth experiment. Nutrient Broth is a basic media with peptone and a beef extract. Peptone and beef extract contribute organic nitrogen compounds with the amide N-H. When mixing nutrient broth with N-halamines, chlorine transfer occurs between them. Ahmed's group[87] confirmed that nutrient broth as shuttle chemicals carried oxidative chlorine after incubation with barbituric acid-bearing N-halamines. They found that the amount of oxidative chlorine in the nutrient broth was higher than in the water because of chlorine exchange. After that, authors incubated barbituric acid-based N-

halamines with a broth medium and found the bacteria failed to grow in a pretreated medium, demonstrating the chlorine shuttle transfer. [88] Among chlorine transfer between nitrogen-containing components, the chlorimides such as sodium dichloroisocyanurate (NaDCC) can easily transfer oxidative chlorine to amides or amines.[48, 89, 90] However, Qian et al.[91] demonstrated the chlorine transfer occurred from 1-chloro-2,2,5,5-tetramethylimidazolidin-4-one (MC, amine) to succinimide in both water and chloroform solutions. In this regard, intermolecular chlorine transfer is possible between nitrogen-containing components.

1.5 Antimicrobial Mechanisms of N-Halamines

Antimicrobial mechanisms of N-halamines are based on the chlorine transport to bacteria. They are similar to dilute bleach products. Sodium hypochlorite (NaOCl) is the main component of disinfectant bleach, in which hypochlorous acid (HOCl) is the active ingredient. Due to its electrical neutrality, weak acid HOCl can passively diffuse into the microbe. The principal antimicrobial activity of HOCl is due to its oxidizing action, as exemplified in **Figure 1-9**.

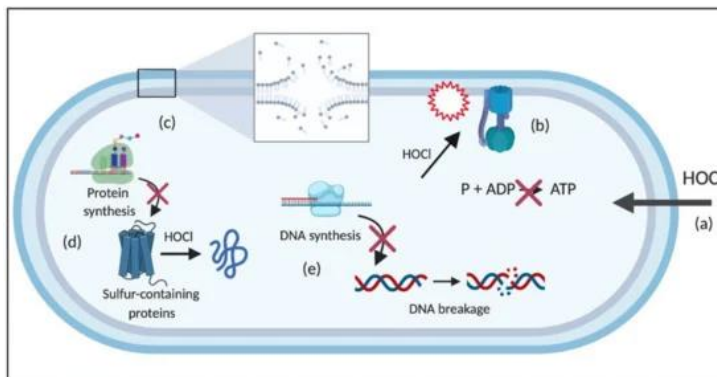


Figure 1-9 A model illustrating the mechanisms of the germicidal actions of HOCl and OCl^- in gram-negative bacterial cells. (a) HOCl penetrates the cell; (b) disruption of ATP production; (c) lipid membrane breakage; (d) protein synthesis disruption; (e) DNA, leading to DNA breakage and impairment of DNA synthesis. HOCl refers to hypochlorous acid; P is phosphate; ADP means adenosine diphosphate; ATP is adenosine triphosphate. Picture reprinted from ref [92].

Compared to OCl^- , the antimicrobial activity of HOCl is approximately 80 times greater. [93] Furthermore, HOCl is a fast-acting antimicrobial agent which reacts with several biomacromolecules, such as sulfur-containing proteins, lipids, nucleic acids, and membrane components, causing severe cellular damage. The reaction of HOCl with acyl chains of unsaturated fatty acids or phospholipids generates chlorohydrin intermediates. [94] The formation of these molecules can increase the permeability of the membrane and

cause the loss of membrane function and structure. Proteins, the most abundant cellular components, are the main target of HOCl, causing damage to membrane transport proteins. The reaction between thiol-containing compounds (R-SH), such as cysteine with HOCl, yields disulfides (R-S-S-R') and sulfonic acids (R-SO₃H). The formation of chloramines and protein carbonylation (aldehyde formation) interferes with protein folding and leads to protein aggregation. The oxidation of these components by HOCl results in the loss of physiological functions. Furthermore, the damage to DNA caused by HOCl results from the DNA derivatives of chlorinated nucleotide bases. [95]

As to the biocidal mechanisms of N-halamines, they may perform a combination of two or three oxidative chlorine transport processes. For example, Ahmed et al. [88] demonstrated that three chlorine transfer mechanisms (i.e., direct transfer, hydrolyzed transfer, and shuttle transfer) provided the antimicrobial function of poly N-halamines. In addition, to improve the chlorine transfer from poly N-halamines to microbes, quaternary ammonium moieties are commonly applied to increase the contact between polymers and microbes, leading to faster chlorine transfer. For instance, Li and Liu et al., [96] designed polymers with hydantoin and quaternary ammonium moieties (see **Figure 1-10**) and immobilized cationic polymer to the substrate. Results demonstrated short-chained (methyl) quaternary ammonium moieties facilitated the oxidative chlorine transfer from N-chlorohydantoin to the negatively charged bacteria because of electrostatic interaction. To further confirm the biocidal mechanism, researchers designed a non-contact killing test by immersing poly N-halamine grafted cotton in PBS buffer and separating PBS buffer. Results revealed there was no bacterial reduction in the extraction buffer. This addressed direct chlorine transfer is the primary biocidal mechanism of N-halamines.

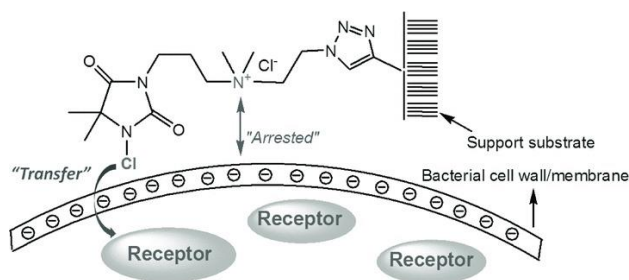


Figure 1-10 Illustration of microbiocidal activity with cation and chloramide groups. Picture adapted from ref [96].

1.6 Factors Influencing Antimicrobial Activity of N-Halamines

Many factors have an effect the antimicrobial activity of N-halamines, including structures of N-hamines[86], the effect of substitution[32, 45], and environmental factors such as soil loads. The structure and substitution effects of N-halamines have been reported in detail by other researchers.[31] In this section, soil loads or organic burdens

are specially addressed. Soil loads are known to influence the effectiveness of antimicrobial agents. From the viewpoint of practical use, antimicrobial agents tend to be challenged with organic materials (e.g., wound exudate, blood sera, or other organic contaminants). [97, 98] The US Environmental Protection Agency reported 5% (v/v) blood serum as one organic soil to evaluate the biocidal activity of antimicrobial agents. [99] Again, water-soluble model soils can be subdivided into low molecular weight molecules, particles, or negatively charged polymers in the environment.

In general, the dilute bleach is highly reactive, and there is a risk to form halogenated organic compounds such as tri-halomethanes. This results in its biocidal reduction in the presence of organic material. However, there is information lacking to discuss the organic material influence with N-halamines. Thus, it is useful to understand the impacts of specific soil types on the antimicrobial activity of poly N-halamine.

The interaction mechanisms between soil loads and poly N-halamines include two main mechanisms: sequestration and consumption of oxidative chlorine. Sequestration of poly N-halamines refers to adsorption at solid/water interfaces with soil particles or by forming polyelectrolyte complexes with oppositely charged water-soluble soils. For polymer adsorption on surfaces, the driving forces are electrostatic and hydrophobic interactions, and this adsorption is irreversible. [100] For polyelectrolyte complexation, the driving force is entropy gain with the release of low molecular weight counterions. [101-103] The formation of polyelectrolyte complexation includes primary complex formation, intracomplexes, and intercomplex aggregation process, as shown in **Figure 1-11**. The interactions in polyelectrolytes include van der Waals, dipole, Coulomb's interactions, hydrogen bonding, or hydrophobic interaction. [104] However, there are always excessive polymers in solution after forming polyelectrolyte complexes and the charge of the excessive polymer determines the net charge of the complexes. In summary, sequestration may inhibit the attachment between polymers and microbes.

As to the consumption of oxidative chlorine, soil loads can exchange chlorine directly with N-halamines, [105] or reduce oxidative chlorine. [106] Chlorine exchange can lower the biocidal activity of N-halamines because of the formation of less or completely inactive products. In Kloth's work, 200 ppm chloramine-T reduced 95% to 100% of *E. coli* growth, but *E. coli* growth was reduced by only 30% to 50% in the presence of fetal bovine serum due to the reduction of oxidative chlorine such as disulfide moieties of protein. [98, 107] Similarly, Gottardi et al. [108] investigated the bactericidal activity of N-halamines in protein load. All investigated N-halamines lost immediately biocidal activity in the presence of proteinaceous material, caused by halogen consumption. Thereafter, consuming oxidative chlorine from N-halamines may negatively interface the antimicrobial activity by reduction reaction. [27] In summary, soil loads impact cationic and anionic synthetic antimicrobial poly N-halamines in various mechanisms. In this regard, the research of poly N-halamines in organic burden is needed to evaluate in terms of their practical use.

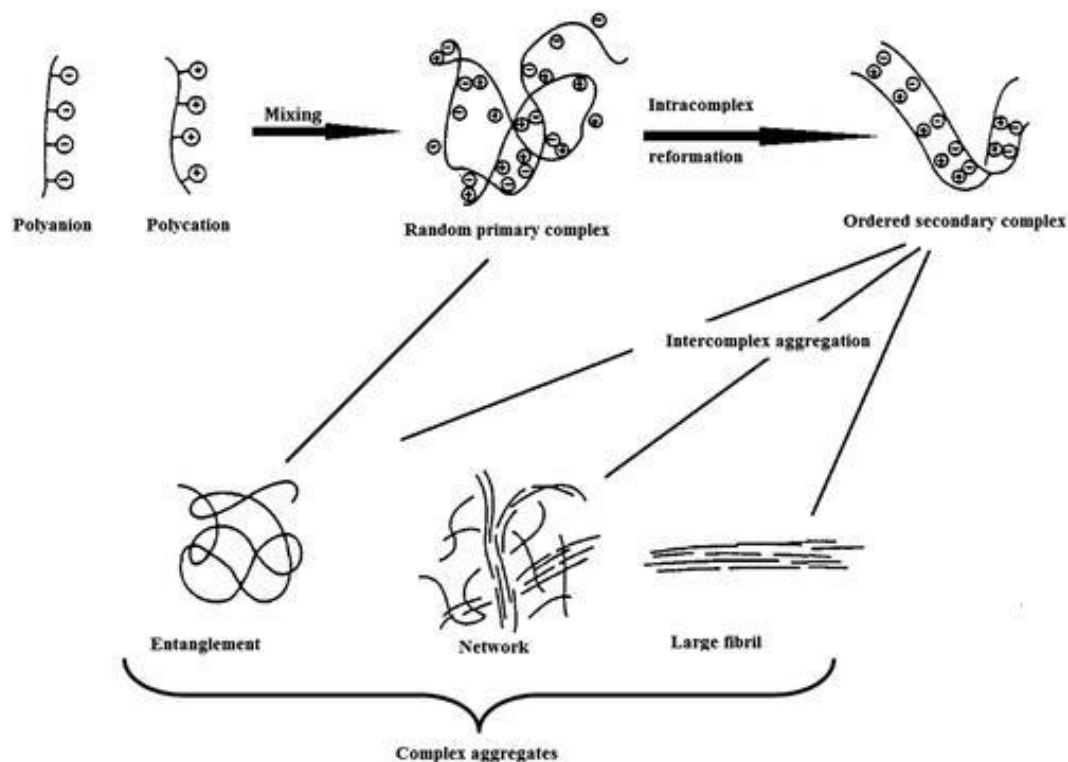


Figure 1-11 Schematic of polyelectrolyte complexation formation, involving primary complex formation; new bond formation process within intracomplexes; intercomplex aggregation process. Picture reprinted from ref [104].

1.7 Examples of Antimicrobial Polymeric N-Halamine Coatings

There is a continued need for the development of antimicrobial coatings that can adapt to the complexity of variable different surfaces such as wood, glass, and textiles. Such coatings should possess long-term biocidal activity, enabling the effective killing of microbes, rather than being limited to specific strains. In this regard, antimicrobial N-halamine polymers have many advantages in high-touch surface applications. For instance, they can be easily modified with desirable functional groups and grafted to the surfaces. [109] On the other hand, household consumer disinfectants are subject to regulations that limit their volatile organic content to a maximum of 1%. [110] As a result, poly N-halamine films or coatings that can be produced using a versatile and cost-effective process are desirable.

Applications of poly N-halamines. In the past decades, researchers have investigated a variety of potential applications such as water treatment [27], air purification [111], or kitchen work surfaces [112]. Although poly N-halamines are effective antimicrobial agents, their toxicology and safety evaluation should be addressed in the future investigations in terms of the strong oxidative property of positive chlorine. At present,

the three main tests such as cytotoxicity, genotoxicity, and protein toxicity, were applied to evaluate the safety of N-halamines. [31] For example, Qiao [113] verified the toxicity of N-halamine compound (1-chloro-2,2,5,5-tetramethyl-4-imidazolidinone) using *in vitro* cytotoxicity testing methods. Similarly, Humpage and co-workers demonstrated the cytotoxic effect of amino acid-containing N-halamines on mammalian cells. [114] In this case, more toxicology work needs to be done when poly N-halamines are coated on high touch surfaces with direct contact with humans such as table desk and knobs. On the other hand, the indirect contact surfaces such as floors, walls, or ceils are suitable for direct poly N-halamine coatings.

Single-component polymer-coated surfaces. Antimicrobial N-halamine polymers form a stable antimicrobial coating through non-covalent or covalent attachment to diverse surfaces, causing complete microbe disintegration. Demir et al. [115] synthesized a copolymer of 2-acrylamido-2-methyl-1-(5-methylhydantoinyl) propane and 3-chloro-2-hydroxypropyl methacrylate (see **Figure 1-12**) and grafted onto a stainless steel surface via covalent attachment. The chlorinated stainless-steel surfaces are robust and regenerable, causing 6 logs reduction of *Staphylococcus aureus* and *Escherichia coli* O157:H7 bacteria within 15 min.

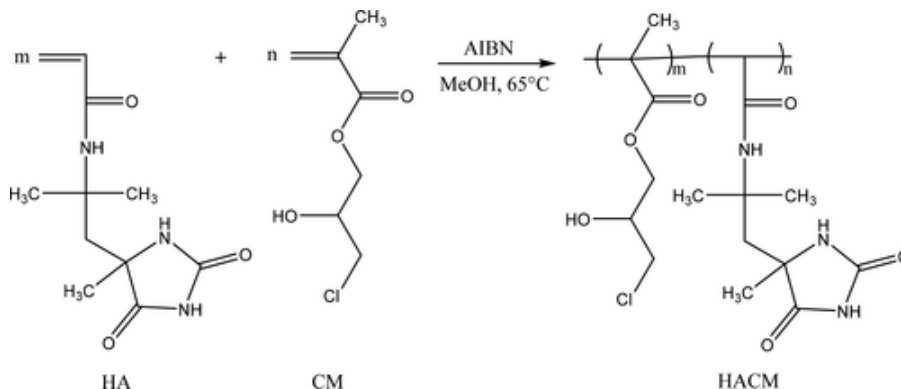


Figure 1-12 Structure of copolymer of 2-acrylamido-2-methyl-1-(5-methylhydantoinyl) propane and 3-chloro-2-hydroxypropyl methacrylate. Reproduced from ref [115].

Sprayable surface coatings of poly N-halamines. For instance, Chien et al. [116] prepared a chlorinated polydopamine (PDA) coating and PDA co-deposited with polyethylenimine (PEI) fabrics to exhibit superior antibacterial activity. Catechol moieties of PDA can react with PEI through Michael addition and Schiff base formation to generate a stable matrix (covalent bonds). [117] One commercial sprayable surface coating was reported by Halomine, Inc. [118, 119] HaloFilm™ is a polymer formulation that consists of a dopamine adhesive part and an N-halamine moiety (see **Figure 1-13**). The adhesive moiety can adhere to various nonporous surfaces (e.g., metals, plastics,

glasses, ceramics, fabrics, etc.) and it can hold free oxidative chlorine to deactivate bacteria, fungi, and viruses after chlorination.

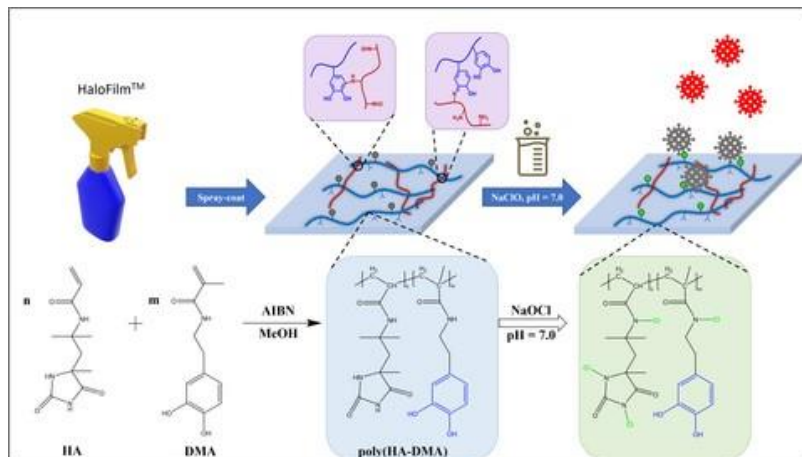


Figure 1-13 Schematic illustration of HaloFilm™ polymer formulation coating on non-porous surfaces, before and after chlorination. Picture from ref [119].

Another polyurethane coating with N-halamine was developed by Worley et al. [120] researchers proposed a biocidal polyurethane coating. The functionalization of a reactive diol with a hydantoin moiety could then be copolymerized with commercial water-borne acrylic polyols and isocyanates to form a polyurethane without a catalyst. After coating, a film can be chlorinated with bleach, to render it biocidal ability. Results showed the coating stayed its biocidal activity for over six months. Recent research focused on the efficacy of single component, antimicrobial poly N-halamines. However, there are many unanswered questions about their surface applications. For example, should the polymer be hydrophobic or hydrophilic? Should the poly N-halamine film be sufficiently water soluble to leave the surface when exposed to water?

Adding poly N-halamines into a polymer matrix. When a polymer matrix is not intrinsically antimicrobial, the strategy of antimicrobial activity can be achieved through the addition of N-halamines into the polymer matrix. In this system, polymeric components include a binder, a liquid component, or additives. [121] A binder refers to the primary material, which is capable of producing a film during the coating process. The most frequently used binders include polyurethane (PU), poly (methacrylic acid) (PMMA), polyvinyl alcohol (PVA), poly (lactic-co-glycolic acid) (PLGA), hydroxyapatite, a hyaluronic acid, and chitosan. [122] A liquid component can be a solvent, a diluent, or a thinner, which confers and/or alters the rheological properties of the coatings, including water, and organic solvents. An additive (such as a biocide) refers to a composition to confer antimicrobial properties to a coating film. For instance, worley's group [123] mixed the polymer of 3-triethoxysilylpropyl-5,5-dimethylhydantoin with commercial floor enamel to produce liquid paint and then brush it onto wood

coupons. Chlorinated siloxane polymers conferred useful biocidal surface coatings. Moreover, Cao et al. [124] developed a “prehalogenation” approach to prepare water-based 4-piperidinol-containing N-halamine-based latex and added it into two commercial water-based latex paints without coagulation and/or phase separation. The antimicrobial activity of paint films stored under 25 °C can be kept over 12 months (see **Figure 1-14**). Furthermore, Kocer et al. [125] found chlorinated homopolymer of hydantoinylacrylamide did not present biocidal property to the paint because of aggregation in the paint. However, the water-miscible copolymers with hydantoinylacrylamide and the sodium salt of 2-(acrylamido)-2-methylpropanesulfonic acid were able to inactivate *Staphylococcus aureus* and *Escherichia coli O157:H7* within 5 min contact.

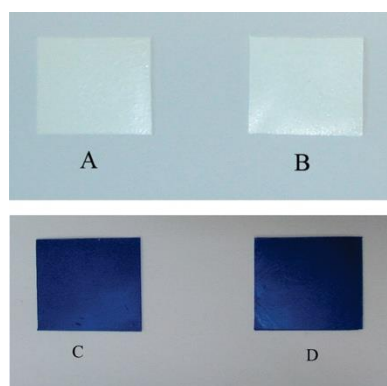


Figure 1-14 Paint films of (A) white paint, (B) white paint with 20 wt % of N-chloro-2,2,6,6-tetramethyl-4-piperidiny methacrylate (poly(Cl-TMPM)), (C) blue paint, and (D) blue paint containing 20 wt % of poly(Cl-TMPM). White paint refers to the color Place exterior latex semigloss house paint and blue paint is Auditions satin latex paint. Reproduced from ref [124].

Polyelectrolyte multilayer coatings. Polyelectrolyte multilayers (PEMs) are suitable for various types of substrates such as glass surfaces in which biocidal compounds can be embedded and released in a controlled manner. [126]

Polyelectrolyte multilayers (PEMs) are assembled by one “molecular layer” at a time and followed by a sequential adsorption process from a polycation or a polyanion. In general, most researchers have used polyacids and polybases to assemble these multilayer thin films and the layer-by-layer process can be operated by spray, spin, or dip coating. [127-129] Another layer-by-layer adsorption process is driven by hydrogen bonds in the assembly process. [130, 131] PEMs represent one of the most successful approaches for incorporating antimicrobial compounds in surface coatings due to their simplicity, versatility, and low cost. For instance, Liu et al. [132] assembled a cationic N-halamine poly((3-acrylamidopropyl) trimethylammonium chloride) and an anionic N-halamine poly(2-acrylamido-2-methylpropane sulfonic acid sodium salt) (AHP) PEMs via a layer-by-layer (LbL) deposition technique and this complex coating inactivated bacteria within

30 min. Additionally, the spray LbL deposition method was developed by Denis-Rohr et al. [133] to coat polypropylene surface with N-halamine containing bilayers of cross-linked polyethyleneimine (PEI) and polyacrylic acid (PAA). Spray LbL fabrication of N-halamines is an attractive coatings technology to fabricate rechargeable antimicrobial surfaces in terms of commercial adoption.

1.8 Objectives

In the research leading to this thesis, I proposed to develop new anionic, antimicrobial polychloramides. The work documented in this thesis aims to achieve four main objectives.

1. To develop new anionic, water-soluble polychloramides to extend the antimicrobial lifetimes of cleaned and disinfected surfaces.
2. To model measurable polymer solution characteristics into bacteria disinfection kinetics.
3. To investigate the impacts of non-microbial soils on polychloramide disinfectants.
4. To enhance the antimicrobial activity of polychloramides with shuttle molecules.

1.9 Outline

Chapter 1 provides an overview of long-lasting antimicrobial N-halamines, their biocidal mechanisms, and their coating applications on high-touch surfaces. In addition, Chapter 1 introduces the objectives of this project and provides an outline of this thesis.

Chapter 2 develops film-forming polychloramides with extending antimicrobial properties on surfaces. Polychloramides were prepared by first reacting poly(ethylene-alt-maleic anhydride) with isopropylamine, followed by chlorination with NaOCl. In addition, water-soluble, highly anionic polyamide PC3 can be grafted to cellulosic filter paper, and then chlorinated and evaluated for antimicrobial activity. This work has been published on *Colloids and Surfaces B: Biointerfaces*.

Chapter 3 proposes the polymer-modified Chick-Watson (PCW) of disinfection kinetics to account for the contributions of polychloramide molecular weight and the polychloramide configuration. The polychloramide properties in the solution are estimated from the overlap concentration, C^* , and chlorine mass fractions. The PCW model concluded that lower molecular weight polymers and polymers with compressed configurations are more effective biocides compared with high MW counterparts. Experimental results are consistent with the model predictions. This work has been published on *Biomacromolecules*.

Chapter 4 demonstrates the impacts of a series of model soils on the biocidal activity of an anionic polychloramide, a cationic polychloramide, and a cationic quaternary

ammonium polymer. The nanoscale soil models contain polyacrylic acid (PAA), cellulose nanocrystals (CNCs), and bovine serum albumin (BSA). The low molecular weight model soils include ammonium chloride, glycine, and (1-(hydroxymethyl)-5,5-dimethylhydantoin (HDMH), a cyclic low molecular weight imide. This chapter is in preparation for publication.

Chapter 5 proposes chlorine transfer from polychloramides to imide molecules and this shuttle process with imide groups enhances the biocidal property of polychloramides. Three model compounds of small imide shuttle molecules, including 1-(hydroxymethyl)-5,5-dimethylhydantoin (HDMH), 5,5-dimethylhydantoin (DMH), and succinimide (SI), were employed to investigate chlorine transfer and biocidal influence of polychloramides. This chapter is in preparation for publication.

Chapter 6 summarizes the contributions of this thesis.

References

1. Ashbee, R., The discovery of chlorine: a window on the chemical revolution. An element of controversy: the life of chlorine in science, medicine, technology and war, **2007**: 15-40.
2. Dakin, H.D., On the use of certain antiseptic substances in the treatment of infected wounds. *British medical journal*, **1915**, 2(2852): 318.
3. Rutala, W.A. and Weber, D.J., Uses of inorganic hypochlorite (bleach) in health-care facilities. *Clinical microbiology reviews*, **1997**, 10(4): 597-610.
4. Wang, M., Duday, D., Scolan, E., Perbal, S., Prato, M., Lasseur, C., and Hołyńska, M., Antimicrobial surfaces for applications on confined inhabited space stations. *Advanced Materials Interfaces*, **2021**, 8(13): 2100118.
5. Cosentino, C.B., Mitchell, B.G., Brewster, D.J., and Russo, P.L., The utility of frailty indices in predicting the risk of health care associated infections: a systematic review. *American journal of infection control*, **2021**, 49(8): 1078-1084.
6. Behzadinasab, S., Williams, M.D., Hosseini, M., Poon, L.L., Chin, A.W., Falkinham III, J.O., and Ducker, W.A., Transparent and sprayable surface coatings that kill drug-resistant bacteria within minutes and inactivate SARS-CoV-2 virus. *ACS Applied Materials & Interfaces*, **2021**, 13(46): 54706-54714.
7. Suleyman, G., Alangaden, G., and Bardossy, A.C., The role of environmental contamination in the transmission of nosocomial pathogens and healthcare-associated infections. *Current Infectious Disease Reports*, **2018**, 20: 1-11.
8. Allegranzi, B., Nejad, S.B., Combescure, C., Graafmans, W., Attar, H., Donaldson, L., and Pittet, D., Burden of endemic health-care-associated infection in developing countries: systematic review and meta-analysis. *The Lancet*, **2011**, 377(9761): 228-241.
9. Inweregbu, K., Dave, J., and Pittard, A., Nosocomial infections. *Continuing Education in Anaesthesia, Critical Care & Pain*, **2005**, 5(1): 14-17.
10. Kollef, M.H., Torres, A., Shorr, A.F., Martin-Loeches, I., and Micek, S.T., Nosocomial infection. *Critical Care Medicine*, **2021**, 49(2): 169-187.
11. Lishchynskiy, O., Shymborska, Y., Stetsyshyn, Y., Raczowska, J., Skirtach, A.G., Peretiako, T., and Budkowski, A., Passive antifouling and active self-disinfecting antiviral surfaces. *Chemical Engineering Journal*, **2022**: 137048.
12. Lei, H., Li, Y., Xiao, S., Yang, X., Lin, C., Norris, S.L., Wei, D., Hu, Z., and Ji, S., Logistic growth of a surface contamination network and its role in disease spread. *Scientific Reports*, **2017**, 7(1): 14826.

13. Saud, Z., Richards, C.A., Williams, G., and Stanton, R.J., Anti-viral organic coatings for high touch surfaces based on smart-release, Cu^{2+} containing pigments. *Progress in Organic Coatings*, **2022**, 172: 107135.
14. Liu, M., Bauman, L., Nogueira, C.L., Aucoin, M.G., Anderson, W.A., and Zhao, B., Antimicrobial polymeric composites for high-touch surfaces in healthcare applications. *Current Opinion in Biomedical Engineering*, **2022**: 100395.
15. Kampf, G., Todt, D., Pfaender, S., and Steinmann, E., Persistence of coronaviruses on inanimate surfaces and their inactivation with biocidal agents. *Journal of Hospital Infection*, **2020**, 104(3): 246-251.
16. Hadavi, I., Hashemi, M., Asadikaram, G., Kalantar-Neyestanaki, D., Hosseininasab, A., Darijani, T., and Faraji, M., Investigation of SARS-CoV-2 genome in the indoor air and high-touch surfaces. *International Journal of Environmental Research*, **2022**, 16(6): 103.
17. Weber, D.J., Rutala, W.A., Miller, M.B., Huslage, K., and Sickbert-Bennett, E., Role of hospital surfaces in the transmission of emerging health care-associated pathogens: norovirus, clostridium difficile, and acinetobacter species. *American journal of infection control*, **2010**, 38(5): S25-S33.
18. Spaulding, E.H., Chemical disinfection and antisepsis in the hospital. *J Hosp Res.*, **1972**, 9: 5-31.
19. Chinn, R.Y. and Schulster, L., Guidelines for environmental infection control in health-care facilities: recommendations of CDC and Healthcare Infection Control Practices Advisory Committee (HICPAC). **2003**.
20. Adlhart, C., Verran, J., Azevedo, N.F., Olmez, H., Keinänen-Toivola, M.M., Gouveia, I., Melo, L.F., and Crijs, F., Surface modifications for antimicrobial effects in the healthcare setting: a critical overview. *Journal of Hospital Infection*, **2018**, 99(3): 239-249.
21. Birkett, M., Dover, L., Cherian Lukose, C., Wasy Zia, A., Tambuwala, M.M., and Serrano-Aroca, Á., Recent advances in metal-based antimicrobial coatings for high-touch surfaces. *International Journal of Molecular Sciences*, **2022**, 23(3): 1162.
22. Dancer, S.J., Controlling hospital-acquired infection: focus on the role of the environment and new technologies for decontamination. *Clinical Microbiology Reviews*, **2014**, 27(4): 665-690.
23. Rutala, W.A. and Weber, D.J., *Guideline for disinfection and sterilization in healthcare facilities*, 2008. **2008**.
24. Deborde, M. and Von Gunten, U., Reactions of chlorine with inorganic and organic compounds during water treatment—kinetics and mechanisms: a critical review. *Water Research*, **2008**, 42(1-2): 13-51.

25. Wojtowicz, J.A., Dichlorine monoxide, hypochlorous acid, and hypochlorites. *Kirk-Othmer Encyclopedia of Chemical Technology*, **2004**, 8: 544-581.
26. de Castro, K.C. and Costa, J.M., Polymeric surfaces with biocidal action: challenges imposed by the SARS-CoV-2, technologies employed, and future perspectives. *Journal of Polymer Research*, **2021**, 28(6): 230.
27. Hui, F. and Debiemme-Chouvy, C., Antimicrobial N-halamine polymers and coatings: A review of their synthesis, characterization, and applications. *Biomacromolecules*, **2013**, 14(3): 585-601.
28. Kovacic, P., Lowery, M.K., and Field, K.W., Chemistry of N-bromamines and N-chloramines. *Chemical Reviews*, **1970**, 70(6): 639-665.
29. Worley, S. and Sun, G., Biocidal polymers. *Trends in Polymer Science*, **1996**, 11(4): 364-370.
30. Worley, S.D., Williams, D., and Crawford, R.A., Halamine water disinfectants. *Critical Reviews in Environmental Science and Technology*, **1988**, 18(2): 133-175.
31. Dong, A., Wang, Y.-J., Gao, Y., Gao, T., and Gao, G., Chemical insights into antibacterial N-halamines. *Chemical Reviews*, **2017**, 117(6): 4806-4862.
32. Chang, J., Yang, X., Ma, Y., Shao, J., Yang, X., and Chen, Z., Alkyl substituted hydantoin-based N-halamine: preparation, characterization, and structure–antibacterial efficacy relationship. *Industrial & Engineering Chemistry Research*, **2016**, 55(35): 9344-9351.
33. Pastoriza, C., Antelo, J.M., Crugeiras, J., and Peña-Gallego, A., Kinetic study of the formation of N-chloro compounds using N-chlorosuccinimide. *Journal of Physical Organic Chemistry*, **2014**, 27(5): 407-418.
34. Postma, T.M. and Albericio, F., Immobilized N-chlorosuccinimide as a friendly peptide disulfide-forming reagent. *ACS Combinatorial Science*, **2014**, 16(4): 160-163.
35. Li, R., Sun, M., Jiang, Z., Ren, X., and Huang, T., N-halamine-bonded cotton fabric with antimicrobial and easy-care properties. *Fibers and Polymers*, **2014**, 15: 234-240.
36. Dong, A., Huang, Z., Lan, S., Wang, Q., Bao, S., Zhang, Y., Gao, G., Liu, F., and Harnode, C., N-halamine-decorated polystyrene nanoparticles based on 5-allylbarbituric acid: from controllable fabrication to bactericidal evaluation. *Journal of Colloid and Interface Science*, **2014**, 413: 92-99.
37. Ahmed, A.E.-S.I., Cavalli, G., Wardell, J.N., Bushell, M.E., and Hay, J.N., N-Halamines from rice straw. *Cellulose*, **2012**, 19: 209-217.

38. Ahmed, A., Hay, J., Bushell, M., Wardell, J., and Cavalli, G., Biocidal polymers (I): preparation and biological activity of some novel biocidal polymers based on uramil and its azo-dyes. *Reactive and Functional Polymers*, **2008**, 68(1): 248-260.
39. Ma, K., Liu, Y., Xie, Z., Li, R., Jiang, Z., Ren, X., and Huang, T.-S., Synthesis of novel N-halamine epoxide based on cyanuric acid and its application for antimicrobial finishing. *Industrial & Engineering Chemistry Research*, **2013**, 52(22): 7413-7418.
40. Kaminski, J.J., Bodor, N., and Higuchi, T., N-Halo derivatives IV: synthesis of low chlorine potential soft N-chloramine systems. *Journal of Pharmaceutical Sciences*, **1976**, 65(12): 1733-1737.
41. Badrossamay, M.R. and Sun, G., Acyclic halamine polypropylene polymer: effect of monomer structure on grafting efficiency, stability and biocidal activities. *Reactive and Functional Polymers*, **2008**, 68(12): 1636-1645.
42. Ma, Y., Li, J., Si, Y., Huang, K., Nitin, N., and Sun, G., Rechargeable antibacterial N-halamine films with antifouling function for food packaging applications. *ACS Applied Materials & Interfaces*, **2019**, 11(19): 17814-17822.
43. Sun, Y. and Sun, G., Novel refreshable N-halamine polymeric biocides: N-chlorination of aromatic polyamides. *Industrial & Engineering Chemistry Research*, **2004**, 43(17): 5015-5020.
44. Sun, X., Cao, Z., Porteous, N., and Sun, Y., Amine, melamine, and amide N-halamines as antimicrobial additives for polymers. *Industrial & Engineering Chemistry Research*, **2010**, 49(22): 11206-11213.
45. Chen, Z. and Sun, Y., N-halamine-based antimicrobial additives for polymers: preparation, characterization, and antimicrobial activity. *Industrial & Engineering Chemistry Research*, **2006**, 45(8): 2634-2640.
46. Abia, L., Armesto, X., Canle, M., Garcia, M., and Santaballa, J., Oxidation of aliphatic amines by aqueous chlorine. *Tetrahedron*, **1998**, 54(3-4): 521-530.
47. Antelo, J.M., Arce, F., and Parajo, M., Kinetic study of the formation of N-chloramines. *International Journal of Chemical Kinetics*, **1995**, 27(7): 637-647.
48. Antelo, J.M., Arce, F., Franco, J., Lopez, M.C.G., Sanchez, M., and Varela, A., Kinetics of the chlorination of secondary amines by N-chlorosuccinimide. *International Journal of Chemical Kinetics*, **1988**, 20(5): 397-409.
49. Hardy, F. and Robson, P., The formation and hydrolysis of substituted N-chloro-N-methylbenzamides in aqueous alkali. *Journal of the Chemical Society B: Physical Organic*, **1967**: 1151-1154.

50. Wayman, M. and Thomm, E., N-Chlorination of secondary amides. III. Kinetics of dechlorination of N-chloroamides. *Canadian Journal of Chemistry*, **1970**, 48(3): 459-466.
51. Pastoriza, C., Antelo, J.M., Amoedo, F.A., and Parajó, M., Kinetic study of the formation reaction of N-chloro-2-oxazolidinone. *Journal of Physical Organic Chemistry*, **2015**, 28(9): 602-611.
52. Buffa, R., Hermannová, M., Sojka, M., Svozil, V., Šulc, P., Halamková, P., Pospíšilová, M., Krejčí, H., and Velebný, V., Hyaluronic acid chloramide—synthesis, chemical structure, stability and analysis of antimicrobials. *Carbohydrate Polymers*, **2020**, 250: 116928.
53. Yan, X., Jie, Z., Zhao, L., Yang, H., Yang, S., and Liang, J., High-efficacy antibacterial polymeric micro/nano particles with N-halamine functional groups. *Chemical Engineering Journal*, **2014**, 254: 30-38.
54. Bastarrachea, L.J. and Goddard, J.M., Antimicrobial coatings with dual cationic and N-halamine character: characterization and biocidal efficacy. *Journal of Agricultural and Food Chemistry*, **2015**, 63(16): 4243-4251.
55. Chang, D., Wang, X., Zhu, C., Dong, A., and Gao, G., N-Halamine polymer from bipolymer to amphiphilic terpolymer with enhancement in antibacterial activity. *Colloids and Surfaces B: Biointerfaces*, **2018**, 163: 402-411.
56. Liu, S. and Sun, G., New refreshable N-halamine polymeric biocides: N-chlorination of acyclic amide grafted cellulose. *Industrial & Engineering Chemistry Research*, **2009**, 48(2): 613-618.
57. Liu, C., Shan, H., Chen, X., Si, Y., Yin, X., Yu, J., and Ding, B., Novel inorganic-based N-halamine nanofibrous membranes as highly effective antibacterial agent for water disinfection. *ACS Applied Materials & Interfaces*, **2018**, 10(51): 44209-44215.
58. Dutta, A., Egusa, M., Kaminaka, H., Izawa, H., Morimoto, M., Saimoto, H., and Ifuku, S., Facile preparation of surface N-halamine chitin nanofiber to endow antibacterial and antifungal activities. *Carbohydrate Polymers*, **2015**, 115: 342-347.
59. Li, R., Hu, P., Ren, X., Worley, S., and Huang, T., Antimicrobial N-halamine modified chitosan films. *Carbohydrate polymers*, **2013**, 92(1): 534-539.
60. Balasubramaniam, B., Prateek, Ranjan, S., Saraf, M., Kar, P., Singh, S.P., Thakur, V.K., Singh, A., and Gupta, R.K., Antibacterial and antiviral functional materials: chemistry and biological activity toward tackling COVID-19-like pandemics. *ACS Pharmacology & Translational Science*, **2020**, 4(1): 8-54.

61. Akdag, A., Okur, S., McKee, M.L., and Worley, S., The Stabilities of N–Cl Bonds in Biocidal Materials. *Journal of Chemical Theory and Computation*, **2006**, 2(3): 879-884.
62. Akdag, A., Kocer, H.B., Worley, S., Broughton, R., Webb, T., and Bray, T.H., Why does Kevlar decompose, while Nomex does not, when treated with aqueous chlorine solutions? *The Journal of Physical Chemistry B*, **2007**, 111(20): 5581-5586.
63. Kocer, H.B., Cerkez, I., Worley, S., Broughton, R., and Huang, T., Polymeric antimicrobial N-halamine epoxides. *ACS Applied Materials & Interfaces*, **2011**, 3(8): 2845-2850.
64. Kocer, H.B., Akdag, A., Ren, X., Broughton, R., Worley, S., and Huang, T., Effect of alkyl derivatization on several properties of N-halamine antimicrobial siloxane coatings. *Industrial & Engineering Chemistry Research*, **2008**, 47(20): 7558-7563.
65. Petterson, R.C. and Wambsgans, A., Photochemical rearrangement of N-chloroimides to 4-chloroimides. A new synthesis of γ -lactones. *Journal of the American Chemical Society*, **1964**, 86(8): 1648-1649.
66. Kocer, H.B., Akdag, A., Worley, S., Acevedo, O., Broughton, R., and Wu, Y., Mechanism of photolytic decomposition of N-halamine antimicrobial siloxane coatings. *ACS Applied Materials & Interfaces*, **2010**, 2(8): 2456-2464.
67. Ren, X., Kou, L., Kocer, H.B., Worley, S., Broughton, R., Tzou, Y., and Huang, T., Antimicrobial modification of polyester by admicellar polymerization. *Journal of Biomedical Materials Research Part B: Applied Biomaterials: An Official Journal of The Society for Biomaterials, The Japanese Society for Biomaterials, and The Australian Society for Biomaterials and the Korean Society for Biomaterials*, **2009**, 89(2): 475-480.
68. Li, J., Liu, Y., Jiang, Z., Ma, K., Ren, X., and Huang, T.-s., Antimicrobial cellulose modified with nanotitania and cyclic N-halamine. *Industrial & Engineering Chemistry Research*, **2014**, 53(33): 13058-13064.
69. Kocer, H.B., Residual disinfection with N-halamine based antimicrobial paints. *Progress in Organic Coatings*, **2012**, 74(1): 100-105.
70. Tsao, T.C., Williams, D.E., Worley, C.G., and Worley, S.D., Novel N-halamine disinfectant compounds. *Biotechnology Progress*, **1991**, 7(1): 60-66.
71. Wang, Z. and Pelton, R., Chloramide copolymers from reacting poly (N-isopropylacrylamide) with bleach. *European Polymer Journal*, **2013**, 49(8): 2196-2201.
72. Wienk, I., Meuleman, E., Borneman, Z., Van Den Boomgaard, T., and Smolders, C., Chemical treatment of membranes of a polymer blend: mechanism of the

- reaction of hypochlorite with poly (vinyl pyrrolidone). *Journal of Polymer Science Part A: Polymer Chemistry*, **1995**, 33(1): 49-54.
73. Stanbro, W.D. and Smith, W.D., Kinetics and mechanism of the decomposition of N-chloroalanine in aqueous solution. *Environmental Science & Technology*, **1979**, 13(4): 446-451.
74. Nweke, A. and Scully Jr, F.E., Stable N-chloroaldimines and other products of the chlorination of isoleucine in model solutions and in a wastewater. *Environmental Science & Technology*, **1989**, 23(8): 989-994.
75. Lichter, J.A., Van Vliet, K.J., and Rubner, M.F., Design of antibacterial surfaces and interfaces: polyelectrolyte multilayers as a multifunctional platform. *Macromolecules*, **2009**, 42(22): 8573-8586.
76. Peterson, P.K. and Quie, P.G., Bacterial surface components and the pathogenesis of infectious diseases. *Annual Review of Medicine*, **1981**, 32(1): 29-43.
77. Wilson, W.W., Wade, M.M., Holman, S.C., and Champlin, F.R., Status of methods for assessing bacterial cell surface charge properties based on zeta potential measurements. *Journal of microbiological methods*, **2001**, 43(3): 153-164.
78. Jiménez-Jiménez, C., Moreno, V.M., and Vallet-Regí, M., Bacteria-assisted transport of nanomaterials to improve drug delivery in cancer therapy. *Nanomaterials*, **2022**, 12(2): 288.
79. Walker, P.J., Siddell, S.G., Lefkowitz, E.J., Mushegian, A.R., Dempsey, D.M., Dutilh, B.E., Harrach, B., Harrison, R.L., Hendrickson, R.C., and Junglen, S., Changes to virus taxonomy and the international code of virus classification and nomenclature ratified by the international committee on taxonomy of viruses (2019). *Archives of Virology*, **2019**, 164(9): 2417-2429.
80. Wisskirchen, K., Lucifora, J., Michler, T., and Protzer, U., New pharmacological strategies to fight enveloped viruses. *Trends in Pharmacological Sciences*, **2014**, 35(9): 470-478.
81. Randolph, H.E. and Barreiro, L.B., Herd immunity: understanding COVID-19. *Immunity*, **2020**, 52(5): 737-741.
82. Rakowska, P.D., Tiddia, M., Faruqui, N., Bankier, C., Pei, Y., Pollard, A.J., Zhang, J., and Gilmore, I.S., Antiviral surfaces and coatings and their mechanisms of action. *Communications Materials*, **2021**, 2(1): 53.
83. Williams, D., Elder, E., and Worley, S., Is free halogen necessary for disinfection? *Applied and Environmental Microbiology*, **1988**, 54(10): 2583-2585.
84. Luo, J., Chen, Z., and Sun, Y., Controlling biofilm formation with an N-halamine-based polymeric additive. *Journal of Biomedical Materials Research Part A: An Official Journal of The Society for Biomaterials, The Japanese Society*

- for Biomaterials, and The Australian Society for Biomaterials and the Korean Society for Biomaterials, **2006**, 77(4): 823-831.
85. Li, C., Hou, J., Huang, Z., Zhao, T., Xiao, L., Gao, G., Harnood, C., and Dong, A., Assessment of 2, 2, 6, 6-tetramethyl-4-piperidinol-based amine N-halamine-labeled silica nanoparticles as potent antibiotics for deactivating bacteria. *Colloids and Surfaces B: Biointerfaces*, **2015**, 126: 106-114.
 86. Qian, L. and Sun, G., Durable and regenerable antimicrobial textiles: Synthesis and applications of 3-methylol-2,2,5,5-tetramethyl-imidazolidin-4-one (MTMIO). *Journal of Applied Polymer Science*, **2003**, 89(9): 2418-2425.
 87. Ahmed, A.E.-S.I., Hay, J.N., Bushell, M.E., Wardell, J.N., and Cavalli, G., Biocidal polymers (II): determination of biological activity of novel N-halamine biocidal polymers and evaluation for use in water filters. *Reactive and Functional Polymers*, **2008**, 68(10): 1448-1458.
 88. Ahmed, A.E.S.I., Hay, J.N., Bushell, M.E., Wardell, J.N., and Cavalli, G., Optimizing halogenation conditions of N-halamine polymers and investigating mode of bactericidal action. *Journal of Applied Polymer Science*, **2009**, 113(4): 2404-2412.
 89. Paine, M.R., Pianegonda, N.A., Huynh, T.T., Manefield, M., MacLaughlin, S.A., Rice, S.A., Barker, P.J., and Blanksby, S.J., Evaluation of Hindered Amine Light Stabilisers and Their N-Chlorinated Derivatives as Antibacterial and Antifungal Additives for Thermoset Surface Coatings. *Progress in Organic Coatings*, **2016**, 99: 330-336.
 90. Liu, Q., Zhang, Y., Liu, W., Wang, L.H., Choi, Y.W., Fulton, M., Fuchs, S., Shariati, K., Qiao, M., and Bernat, V., A broad-spectrum antimicrobial and antiviral membrane inactivates SARS-CoV-2 in minutes. *Advanced Functional Materials*, **2021**, 31(47): 2103477.
 91. Qian, L. and Sun, G., Durable and regenerable antimicrobial textiles: chlorine transfer among halamine structures. *Industrial & Engineering Chemistry Research*, **2005**, 44(4): 852-856.
 92. da Cruz Nizer, W.S., Inkovskiy, V., and Overhage, J., Surviving reactive chlorine stress: responses of gram-negative bacteria to hypochlorous acid. *Microorganisms*, **2020**, 8(8): 1220.
 93. Fukuzaki, S., Mechanisms of actions of sodium hypochlorite in cleaning and disinfection processes. *Biocontrol Science*, **2006**, 11(4): 147-157.
 94. Niki, E., Lipid peroxidation: physiological levels and dual biological effects. *Free Radical Biology and Medicine*, **2009**, 47(5): 469-484.

95. Dukan, S. and Touati, D., Hypochlorous acid stress in *Escherichia coli*: resistance, DNA damage, and comparison with hydrogen peroxide stress. *Journal of Bacteriology*, **1996**, 178(21): 6145-6150.
96. Li, L., Pu, T., Zhanel, G., Zhao, N., Ens, W., and Liu, S., New biocide with both N-chloramine and quaternary ammonium moieties exerts enhanced bactericidal activity. *Advanced Healthcare Materials*, **2012**, 1(5): 609-620.
97. Rahma, H., Asghari, S., Logsetty, S., Gu, X., and Liu, S., Preparation of hollow N-chloramine-functionalized hemispherical silica particles with enhanced efficacy against bacteria in the presence of organic load: synthesis, characterization, and antibacterial activity. *ACS Applied Materials & Interfaces*, **2015**, 7(21): 11536-11546.
98. Kawamura-Sato, K., Wachino, J.-i., Kondo, T., Ito, H., and Arakawa, Y., Reduction of disinfectant bactericidal activities in clinically isolated acinetobacter species in the presence of organic material. *Journal of Antimicrobial Chemotherapy*, **2008**, 61(3): 568-576.
99. Product performance test guidelines OCSPP 810.2000: general considerations for testing public health antimicrobial pesticides guidance for efficacy testing. **2018**, Environmental Protection Agency.
100. Fler, G., Stuart, M.C., Scheutjens, J.M., Cosgrove, T., and Vincent, B., *Polymers at interfaces*. **1993**, London: Chapman & Hall.
101. Philipp, B., Dautzenberg, H., Linow, K.-J., Kötz, J., and Dawydoff, W., Polyelectrolyte complexes—recent developments and open problems. *Progress in Polymer Science*, **1989**, 14(1): 91-172.
102. Meka, V.S., Sing, M.K., Pichika, M.R., Nali, S.R., Kolapalli, V.R., and Kesharwani, P., A comprehensive review on polyelectrolyte complexes. *Drug Discovery Today*, **2017**, 22(11): 1697-1706.
103. Bohidar, H., Dubin, P., Majhi, P., Tribet, C., and Jaeger, W., Effects of protein–polyelectrolyte affinity and polyelectrolyte molecular weight on dynamic properties of bovine serum albumin– poly (diallyldimethylammonium chloride) coacervates. *Biomacromolecules*, **2005**, 6(3): 1573-1585.
104. Kulkarni, A.D., Vanjari, Y.H., Sancheti, K.H., Patel, H.M., Belgamwar, V.S., Surana, S.J., and Pardeshi, C.V., Polyelectrolyte complexes: mechanisms, critical experimental aspects, and applications. *Artificial Cells, Nanomedicine, and Biotechnology*, **2016**, 44(7): 1615-1625.
105. Williams, D.E., Elder, E.D., and Worley, S.D., Is free halogen necessary for disinfection? *Applied and Environmental Microbiology*, **1988**, 54(10): 2583-2585.
106. Debiemme-Chouvy, C., Haskouri, S., and Cachet, H., Study by XPS of the chlorination of proteins aggregated onto tin dioxide during electrochemical

- production of hypochlorous acid. *Applied Surface Science*, **2007**, 253(12): 5506-5510.
107. Kloth, L.C., Berman, J.E., Laatsch, L.J., and Kirchner, P.A., Bactericidal and cytotoxic effects of chloramine-T on wound pathogens and human fibroblasts in vitro. *Advances in Skin & Wound Care*, **2007**, 20(6): 331-345.
 108. Gottardi, W., Klotz, S., and Nagl, M., Superior bactericidal activity of N-bromine compounds compared to their N-chlorine analogues can be reversed under protein load. *Journal of Applied Microbiology*, **2014**, 116(6): 1427-1437.
 109. Kaur, R. and Liu, S., Antibacterial surface design—contact kill. *Progress in Surface Science*, **2016**, 91(3): 136-153.
 110. Lan, T., Hanna, S.J., Sloan, G.P., Aylward, B.P., Welch, K.T., Shireman, D.E., Kavchok, K.A., and Hawes, C.L., Surface disinfectant with residual biocidal property. **2020**: US 10,834,922 B2.
 111. Demir, B., Cerkez, I., Worley, S., Broughton, R., and Huang, T.-S., N-Halamine-modified Antimicrobial Polypropylene Nonwoven Fabrics for Use against Airborne Bacteria. *ACS Applied Materials & Interfaces*, **2015**, 7(3): 1752-1757.
 112. Williams, J., Suess, J., Santiago, J., Chen, Y., WANG, I., and Wu, R., Antimicrobial Properties of Novel N-Halamine Siloxane Coatings. *Surface coatings international. Part B, Coatings transactions*, **2005**, 88(1): 35-39.
 113. Qiao, M., Application and Toxicity Assessment of Antimicrobial N-Halamines for Food Safety Controls. **2017**.
 114. Laingam, S., Frosco, S., Bull, R., and Humpage, A., In Vitro Toxicity and Genotoxicity Assessment of Disinfection by-products, Organic N-Chloramines. *Environmental and Molecular Mutagenesis*, **2012**, 53(2): 83-93.
 115. Demir, B., Broughton, R., Huang, T., Bozack, M., and Worley, S., Polymeric antimicrobial N-halamine-surface modification of stainless steel. *Industrial & Engineering Chemistry Research*, **2017**, 56(41): 11773-11781.
 116. Chien, H.-W. and Chiu, T.-H., Stable N-halamine on polydopamine coating for high antimicrobial efficiency. *European Polymer Journal*, **2020**, 130: 109654.
 117. Tian, Y., Cao, Y., Wang, Y., Yang, W., and Feng, J., Realizing ultrahigh modulus and high strength of macroscopic graphene oxide papers through crosslinking of mussel-inspired polymers. *Advanced Materials*, **2013**, 25(21): 2980-2983.
 118. Qiao, M., Liu, Q., Yong, Y., Pardo, Y., Worobo, R., Liu, Z., Jiang, S., and Ma, M., Scalable and rechargeable antimicrobial coating for food safety applications. *Journal of Agricultural and Food Chemistry*, **2018**, 66(43): 11441-11450.
 119. Zhang, Y., Choi, Y.W., Demir, B., Ekbataniamiri, F., Fulton, M.L., Ma, M., Schang, L.M., Purevdorj-Gage, L., and Qiao, M., Novel chlorine-extending

- polymer coating with prolonged antiviral activity against SARS-CoV-2. *Letters in Applied Microbiology*, **2022**, 75(5): 1346-1353.
120. Worley, S., Li, F., Wu, R., Kim, J., Wei, C., Williams, J., Owens, J., Wander, J., Bargmeyer, A., and Shirliff, M., A novel N-halamine monomer for preparing biocidal polyurethane coatings. *Surface Coatings International Part B: Coatings Transactions*, **2003**, 86: 273-277.
 121. McDaniel, C.S., Coating compositions having peptidic antimicrobial additives and antimicrobial additives of other configurations. **2013**: US 8,618,066 B1.
 122. Campoccia, D., Montanaro, L., and Arciola, C.R., A review of the biomaterials technologies for infection-resistant surfaces. *Biomaterials*, **2013**, 34(34): 8533-8554.
 123. Liang, J., Wu, R., Wang, J., Barnes, K., Worley, S., Cho, U., Lee, J., Broughton, R., and Huang, T., N-Halamine biocidal coatings. *Journal of Industrial Microbiology and Biotechnology*, **2007**, 34(2): 157-163.
 124. Cao, Z. and Sun, Y., Polymeric N-halamine latex emulsions for use in antimicrobial paints. *ACS Applied Materials & Interfaces*, **2009**, 1(2): 494-504.
 125. Kocer, H.B., Cerkez, I., Worley, S., Broughton, R., and Huang, T., N-Halamine copolymers for use in antimicrobial paints. *ACS Applied Materials & Interfaces*, **2011**, 3(8): 3189-3194.
 126. Séon, L., Lavallo, P., Schaaf, P., and Boulmedais, F., Polyelectrolyte multilayers: a versatile tool for preparing antimicrobial coatings. *Langmuir*, **2015**, 31(47): 12856-12872.
 127. Schlenoff, J.B., Dubas, S.T., and Farhat, T., Sprayed polyelectrolyte multilayers. *Langmuir*, **2000**, 16(26): 9968-9969.
 128. Sohn, B.-H., Kim, T.-H., and Char, K., Process-dependent photocatalytic properties of polymer thin films containing TiO₂ nanoparticles: dip vs spin self-assembly methods. *Langmuir*, **2002**, 18(21): 7770-7772.
 129. Shiratori, S.S. and Rubner, M.F., pH-dependent thickness behavior of sequentially adsorbed layers of weak polyelectrolytes. *Macromolecules*, **2000**, 33(11): 4213-4219.
 130. Kharlampieva, E. and Sukhishvili, S.A., Hydrogen-bonded layer-by-layer polymer films. *Journal of Macromolecular Science, Part C: Polymer Reviews*, **2006**, 46(4): 377-395.
 131. Yang, S.Y. and Rubner, M.F., Micropatterning of polymer thin films with pH-sensitive and cross-linkable hydrogen-bonded polyelectrolyte multilayers. *Journal of the American Chemical Society*, **2002**, 124(10): 2100-2101.

132. Liu, Y., Li, J., Cheng, X., Ren, X., and Huang, T., Self-assembled Antibacterial coating by N-Halamine Polyelectrolytes on A Cellulose Substrate. *Journal of Materials Chemistry B*, **2015**, 3(7): 1446-1454.
133. Denis-Rohr, A., Bastarrachea, L.J., and Goddard, J.M., Antimicrobial efficacy of N-halamine coatings prepared via dip and spray layer-by-layer deposition. *Food and Bioproducts Processing*, **2015**, 96: 12-19.

Chapter 2

Water-soluble Anionic Polychloramide Biocides Based on Maleic Anhydride Copolymers

In this chapter, a flexible synthetic platform of water-soluble, anionic polychloramides were prepared and could be applied to provide residual antimicrobial activity. The reaction of primary amines with poly (ethylene-alt-maleic anhydride), PEMA, followed by hydrolysis, is a convenient route to obtain PC3, a family of anionic, water-soluble polyamides. After chlorination with bleach, it can give bactericidal activities. In addition, the PEMA polymers can be grafted to the cellulose surfaces by the catalyst and reagent-free anhydride reactions. After chlorination, the PC3-treated filter paper has antimicrobial activity.

The data within this chapter were collected and summarized by me and wrote the first drafts of the paper. Dr. Tian and Prof. Hosseinidoust provided laboratory facilities and trained me in microbiological work. Dr. Fatona and Wu gave help with polymer characterization and training. Dr. Zhang guided the paper grafting work. Dr. Liu and Fefer provided funding and advice from an industrial perspective. Dr. Robert Pelton helped me analyze the data and re-write parts of the draft to the final version.

This chapter and supporting information are allowed to reprint as they appear on *Colloids and Surfaces B: Biointerfaces* with permission from Elsevier.

Water-soluble anionic polychloramide biocides based on maleic anhydride copolymers

Gaoyin He, Lei Tian, Ayodele Fatona, Xiao Wu, Hongfeng Zhang, Jun Liu, Michael Fefer, Zeinab Hosseinidoust, Robert H. Pelton.

Colloids and Surfaces B: Biointerfaces 2022, 215: 112487.

<https://doi.org/10.1016/j.colsurfb.2022.112487>

Water-Soluble Anionic Polychloramide Biocides Based on Maleic Anhydride Copolymers

Gaoyin He ^a, Lei Tian ^a, Ayodele Fatona ^a, Xiao Wu ^a, Hongfeng Zhang ^a, Jun Liu ^b, Michael Fefer ^b, Zeinab Hosseinidoust ^a, Robert H. Pelton ^{a *}

^a Department of Chemical Engineering, McMaster University, 1280 Main Street West, Hamilton, ON, L8S 4L7, Canada

^b Suncor AgroScience, 2489 North Sheridan Way, Mississauga, ON L5K 1A8, Canada

*Corresponding author: peltonrh@mcmaster.ca, Department of Chemical Engineering, McMaster University, 1280 Main Street West, Hamilton, ON, L8S 4L7, Canada

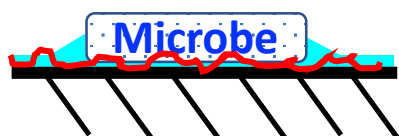
Keywords

antimicrobial polymers, grafted biocide, chloramides, cellulose grafting

Abstract

Our goal was to develop film-forming polymers to extend the antimicrobial lifetimes of cleaned and disinfected surfaces. Antimicrobial polymers were prepared by first reacting poly(ethylene-alt-maleic anhydride) with isopropylamine, partially consuming the anhydride groups, followed by hydrolysis to give water-soluble, highly anionic polyamide PC3. Chlorination with NaOCl gave PC3Cl with oxidative chlorine contents up to 9 wt%. Dried, 5 μm thick, PC3Cl films, gave log 4 reductions in the concentration of *Escherichia coli* or *Staphylococcus aureus* exposed to films. A unique feature of the maleic anhydride copolymer platform was the ability to form covalent grafts to surfaces via anhydride reactions. PC3 solution was impregnated into cellulosic filter paper, heated to form ester linkages with cellulose, followed by chlorination with sodium dichloroisocyanurate dihydrate giving grafted PC3Cl. The treated paper (0.3 wt% PC3Cl) gave a log 4 reduction of *E. coli* concentration in 30 min.

Graphical Abstract



Anionic Polychloramide
Contact Killing

Introduction

The Covid pandemic has emphasized the need for surface disinfection technologies applicable to both public and private spaces. [1] Dilute chlorine bleach ($\text{NaOCl} + \text{NaOH}$) is widely used as both a cleaner and a disinfectant because it is inexpensive, effective, and with care, is safe. [2] However, when dried on a surface, bleach offers little residual antimicrobial activity. HOCl is more volatile than water [3] leading to oxidant loss to the air. [4, 5] Our overall goal was to understand the factors influencing the efficacy of single component, film-forming, antimicrobial polymers that extend the non-infectious lifetime of bleach-cleaned surfaces. Specifically, we had many unanswered questions including the following. Should the polymer be hydrophobic or hydrophilic? Should the polymer be sufficiently water soluble to leave the surface when exposed to water? Should the polymer be anionic versus cationic? Must the biocide detach from the polymer to be effective or is direct contact between microbe and immobilized polymer sufficient? To answer these questions, we developed a first-generation antimicrobial polymer platform: that is a single component with no co-additives; that easily provides a range of hydrophobicities; that could be very water soluble yet easily grafted to surfaces; that can have appended two or more types of antimicrobial agents; and, that is based on the modification of a commercial polymer. This contribution describes the polymer synthesis, stability, antimicrobial behaviors. The following paragraphs outline our design philosophy.

The antimicrobial polymers literature is daunting with over 1000 publications in 2018. [6] Several good reviews help one understand the landscape. [6-11] Except for a few synthetic cationic polyelectrolytes [12] and antimicrobial peptides, [6] most commercial waterborne polymers are not antimicrobial. The literature mainly describes two synthetic routes to antimicrobial polymers: 1) copolymerization with a monomer that has or could be modified to have biocidal activity; and, 2) fixation of a biocide to an existing polymer. [13] We chose the second method as polymer modification should be an easier route to a library of biocidal polymers.

For choosing a biocide, Chapman *et al.* proposed that the commodity disinfection chemicals (i.e. not antibiotics) worked by one of three mechanisms: membrane disruption agents such as hydrophobically modified quaternary ammoniums; electrophilic agents including HOCl that attack protein sulfhydryl groups and other nucleophilic centers; and, free radical generating chemicals such as peroxides. [14] Of these, we chose oxidative chlorine agents since they seem the logical choice for our work when designing a polymer to be applied to surfaces after bleach disinfection.

Organic oxidative chlorine is most commonly present as nitrogen-chlorine bonds that can oxidize thiols and chlorinate proteins. Hydrolysis regenerates hypochlorous acid ($\text{R}_2\text{N-Cl} + \text{H}_2\text{O} \rightarrow \text{HOCl} + \text{R}_2\text{NH}$). The hydrolytic reactivity of $\text{R}_2\text{N-Cl}$ bonds is imides > amides > primary amines. [13] [15] [16] We have chosen chloramides and chlorimides, as the biocidal agents for our research.

Poly(ethylene-alt-maleic anhydride), PEMA, a commercially available polymer, was chosen as the supporting polymer. The succinic anhydride moieties on PEMA can be modified in organic solvents to give pendent amides, imines, and esters in high yields. Whereas the anhydride groups on PEMA hydrolyze in water to give two carboxylic acid groups on every repeat unit, giving a polymer with the same acid content as polyacrylic acid. PEMA offers enormous flexibility. [17-19] Residual anhydride groups can be crosslinked to give insoluble films or used to graft to surfaces such as cellulose. [20] By using a series of alkyl amines it is possible to systematically vary the overall hydrophobicity.

Figure 2-1 summarizes our approach for this contribution. A near quantitative reaction with isopropylamine produces PC3, a polyamide with at least one carboxylic acid group on every repeat unit. Exposure of PC3 to NaOCl partially converts amides to the corresponding chloramides, giving the polychloramide PC3Cl. As the first contribution from this project, the focus of this paper is on one polymer, PC3Cl, where 96% of the anhydride groups were converted to N-isopropylamides plus carboxylic acids. The following paragraphs highlight the most relevant literature.

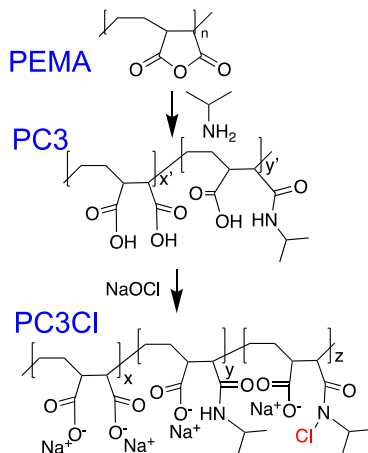


Figure 2-1 The conversion of PEMA to PC3 and PC3Cl.

We have found only a few examples of synthetic anionic, water-soluble antimicrobial polymers. Possibly the closest example to our work was a recent publication from Auburn University. [21] They reported anionic copolymers of acrylic acid and an amide monomer with a pendant dimethylhydantoin moiety which was linked via one of the methyl groups leaving both the imide and amide hydantoin nitrogens available for chlorination. Cotton fabric was impregnated with the polymer and the authors stated “To the best of our knowledge, these are the most efficacious results in terms of contact times ever observed for an antibacterial coating, N-halamine or otherwise.” They proposed the treated cotton would be a single-use product since the copolymer was not grafted to the cellulose. We will see below that PC3 will graft to cellulose without catalysts or other reagents.

A completely different concept was a polysulfonic acid copolymer where low molecular weight, cationic amphiphilic counterions were the microbiocidal agents. [22] Although not a polymer, Meyers' anionic amphiphilic dendrimers with carboxylic acids on one end and hydrophobic chains on the other, highlights that not all biocides must be cationic. [23]

Wang's 2019 paper describes a copolymer of acrylic acid and an allylic derivative of dimethylhydantoin, coupled through the imide nitrogen. [24] The polymer composition was not given, and the oxidative chlorine contents were low possibly reflecting the difficulty in copolymerizing allylic monomers. Nevertheless, their polymers did kill microbes. Summarizing the literature, we have found very few examples of synthetic, anionic, water-soluble antimicrobial polymers.

Reported herein are the synthesis, characterization, solubility, chemical stability, and antimicrobial activity of PC3Cl. In addition, PC3 was grafted to filter paper and then chlorinated and evaluated for antimicrobial activity.

Experimental

Materials. Isopropylamine ($\geq 99\%$), poly(ethylene-alt-maleic anhydride) (PEMA, average Mw 100–500 kDa), sodium thiosulfate ($\text{Na}_2\text{S}_2\text{O}_3$, $>99\%$), N, N-Dimethylformamide anhydrous (DMF, 99.8%), sodium hypochlorite (NaOCl, 10–15%), sodium dichloroisocyanurate dihydrate (NaDCC), phosphate-buffered saline (PBS) buffer, Luria-Bertani (LB) broth, LB agar, and 5,5'-dithiobis(2-nitrobenzoic acid) (DTNB, 99%), and L-cystine ($\geq 98\%$) were obtained from Sigma-Aldrich (Canada) and used as received. The concentration of sodium hypochlorite was determined by the iodometric titration method. [25] Starch solution stabilized for iodometry was from Thermo Fisher Scientific. MilliQ water ($\sim 18.2 \text{ M}\Omega \text{ cm}$) was purified by an EMD Millipore Milli-Q[®] Advantage A10 System (Thermo Scientific).

PC3 Synthesis. PEMA (0.5 g, 4 mmol anhydride groups) was dissolved into 10 mL anhydrous DMF and stirred at room temperature. Then, isopropylamine (0.24 g, 4 mmol) in 2 mL DMF was added into the PEMA solution. The reaction mixture was stirred overnight at room temperature. Thereafter, 5 mL 0.01 M HCl was added to stop the reaction and the solution was transferred to a 12-14 kDa dialysis tube against 1 L 0.01 M HCl for 6 h. Finally, the PC3 solution was dialyzed against deionized water for 36 h and the modified polymer was then recovered by freeze-drying.

PC3 Chlorination to Give PC3Cl. PC3 was chlorinated with an aqueous NaOCl solution. Typically, 5 mL PC3 solution (3 g/L) and 10 mL 400 mM NaOCl were mixed in a vial and the solution pH was adjusted to 10.5. Thereafter, the vial was immersed in a 90 °C water bath for 2 h. The PC3Cl was dialyzed in cellulose membrane tubes against 4 L water with stirring for 5 h to remove excess NaOCl and salt. The chlorinated polymers PC3Cl were isolated by freeze-drying and stored at a 4 °C fridge. For the chlorinated polymer, it can be named as PC3Cl.

Chlorine Contents by Iodometric Titration. To determine oxidative chlorine (Cl^+) content of PC3Cl, a standard KI/starch/thiosulfate titration method was employed. [25] Typically, 0.1 g KI was added to 5 mL 1 g/L PC3Cl (~5 mg) solution and the solution pH was adjusted to around 3. Sodium thiosulfate was performed to titrate polymers after adding 2 mL 1% starch indicator. The weight percentage of oxidative Cl^+ in the polymers was calculated using the following formula: where C is the concentration (mol/L) and V volume (L) of sodium thiosulfate in the titration, and w is the mass of the chlorinated PC3Cl polymer (g). Sodium dichloroisocyanurate dihydrate (NaDCC) was used to calibrate sodium thiosulfate concentration – see **Figure S2-1**.

$$\text{Cl} (\%) = \frac{C \times V \times 35.45}{2 \times w} \times 100 \quad \text{Equation 2-1}$$

Chlorine Contents of Dry PC3Cl Film by the TNB Assay. The iodometric titration assay was not suitable for chlorine analysis in small film samples because the amounts of active chlorine in small film samples are too small to be measured by the titration method. Instead, the chlorine contents of PC3Cl films were measured by the TNB assay which is based on the consumption of TNB which adsorbs light at 412 nm. [26]

TNB solutions were prepared by mixing 2 equivalents of 4 mM cysteine (Cys) to 1 equivalent of 2 mM 5,5'-dithiobis(2-nitrobenzoic acid) (DTNB) in a 10 mM pH 7 phosphate buffer solution. The highly colored yellow solutions (TNB) were stored at 4 °C overnight. Dry PC3Cl film samples were dissolved into 6 mL of 10 mM phosphate buffer. Then, equal volumes of TNB solution and PC3Cl solution were mixed, and the absorbance was measured at 412 nm. The chlorine contents were obtained from the standard plot of absorbance versus the known chlorine concentration from NaDCC solutions – see **Figure S2-2**.

Polymer Characterization. ^1H NMR spectra of our polymers, in D_2O , were measured with a Bruker NEO 600 spectrometer (600 MHz). Carbon/nitrogen ratios were determined by elemental analysis, UNICUBE in C/H/N/S mode, Elementar, (Langensfeld, Germany). Each sample was measured three times.

Conductometric Titration. Conductometric titration of carboxylic groups was performed at room temperature employing Mantech Inc. Benchtop Titrator Model, MT-10. In detail, a freeze-dried sample PC3 or PC3Cl (dry mass ~10 mg) was added to 50 mL 1 mM NaCl solution and the initial pH was adjusted below 3.0 by adding 1 M HCl. Then, 0.1 M NaOH solution was used to titrate the sample and each sample was titrated in triplicate. The volume of base consumed by the weak carboxyl groups was determined by the points of intersection of three trendlines going through the linear sections of the titration curve.

Cloud-point Temperatures. The transmittance of PC3 and PC3Cl in 1 mM NaHCO_3 solution at 500 nm was recorded with a DU800 UV-Vis spectrophotometer (Beckman Coulter) as a function of temperature. The transmittance values were normalized by

dividing the results by the values at low temperatures and pH values sufficiently high to ensure solubility.

PC3Cl Film Formation. Typically, 200 μL 0.4 wt/v% PC3Cl in 1 mM NaHCO_3 solution was dropped on glass slides to form a circular and transparent polymer film and dried around 3 h in a humidity chamber (ESPEC) at 35 $^\circ\text{C}$ and 40% relative humidity. Photographs of the dried films are shown in **Figure S2-3** and ImageJ was used to calculate the area of the films. Four replicates were prepared for each thickness and the standard deviation ranged from 5% to 7% of the mean thickness.

Photostability Test of PC3Cl Films. A Heliospectra LED Grow Light - RX30 (Spectral distribution from 370 nm to 750 nm, 5700K white) was used to evaluate the light stability of PC3Cl deposit films. PC3Cl films were exposed at a distance of 40 cm from the light to the film, corresponding to an intensity of 0.35 W/cm^2 .

Gel Permeation Chromatography (GPC). Freeze-dried PC3Cl was dissolved in 1 \times PBS with 0.05% sodium azide and the filtered solution was injected into an Agilent 1260 Infinity II GPC with an Agilent 1260 infinity RI detector. The GPC was fitted with a Superose 6 column 10/300 GL (GE Healthcare). The column was calibrated using polyethylene glycol (PEG) standards and the flow rate was 0.5 mL/min.

Dry Film Antimicrobial Assay. The antibacterial experiments were carried out with gram-negative bacteria *E. coli* 13127 and gram-positive bacteria *Staphylococcus aureus* MZ100. The *S. aureus* MZ100 was generously provided by Dr. Michael Surette from Hamilton Health Sciences McMaster University and the *E. coli* 13127 was purchased from the German Collection of Microorganisms and Cell Cultures GmbH. 10 μL bacterial suspensions (*S. aureus* and *E. coli*) were incubated in sterilized LB broth at 37 $^\circ\text{C}$ overnight and then were diluted to the appropriate concentration (around 10^7 CFU/mL) with 990 μL sterilized PBS buffer. Next, 10 μL of *E. coli* PBS suspension was spotted on the center of the circular PC3Cl dried films, supported on glass slides. The spotted films were sealed in sterilized Petri dishes and incubated at room temperature. After the contact time, the bacteria were washed with 200 μL sterile 0.1 N $\text{Na}_2\text{S}_2\text{O}_3$ solution to neutralize the unreacted active chlorine. Although this neutralization strategy has been reported by others, [27, 28] we confirmed that there was no loss of live bacteria due to this treatment – see **Table S2-2**. As an additional precaution, each round of experiments included polychloramide-free controls that did undergo 0.1 N $\text{Na}_2\text{S}_2\text{O}_3$ neutralization.

After chlorine neutralization, the suspension was then serially diluted (10^1 , $\times 10^2$, $\times 10^3$, $\times 10^4$, $\times 10^5$, $\times 10^6$) and then were plated on nutrient LB agar plates and incubated at 37 $^\circ\text{C}$ overnight before colony counting. The concentrations of colony-forming units (CFU/mL) were determined in triplicate and all the standard deviations were less than the mean and most were less than 40% of the mean – see **Figure S2-4**.

PC3 Fixation on Filter Paper. In a typical impregnation experiment, 3 mL of 2 wt% PC3 solution at pH 4 was added dropwise across the surface of a Whatman filter paper, Grade 2, (~ 2 g) over about 2 min. The wet filter paper was then placed between two

blotter papers and rolled with two passes using a TAPPI-standard brass couch roller (102 mm diameter and 13 kg mass) to remove excess polymer solution. The filter paper was weighed before impregnation and after pressing to facilitate calculating the mass of the applied polymer. The impregnated filter paper was cured between two blotting papers on a speed dryer (Labtech Instruments Inc.) at 150 °C for 10 min. The grafted filter paper was washed with 1 mM NaCl solution.

Chlorination and Titration of PC3 Grafted Papers. The weighed dry PC3 grafted paper was soaked in NaDCC solution, unless otherwise stated, at pH 6 and room temperature. In detail, the PC3-coated paper was cut in 2.54 × 2.54 cm pieces and chlorinated by soaking in 30 mL aqueous NaDCC solution at room temperature for 24 h. Subsequently, the chlorinated paper was immersed and washed thoroughly in 2 L distilled water to remove free chlorine for 1 h twice. The resulting wet papers were pressed between two blotters to absorb excessive water. Whatman filter papers were applied as control samples.

The oxidative chlorine content of the chlorinated PC3-impregnated paper was quantified by the iodometric/thiosulfate titration method. Typically, 0.4 g paper was soaked in 20 mL water and 0.5 g KI with H₂SO₄ to adjust pH < 3. Then, samples were vortexed at room temperature for 30 min in sealed 80 mL sterile plastic cups (Starplex Scientific). Next, 2 mL of a 1% starch solution was added to the above solution and then the solution was titrated by 8.86 mM Na₂S₂O₃ solution.

Contact Killing against Bacteria. The biocidal activities of the PC3Cl grafted paper against *E. coli* were evaluated by a “sandwich test”. [21] In a typical experiment, 25 µL *E. coli* bacterial suspension (10⁷~10⁸ CFU/mL) was added to the center of a pair of dry paper squares (2.54 × 2.54 cm). Both paper swatches were pressed by a sterile weight to ensure tight contact. After 30 min of contact, surfaces were transferred to a tube with 5.0 mL 0.02 mol/L sodium thiosulfate solution to quench excessive chlorine of paper samples, and then solutions were vigorously vortexed for 2 min to recover the adhered bacteria into media. The recovered bacteria suspensions were serially diluted with ×1 PBS buffer and 50 µL of each dilution was plated onto LB agar plates in triplicate. The plates were incubated at 37 °C for 24 h, overnight. Control samples include pure filter papers and PC3 coated papers. The corresponding detection limit (1 CFU, no dilution) was 4000 CFU/mL.

Results and Discussion

Polymer Modification and Characterization. The focus of this work is the synthesis, characterization, and properties of antimicrobial polymer PC3Cl – see **Figure 2-1**. The extent of amide formation in the first step, giving PC3, and the degree of chlorination in the second step can be varied potentially giving a wide range of structures. ¹H NMR

spectra of hydrolyzed PEMA, PC3 and PC3Cl are given in **Figure S2-5** in the supplementary material. Herein we focus on a single PC3 where most of the amides are substituted (i.e. $y' = 0.96$, see **Figure 2-1**). Conductometric titration of PC3 gave a carboxylic acid content of PC3 was 5.64 meq/g which also corresponds to $y' = 0.96$. The C/N ratio for PC3 is 8.3 which corresponds to $y' = 0.89$. We have the most confidence in the NMR and titration value of $y' = 0.96$.

PC3Cl was prepared by treatment of PC3 with NaOCl at pH 10.5. The chlorine contents of products after dialysis were determined by iodometric titration. **Figure 2-2** shows the influences of chlorination time and NaOCl concentration on the mass fractions of Cl in PC3Cl. The ongoing work focuses on two polymers PC3Cl2 (2h, 30 °C) and PC3Cl9 (2h, 90 °C) where the final number in the name, is the chlorine mass fraction.

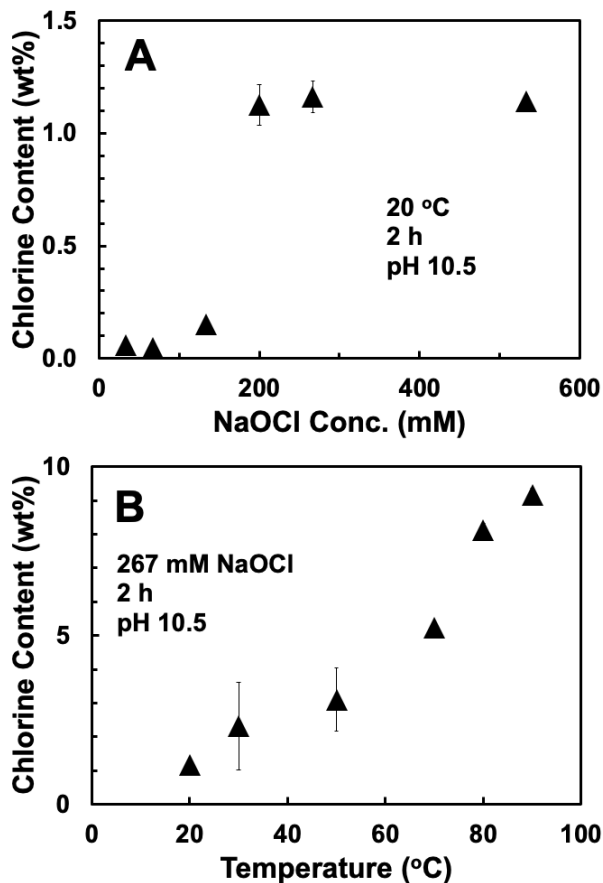


Figure 2-2 The influence of chlorination conditions on the mass fractions of Cl in PC3Cl.

The polymer compositions of PC3, PC3Cl2, and PC3Cl9 were determined by a combination of NMR, atomic composition, and active chlorine titration. The details are given in **Table S2-1** and the associated text in the SI file. In terms of the coefficients shown in **Figure 2-1**, PC3 ($x' = 0.04$, $y' = 0.96$), PC3Cl2 ($x = 0.170$, $y = 0.695$, $z = 0.135$), and

PC3C19 ($x=0.200$, $y=0.220$, $z=0.580$). Based on these compositions, 14-17% of amides groups were lost with chlorination, possibly by hydrolysis. The hydrolysis of polyacrylamide during chlorination has been reported. [29, 30] **Figure 2-3** compares the GPC curves of PC3 to that of the chlorination product PC3C19. The weight average molecular mass decreased from 118 to 18 kDa as a result of chlorination with 267 mM.

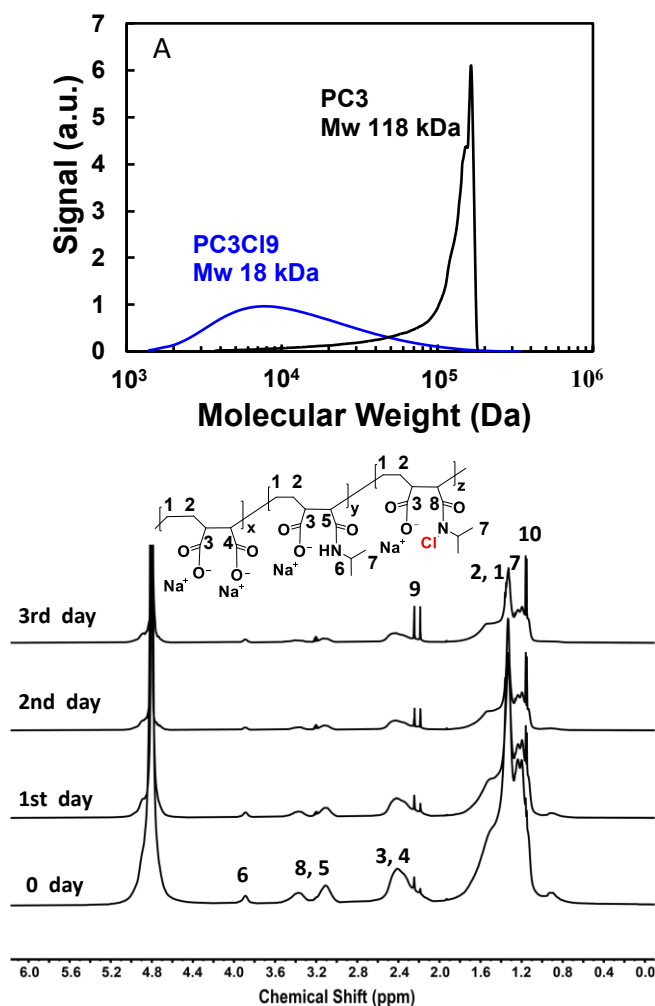


Figure 2-3 Left) Molecular weight distributions for PC3, and PC3C19 dissolved in PBS + 0.05% sodium azide. The molecular weight assignments were based on polyethylene glycol standards. Right) The proton NMR of PC3C19 in D_2O over 3 days of aging at room temperature.

To further evaluate polychloramide stability, PC3C19 was dissolved in D_2O and proton NMR spectra were recorded over 3 days. The spectra, shown in **Figure 2-3** reveal the emergence of fine lines indicating the presence of low molecular weight degradation products. The peak labeled 10 indicates methyl groups likely originating from isopropylamine released by hydrolysis.

Whereas PC3Cl aqueous solutions experience degradation, dried PC3Cl is more stable. Freeze-dried PC3Cl9 shows 20% chlorine loss over 40 days of dark storage at 4 °C, see **Figure 2-4A**. If a dry film of polychloramide is going to protect a surface exposed to air and light, the dry film the loss rate of oxidative chlorine must be low until the surface is challenged by a wet microbe. **Figure 2-4B** shows film chlorine contents as a function of aging time. There was little chlorine loss over 5 days. Chlorine loss was only slightly faster when illuminated. For applications such as floors in public spaces, the polychloramide films should retain activity until it is replaced in the next cleaning cycle. Note that the Cl contents of the films were measured by the TNB method because masses of polymer were too low for iodometric titration.

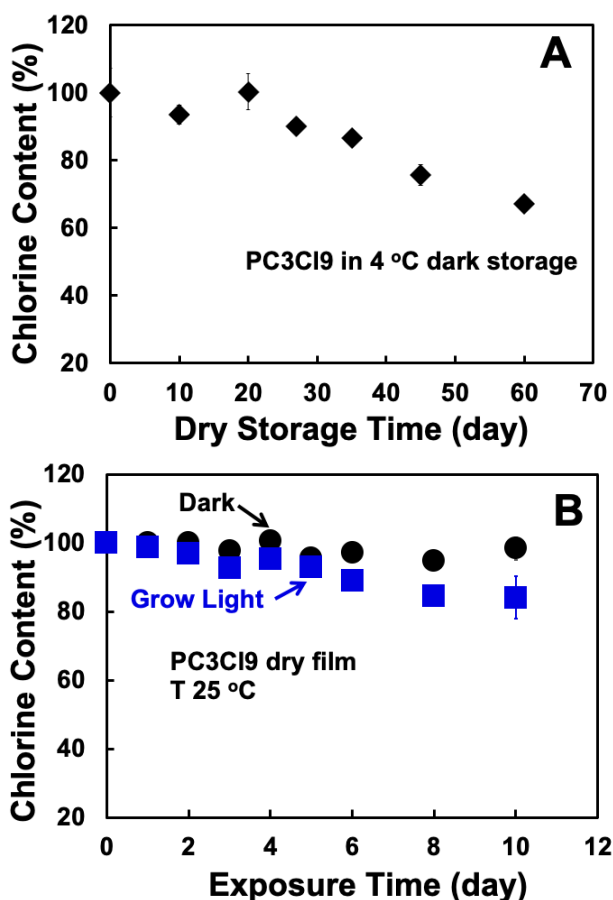


Figure 2-4 Chlorine contents of PC3Cl9, as a percentage of the initial content, as functions of aging time: **A**) as a dry solid, 4 °C in dark; and, **B**) as thin films in dark and under a Heliospectra RX30 grow light.

To summarize, in our view, the structures of the starting PEMA, and the amide derivative, PC3, are very well defined. By contrast, we consider the x-y-z values for the chlorinated products more approximate because of side reactions during chlorination. We speculated

that amide hydrolysis and chain scission are the major side reactions of chlorination. Note that chlorinated products were dialyzed and then freeze-dried to remove most of the low molecular weight oxidation products before use. The purified freeze-dried chlorinated polymers either as powders in the freezer or films on a surface have reasonable stability whereas aqueous solutions degrade in days.

PC3 and PC3Cl Solubility. Polychloramides are more hydrophobic than the parent polyamides. [25] The optical transmittance at 500 nm of PC3 and PC3Cl9 solutions were measured as functions of pH and temperature – see **Figure 2-5**. The highly carboxylated PC3 is soluble over the whole pH range investigated. However, at pH 2 where it is not ionized, PC3 has a cloud point temperature of 25 °C. The more hydrophobic PC3Cl9 was insoluble at pH values below 5.

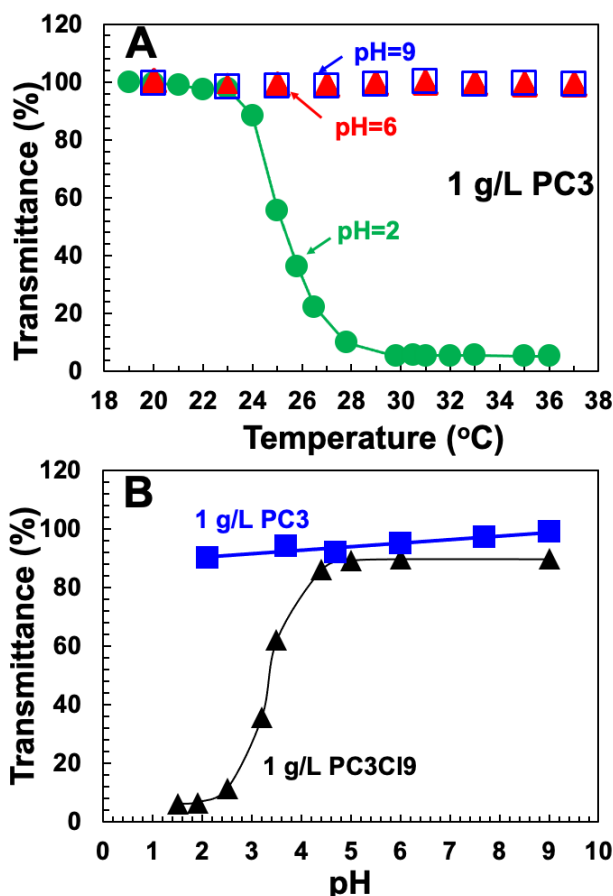


Figure 2-5 Transmittance of PC3 and PC3Cl9 solutions at 500 nm as functions of temperature and pH.

Dry Film Antimicrobial Properties. We developed the following assay to determine if dried PC3Cl films would kill bacteria that happen to land on the film. Gram-negative *E.*

coli 13127 and gram-positive *S. aureus* MZ100 were selected as the representative bacteria strains. To prepare the antimicrobial polymer films, 200 μL of PC3Cl solution was dropped onto a clean glass slide and allowed to dry, forming circular films – photographs are shown in **Figure S2-3**. The average thicknesses of the dry PC3Cl films were calculated from their surface areas assuming the polymer density was 0.9 g/mL. A 10 μL drop of bacterial suspension was spotted on each dry polymer film and the drops spontaneously spread to cover the entire polymer films, without further spreading. After a fixed contact time, the polymer and bacteria were washed from the supporting slide with 0.1 N $\text{Na}_2\text{S}_2\text{O}_3$ which served to deactivate the residual chlorine. The bacteria concentration was determined by conventional plating and counting.

The antimicrobial results of dry films are summarized in **Figure 2-6**. The bacteria concentrations, expressed as $\log(\text{CFU}/\text{mL})$, were calculated as the total CFU washed from the slide divided by 10 μL , the volume of bacteria suspension originally applied to the antimicrobial film. The corresponding detection limit was 100 CFU/mL. Upon exposure to the bacteria suspension, the thin water-soluble PC3Cl films swell and possibly dissolve. However, visual inspection revealed that the free water evaporated in about 30 min after bacteria spotting. The antimicrobial polymer films are thin and therefore it is reasonable to assume that the total available oxidative chlorine increased linearly with the dry PC3Cl film thickness. **Figure 2-6A** shows the influence of film thickness. For both *E. coli* and *S. aureus*, the thicker the PC3Cl film, the greater the CFU reduction. Disinfection of *S. aureus* requires higher concentrations of chloramide biocides compared to *E. coli*. Figure S6 in the Supplementary Materials section compares scanning electron microscope images of bacteria before and after being exposed to PC3Cl9 films. There are some indications of macroscopic damage to bacteria exposed to PC3Cl9 films.

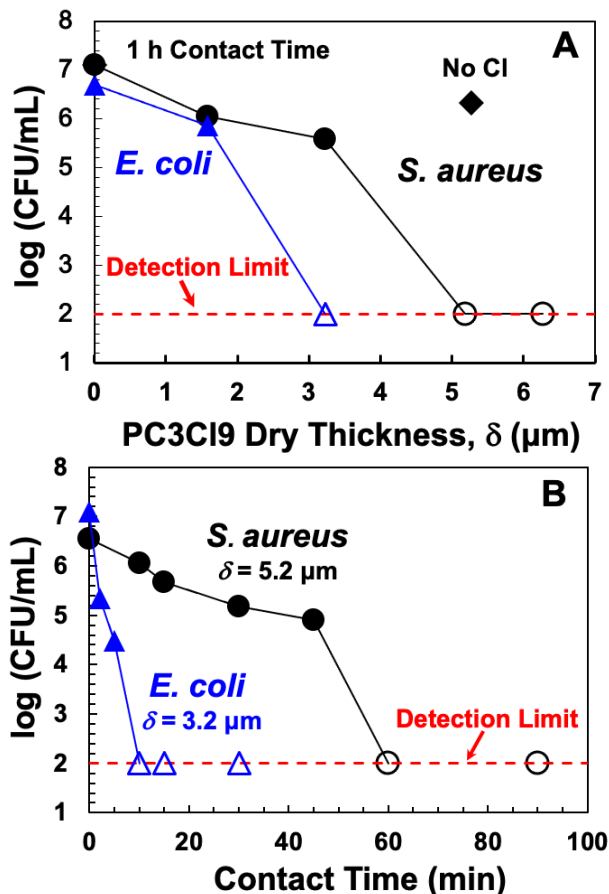


Figure 2-6 (A) The influence of PC3Cl9 film thickness, δ , (A) or contact time (B) on the concentrations of *E. coli* and *S. aureus*. The “No Cl” result corresponds to PC3 containing no Cl. The open symbols represent conditions where no colonies were observed and were plotted at the detection limit.

Figure 2-6B shows the influence of contact time. As expected, the longer the exposure time, the greater the CFU reductions. These results support the concept that a dried polychloramide film will kill wet bacteria that land on the films. However, from a mechanistic perspective, these are poorly defined experiments. The available water and thus all concentrations are unknown functions of time, temperature, and relative humidity. Indeed, we do not know if the PC3Cl films completely dissolved into the bacteria suspension before the water evaporated. Nevertheless, these results demonstrate the concept of a dry, thin polychloramide film giving residual antimicrobial activity.

Bacterial Killing by PC3Cl Grafted on Paper. The following describes the grafting PC3 to cellulose filter paper, and the assessment of bacterial killing efficacy after chlorination. In another project, we have shown that paper impregnated with hydrolyzed PEMA will form ester linkages with cellulose if dried and heated above 150 °C for 10 min.[20] The

reaction mechanism involves the regeneration of anhydride group intermediates from succinic acid moieties in the PC3 chain. Those anhydrides in contact with cellulose react to form esters with cellulosic hydroxyl groups. [31-33] Four percent of the repeat units on PC3 are succinic acid moieties that can revert to anhydrides with heating, leading to grafting. Based on the number average chain length of the starting PEMA, 4% corresponds to a potential 68 grafting sites per chain.

Initially, we employed NaOCl as the chlorinating agent, however, the filter paper decomposed to a suspension of individualized pulp fibers when treated with NaOCl solution at 90 °C. Therefore, we employed sodium dichloroisocyanurate dihydrate (NaDCC) at room temperature as the chlorinating agent, leaving the paper intact. **Figure 2-7** shows the influence of chlorination pH and the PC3 content on the oxidative chlorine contents in the paper. Lower pH chlorination was the most effective and the active chlorine content of the paper was proportional to the PC3 contents. The observation that **Figure 2-7B** is linear suggests that the chlorine content of the grafted polymer, PC3Cl, was independent of the content of PC3 in the paper before chlorination. The mass fraction of Cl in PC3Cl polymer was 7.5% based on the slope in **Figure 2-7B**.

The bactericidal activity of PC3Cl grafted on paper was measured with a sandwich assay where the bacterial suspension is spotted between two paper sheets. **Figure 2-8** shows the *E. coli*. concentration as a function of the mass fraction of PC3 in the filter paper. The detection limit of 3.6 log(CFU/mL), corresponding to a log reduction >3, was achieved with a polymer content (mass polymer/mass cellulose) of 0.3% and a 30 min exposure time. The blue PC3 results correspond to unchlorinated paper. This example illustrates the utility of PEMA-based chloramide polymers that can graft onto cellulose.

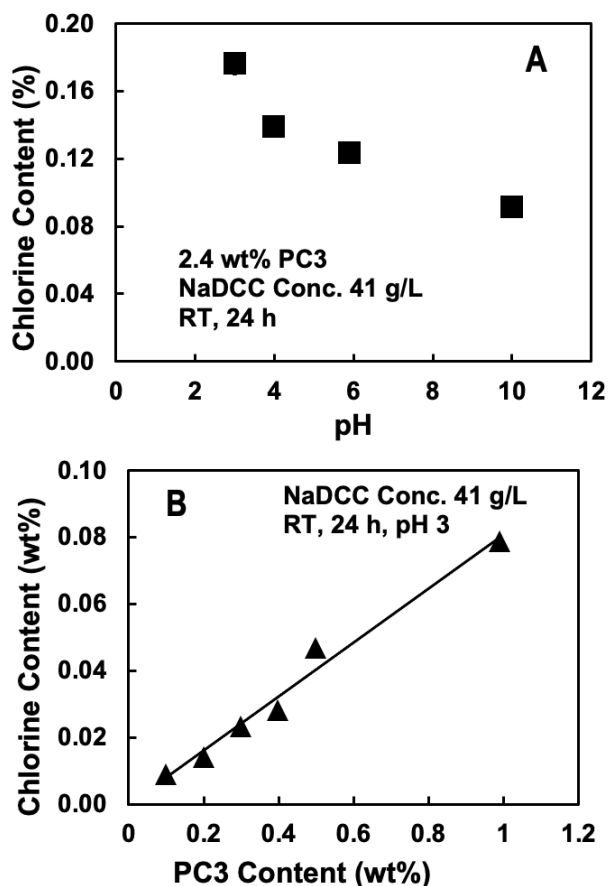


Figure 2-7 The influence of chlorination pH (A) and the PC3 content, before chlorination (B) on the mass fraction of oxidative chlorine in the filter paper. NaDCC is chlorinating agent sodium dichloroisocyanurate dihydrate.

Many publications describe antimicrobial paper based on many approaches including biocide-loaded polymer micelles loaded, [34] silver nanoparticles, [35] guanidine polymers, [36] and, photocatalytic oxidation [37]. Additionally, there are many commercial papers or nonwoven fabric wipes that are impregnated with antimicrobial agents. Our results, described above, serve as a proof-of-concept demonstrating the easy grafting of PC3 to cellulose and subsequent chlorination to form antimicrobial paper. No comparisons have been made with other antibacterial paper technologies. Beyond lignocellulosic surfaces, the maleic acid/anhydride groups in PC3 will graft to any surface bearing alcohol or primary amine groups [19].

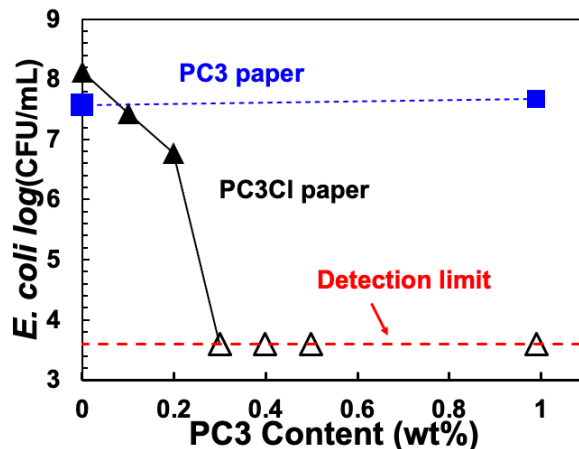


Figure 2-8 *E. coli* concentration after 30 min contact with PC3Cl treated filter paper. The PC3 result corresponds to filter paper before chlorination.

Conclusions

The reaction of primary amines with poly (ethylene-alt-maleic anhydride), PEMA, followed by hydrolysis, is a convenient route to PC3, a family of anionic, water-soluble polyamides that can be chlorinated with bleach to give bactericidal properties. Although our goals were to develop a flexible synthetic platform for mechanistic studies linking antimicrobial activity to polymer structure, this work has shown that anionic water-soluble polychloramides could be used to provide residual antimicrobial resistance on bleach disinfected surfaces such as floors in public spaces. The specific conclusions are:

1. PC3 with 96% of the PEMA anhydrides converted to the corresponding isopropylamides plus carboxylic acid groups (**Figure 2-1**), was water soluble from pH 2-11 whereas PC3Cl with 58 % of the amides chlorinated was water soluble only if the pH > 5, reflecting the increased hydrophobicity of the chloramide groups.
2. Aggressive chlorination conditions, (90 °C, 2h, 267 mM NaOCl, and pH 10.5) converted 73% of the remaining amides to chloramides (dsCl in **Table S2-1**) giving PC3Cl9 with a Cl mass fraction of 9.2%. However, these conditions cause some polymer chain scission and a 17% loss of amide groups.
3. Purified (dialyzed followed by freeze-drying) PC3Cl9 showed good storage stability. Furthermore, cast dry films of PC3Cl films showed good stability in the dark and under grow-light exposure.
4. Thin (5.2 μm) PC3Cl9 films can kill 5 log CFU of soil-free suspensions of *E. coli* and *S. aureus* within 60 min showing PC3Cl9 is an effective anionic, water-soluble antimicrobial polymer.

5. A unique feature of the PEMA polymers is the ability to graft to surfaces as demonstrated by the catalyst and reagent-free grafting of PC3 onto cellulose filter paper. After chlorination, the PC3-treated paper was antibacterial.

Supporting Information

The file includes the sodium thiosulfate calibration curve, the calibration curve for the TNB oxidative chlorine assay, photographs of polychloramide films on glass coverslips, standard deviations of bacteria CFU/mL versus the mean, and NMR spectra with peak assignments.

Acknowledgments

We thank the Natural Sciences and Engineering Research Council of Canada (NSERC) and Suncor Energy for funding this project. We thank Mr. Chaochen Song for assistance with the PC3 grafting to filter paper and Mr. Alexander Jesmer for performing the GPC measurements. Prof. Ryan Wylie is thanked for giving access to his GPC.

References

1. Kampf, G., Todt, D., Pfaender, S., and Steinmann, E., Persistence of coronaviruses on inanimate surfaces and their inactivation with biocidal agents. *Journal of Hospital Infection*, **2020**, 104(3): 246-251.
2. Rutala, W.A. and Weber, D.J., Guideline for disinfection and sterilization in healthcare facilities, 2008 Update: May 2019. **2019**, Centers for Disease Control (CDC) p. 1-163.
3. Wojtowicz, J.A., Dichlorine monoxide, hypochlorous acid, and hypochlorites. *Kirk-Othmer Encyclopedia of Chemical Technology*, **2004**, 8: 544-581.
4. Odabasi, M., Halogenated volatile organic compounds from the use of chlorine-bleach-containing household products. *Environmental Science & Technology*, **2008**, 42(5): 1445-1451.
5. Wong, J.P.S., Carslaw, N., Zhao, R., Zhou, S., and Abbatt, J.P.D., Observations and impacts of bleach washing on indoor chlorine chemistry. *Indoor Air*, **2017**, 27(6): 1082-1090.
6. Ergene, C., Yasuhara, K., and Palermo, E.F., Biomimetic antimicrobial polymers: recent advances in molecular design. *Polymer Chemistry*, **2018**, 9(18): 2407-2427.
7. Kenawy, E.-R., Worley, S., and Broughton, R., The chemistry and applications of antimicrobial polymers: a state-of-the-art review. *Biomacromolecules*, **2007**, 8(5): 1359-1384.
8. Hui, F. and Debiecme-Chouvy, C., Antimicrobial N-halamine polymers and coatings: A review of their synthesis, characterization, and applications. *Biomacromolecules*, **2013**, 14(3): 585-601.
9. Ganewatta, M.S. and Tang, C., Controlling macromolecular structures towards effective antimicrobial polymers. *Polymer*, **2015**, 63: A1-A29.
10. Kaur, R. and Liu, S., Antibacterial surface design—contact kill. *Progress in Surface Science*, **2016**, 91(3): 136-153.
11. Dong, A., Wang, Y.-J., Gao, Y., Gao, T., and Gao, G., Chemical insights into antibacterial N-halamines. *Chemical Reviews*, **2017**, 117(6): 4806-4862.
12. Westman, E.-H., Ek, M., Enarsson, L.-E., and Wågberg, L., Assessment of antibacterial properties of polyvinylamine (PVAm) with different charge densities and hydrophobic modifications. *Biomacromolecules*, **2009**, 10(6): 1478-1483.
13. Worley, S.D. and Wojtowicz, J.A., N-Halamines. *Kirk-Othmer Encyclopedia of Chemical Technology*, **2004**, 13: 98-122.

14. Chapman, J.S., Diehl, M.A., and Lyman, R.C., Biocide susceptibility and intracellular glutathione in *Escherichia coli*. *Journal of Industrial Microbiology*, **1993**, 12(6): 403-407.
15. Qian, L. and Sun, G., Durable and regenerable antimicrobial textiles: Synthesis and applications of 3-methylol-2,2,5,5-tetramethyl-imidazolidin-4-one (MTMIO). *Journal of Applied Polymer Science*, **2003**, 89(9): 2418-2425.
16. Akdag, A., Okur, S., McKee, M.L., and Worley, S., The stabilities of N–Cl bonds in biocidal materials. *Journal of Chemical Theory and Computation*, **2006**, 2(3): 879-884.
17. Chitanu, G.-C., Zaharia, L.-I., and Carpov, A., Analysis and characterization of maleic copolymers. *International Journal of Polymer Analysis and Characterization*, **1997**, 4(1): 1-20.
18. Rätzsch, M., Alternating maleic anhydride copolymers. *Progress in Polymer Science*, **1988**, 13(4): 277-337.
19. Pompe, T., Zschoche, S., Herold, N., Salchert, K., Gouzy, M.-F., Sperling, C., and Werner, C., Maleic anhydride copolymers a versatile platform for molecular biosurface engineering. *Biomacromolecules*, **2003**, 4(4): 1072-1079.
20. Zhang, H., Bicho, P., Doherty, E.A., Riehle, R.J., Moran-Mirabal, J., and Pelton, R.H., High-yield grafting of carboxylated polymers to wood pulp fibers. *Cellulose*, **2021**, 28: 7311-7326.
21. Zhang, S., Demir, B., Ren, X., Worley, S.D., Broughton, R.M., and Huang, T.-S., Synthesis of antibacterial N-halamine acryl acid copolymers and their application onto cotton. *Journal of Applied Polymer Science*, **2019**, 136(16).
22. Qian, Y., Cui, H., Shi, R., Guo, J., Wang, B., Xu, Y., Ding, Y., Mao, H., and Yan, F., Antimicrobial anionic polymers: the effect of cations. *European Polymer Journal*, **2018**, 107: 181-188.
23. Meyers, S.R., Juhn, F.S., Griset, A.P., Luman, N.R., and Grinstaff, M.W., Anionic amphiphilic dendrimers as antibacterial agents. *Journal of the American Chemical Society*, **2008**, 130(44): 14444-14445.
24. Wang, X., Hao, X., Chang, D., Zhu, C., Chen, L., Dong, A., and Gao, G., Novel hydrophilic N-halamine polymer with enhanced antibacterial activity synthesized by inverse emulsion polymerization. *Journal of Applied Polymer Science*, **2019**, 136(17): 47419.
25. Wang, Z. and Pelton, R., Chloramide copolymers from reacting poly (N-isopropylacrylamide) with bleach. *European Polymer Journal*, **2013**, 49(8): 2196-2201.
26. Nazi, N., Humblot, V., and Debiemme-Chouvy, C., A new antibacterial N-halamine coating based on polydopamine. *Langmuir*, **2020**, 36(37): 11005-11014.

27. Dong, A., Huang, Z., Lan, S., Wang, Q., Bao, S., Siriguleng, Zhang, Y., Gao, G., Liu, F., and Harnode, C., N-halamine-decorated polystyrene nanoparticles based on 5-allylbarbituric acid: From controllable fabrication to bactericidal evaluation. *Journal of Colloid and Interface Science*, **2014**, 413: 92-99.
28. Yan, X., Jie, Z., Zhao, L., Yang, H., Yang, S., and Liang, J., High-efficacy antibacterial polymeric micro/nano particles with N-halamine functional groups. *Chemical Engineering Journal*, **2014**, 254: 30-38.
29. Liu, S. and Sun, G., Durable and regenerable biocidal polymers: acyclic N-halamine cotton cellulose. *Industrial & Engineering Chemistry Research*, **2006**, 45(19): 6477-6482.
30. Liu, S. and Sun, G., New refreshable N-halamine polymeric biocides: N-chlorination of acyclic amide grafted cellulose. *Industrial & Engineering Chemistry Research*, **2009**, 48(2): 613-618.
31. Yang, C.Q., Infrared spectroscopy studies of the cyclic anhydride as the intermediate for the ester crosslinking of cotton cellulose by polycarboxylic acids. I. Identification of the cyclic anhydride intermediate. *Journal of Polymer Science, Part A: Polymer Chemistry*, **1993**, 31(5): 1187-1193.
32. Yang, C.Q. and Wang, X., Infrared spectroscopy studies of the cyclic anhydride as the intermediate for the ester crosslinking of cotton cellulose by polycarboxylic acids. II. Comparison of different polycarboxylic acids. *Journal of Polymer Science, Part A: Polymer Chemistry*, **1996**, 34(8): 1573-1580.
33. Yang, C.Q., Xu, Y., and Wang, D., FT-IR spectroscopy study of the polycarboxylic acids used for paper wet strength improvement. *Industrial & Engineering Chemistry Research*, **1996**, 35(11): 4037-4042.
34. Mansur-Azzam, N., Woo, S.G., Eisenberg, A., and van de Ven, T.G., Binder-block copolymer micelle interactions in bactericidal filter paper. *Langmuir*, **2013**, 29(31): 9783-9789.
35. Dankovich, T.A. and Gray, D.G., Bactericidal paper impregnated with silver nanoparticles for point-of-use water treatment. *Environmental Science & Technology*, **2011**, 45(5): 1992-1998.
36. Guan, Y., Qian, L., Xiao, H., and Zheng, A., Preparation of novel antimicrobial-modified starch and its adsorption on cellulose fibers: Part I. Optimization of synthetic conditions and antimicrobial activities. *Cellulose*, **2008**, 15(4): 609-618.
37. Carpenter, B.L., Scholle, F., Sadeghifar, H., Francis, A.J., Boltersdorf, J., Weare, W.W., Argyropoulos, D.S., Maggard, P.A., and Ghiladi, R.A., Synthesis, characterization, and antimicrobial efficacy of photomicrobicidal cellulose paper. *Biomacromolecules*, **2015**, 16(8): 2482-2492.

Supporting Information

Water-Soluble Anionic Polychloramide Biocides Based on Maleic Anhydride Copolymers

Gaoyin He,^a Lei Tian,^a Ayodele Fatona,^a Xiao Wu,^a Hongfeng Zhang,^a Jun Liu,^b Michael Fefer,^b Zeinab Hosseinidoust,^a Robert H. Pelton^{a*}

^a Department of Chemical Engineering, McMaster University, 1280 Main Street West, Hamilton, ON, L8S 4L7, Canada

^b Suncor AgroScience, 2489 North Sheridan Way, Mississauga, ON L5K 1A8, Canada

*Corresponding author: peltonrh@mcmaster.ca

Iodometric Titration of NaDCC. A series of volumes of sodium dichloroisocyanurate dihydrate (NaDCC) solution with known chlorine content were prepared. Then, the titration process of NaDCC was done as previously described.

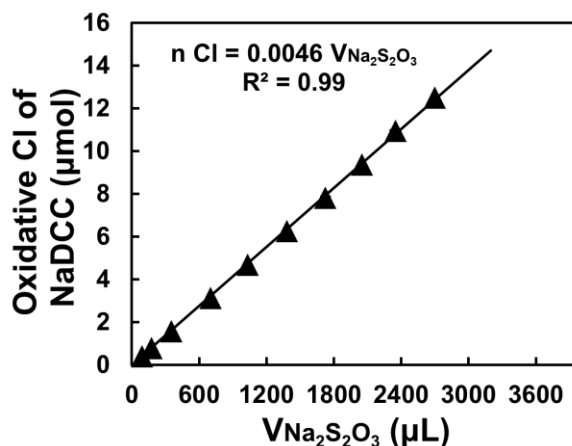
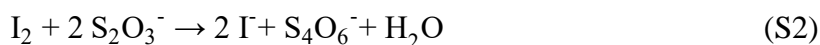
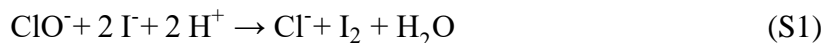


Figure S2-1 Concentration calibration curve of sodium thiosulfate with NaDCC.



TNB Assay. The oxidative chlorine of PC3Cl film was measured by the TNB method. The N-Halamine presence of PC3Cl was confirmed by measuring the UV absorbance of a 5-thio-2-nitrobenzoic acid (TNB) solution at 412 nm. Fresh TNB solution was produced before each experiment via the addition of 2 equivalents of 4 mM cysteine (Cys) to 1 equivalent of 2 mM 5,5'-dithiobis(2-nitrobenzoic acid) (DTNB) in 10 mM phosphate buffer solution at pH 7 following the reaction (S3). A highly colored yellow solution (TNB) was stored at a 4 °C fridge overnight after cysteine and DTNB were mixed. Then, this stock solution was mixed with variable polychloramide solutions in equal volumes to measure the oxidative chlorine concentration. The standard curve of TNB UV-vis absorbance as a function of PC3Cl concentration is presented in **Figure S2-2**.

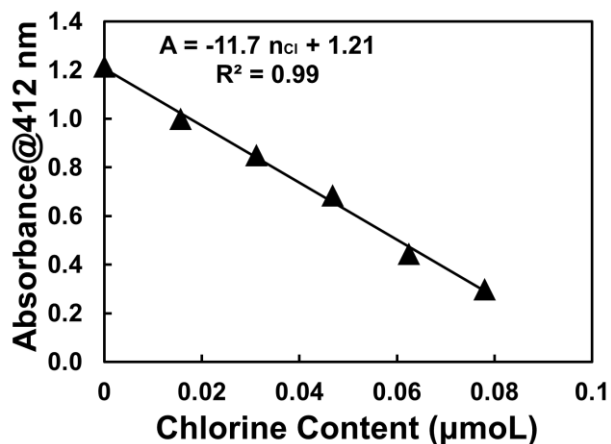
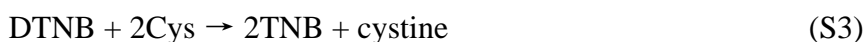


Figure S2-2 The standard UV-Vis absorbance curve of the TNB vs oxidative chlorine contents of NaDCC solution in 10 mM phosphate buffer.

PC3C19 Films Polymer films were formed by drying sessile drops onto glass coverslips. There is some coffee ring formation.

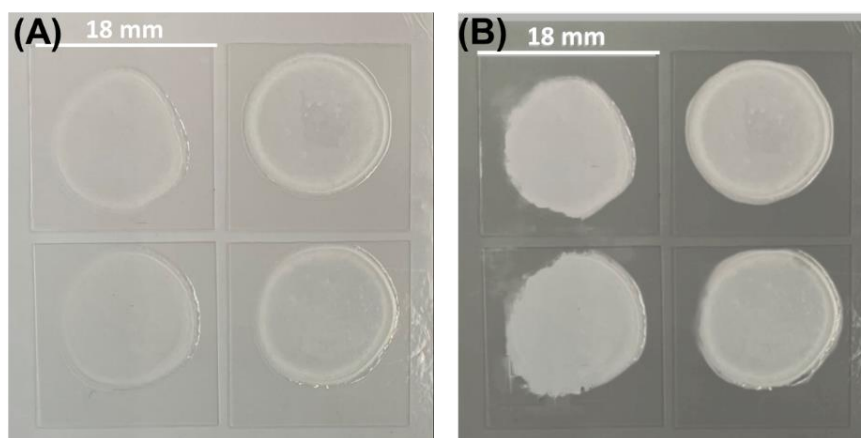


Figure S2-3 Photographs of PC3C19 films on coverslips. A shows the original images and B shows the images after background subtraction with the “color splash function” on Fotor software. (<https://www.fotor.com/photo-editor-app/editor/goart>)

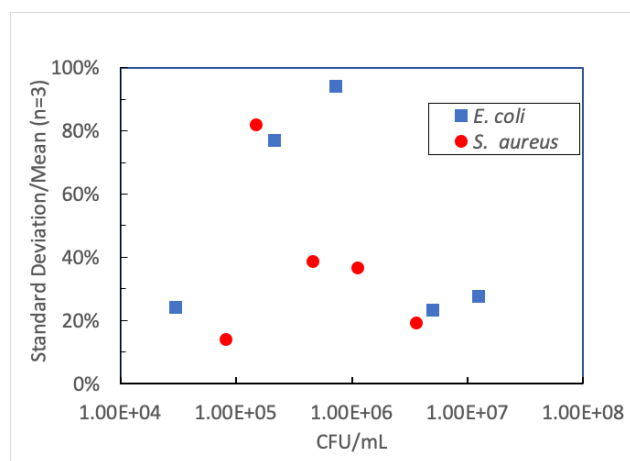


Figure S2-4 Standard deviations as a percentage of means versus the mean values from the bacterial counting experiments.

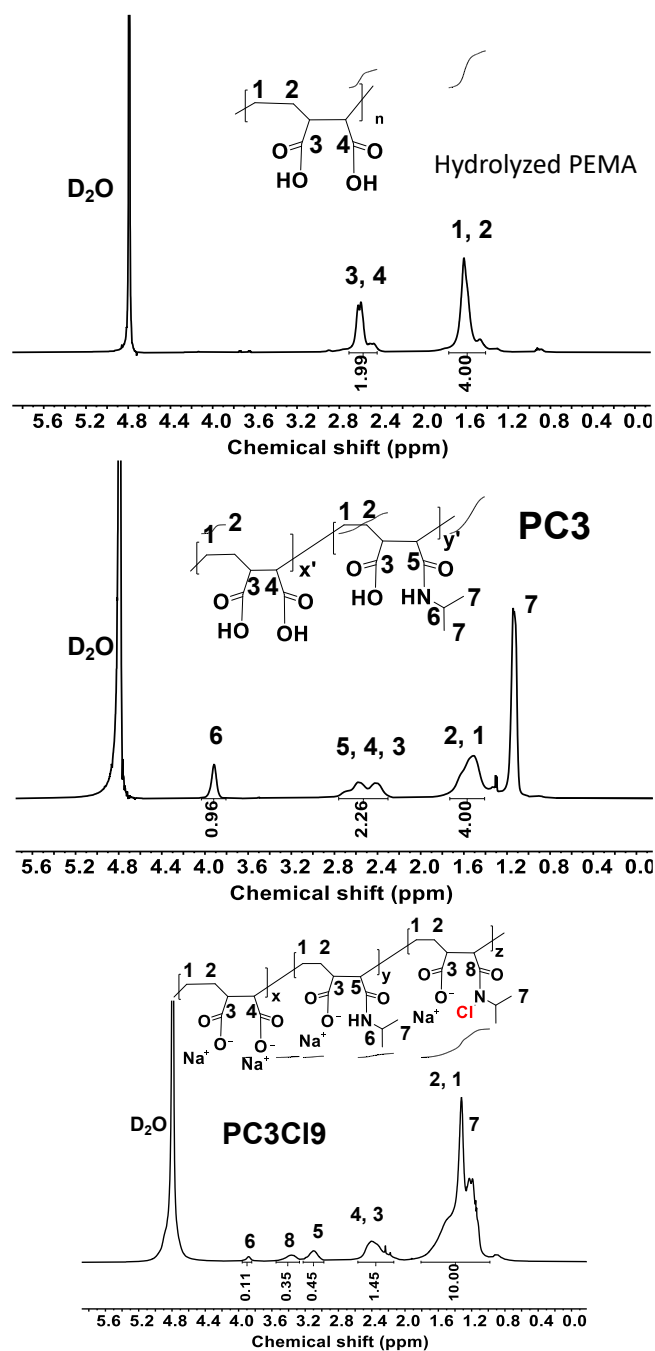
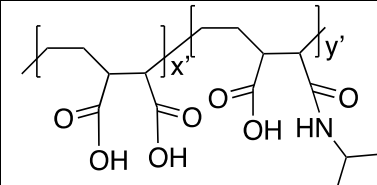
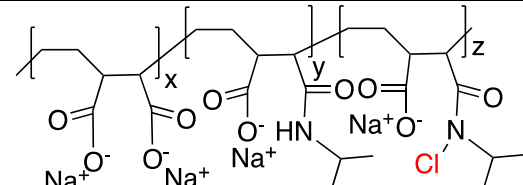


Figure S2-5 Proton NMR spectra of hydrolyzed PEMA, PC3, and PC3Cl9 in D₂O. *y'* in PC3 was determined from the peak areas of peak 6 relative to peak 2.

Compositions of PC3, PC3Cl2, and PC3Cl9. The compositions of PC3, PC3Cl2, and PC3Cl9 are summarized in **Table S2-**. PC3 composition was based on NMR as described above. Extracting the composition of PC3Cl9 was more complicated because the NMRs of the chlorinated polymers were complex. Furthermore, the experimental carbon/nitrogen mass ratios increased with chlorination suggesting loss of amide groups during chlorination. The PC3Cl composition is defined by x , y , and z (see structure in **Table S2-**), where $x+y+z=1$. Two other experimental values are linked to the PC3Cl composition, the carbon/nitrogen mass ratio (CNR), and the mass fraction of active chlorine in the polymer, Cl%, measured by titration. The experimental Cl% and corresponding CNR values were used to assign values for x , y , and z , as follows.

Table S2-1 Summary of polymer properties. COOH, Cl, and C/N are experimental data used with the NMR to calculate the structural parameters x , y , z , dsN, and dsCl.

			
Property*	PC3	PC3Cl2	PC3Cl9
COOH meq/g	5.64	5.70	6.15
Cl (wt%)	0	2.3	9.2
CNR	8.5	8.9	9.3
x or x'	0.04	0.170	0.200
y or y'	0.96	0.695	0.220
z	-	0.135	0.580
dsN	0.96	0.831	0.800
dsCl	-	0.163	0.725

*COOH is the carboxylic acid content. Cl is the mass fraction of chlorine. CNR is the carbon-nitrogen ratio from elemental analysis. dsN = $y+z$ is the fraction repeat units present as amides. dsCl = $z/(y+z)$ the fraction of amides chlorinated.

It is convenient to define two alternate structural parameters - the fraction of repeat units with an amide group, dsN = $y+z$, and the fraction of amide groups that are chlorinated, dsCl = $z/(y+z)$. Based on these definitions and the PC3Cl structure, the following expressions arise for the CNR and the Cl%. MW_x is the molecular weight for substructure x in PC3Cl, and AM_C , AM_N , and AM_{Cl} are the atomic masses for C, N, and Cl.

$$CNR = \frac{AM_C \left(\frac{(1-dsN) \cdot 6}{MW_x} + \frac{dsN \cdot dsCl \cdot 9}{MW_z} + \frac{dsN \cdot (1-dsCl) \cdot 9}{MW_y} \right)}{AM_N \left(\frac{dsN \cdot dsCl}{MW_z} + \frac{dsN \cdot (1-dsCl)}{MW_y} \right)} \quad \text{Equation S2-1}$$

$$Cl\% = \frac{AM_{Cl} \cdot dsCl \cdot dsN}{(1-dsN) \cdot MW_x + (1-dsCl) \cdot dsN \cdot MW_y + dsN \cdot dsCl \cdot MW} \quad \text{Equation S2-2}$$

Experimental CNR and Cl% values for PC3Cl2 and PC3Cl9 were used to determine the corresponding dsN, and dsCl for each polymer by solving the above two equations using the solver in MathCad Prime 7 software. Given the ds values, the corresponding x,y,z values were calculated and the values also are given in **Table S2-**. Based on the dsN values, 0.96 of the repeat units contained amide groups in PC3, only 0.80 of the repeat units were amides in PC3Cl9 and 0.83 in PC3Cl2. Thus 14-17% of amides groups were lost with chlorination, possibly by hydrolysis. The hydrolysis of polyacrylamide during chlorination has been reported. [1, 2]

Influence of Na₂S₂O₃ on bacteria viability.

Table S2-2 Bacteria in 1× PBS and Na₂S₂O₃ solution.

Sample	Replication 1 (CFU/mL)	Replication 2 (CFU/mL)	Replication 3 (CFU/mL)	Ave (CFU/mL)
<i>E. coli</i> in PBS solution	1.2×10 ⁷	8×10 ⁶	1 ×10 ⁷	1 ×10⁷
<i>E. coli</i> in Na ₂ S ₂ O ₃ solution	1.6×10 ⁷	8×10 ⁶	1.6×10 ⁷	1.3×10⁷
<i>S. aureus</i> in PBS solution	8.5×10 ⁶	5.1×10 ⁶	4.2×10 ⁶	5.9×10⁶
<i>S. aureus</i> in Na ₂ S ₂ O ₃ solution	6.1×10 ⁶	5.3×10 ⁶	3.8×10 ⁶	5.1×10⁶

Experimental procedures: 10 μL original bacteria suspension was added to 190 μL 0.1 N Na₂S₂O₃ or PBS buffer solution and then was transferred to LB agar plates. The number of bacterial colonies was recorded after LB agar plates were incubated at 37 °C overnight.

SEMs of Bacteria Before and After Exposure to PC3Cl9 films. For the SEM imaging, a 100 μL droplet of 0.1 mg/L poly-L-lysine was added to a clean glass coverslip (1×1 cm). After drying at room temperature, the coverslips were rinsed in a stream of distilled water and dried by N₂.

50 μL untreated and treated bacterial suspensions, isolated from PC3Cl9 coated coverslips were centrifuged at 2000 g for 10 min leaving PC3Cl9 in the supernatant. Redispersed cell solutions were dropped to the poly-L-lysine coated glass slide, air-dried

for 1 h. Next, bacterial cells were fixed with 2.5 wt% glutaraldehyde solution at room temperatures for 15 min. Cells were dehydrated by sequential treatment with 50%, 70%, 90%, and 100% ethanol for 2 min each followed by critical point drying and sputter-coated with gold. The microscopic images were obtained with the TESCAN VEGA-II LSU SEM. Although the number of microbes is low, there are indications that there are debris and misshapen cells after exposure to PC3C19 films.

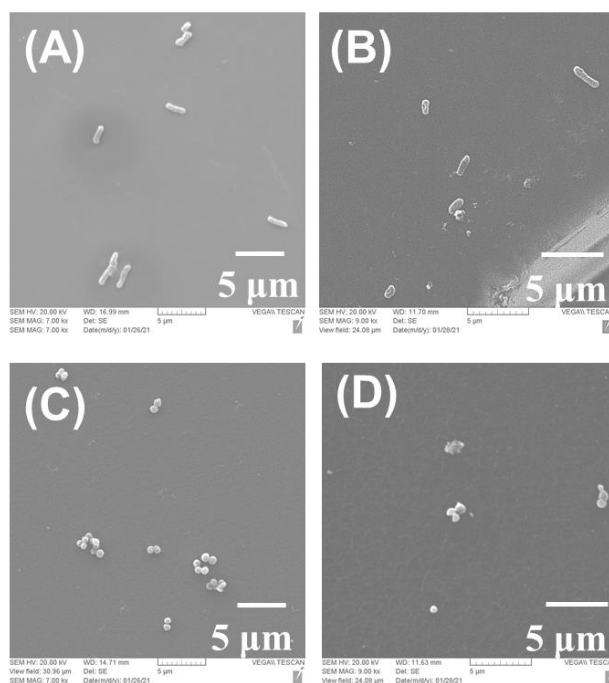


Figure S2-6 SEM micrographs of *E. coli* and *S. aureus* bacteria treated for 1 h with PC3C19 film. (A) Live *E. coli* and (B) treated *E. coli* (C) Live *S. aureus* (D) treated *S. aureus*.

References

1. Liu, S. and Sun, G., Durable and regenerable biocidal polymers: acyclic N-halamine cotton cellulose. *Industrial & Engineering Chemistry Research*, **2006**, 45(19): 6477-6482.
2. Liu, S. and Sun, G., New refreshable N-halamine polymeric biocides: N-chlorination of acyclic amide grafted cellulose. *Industrial & Engineering Chemistry Research*, **2009**, 48(2): 613-618.

Chapter 3

Modeling the Impact of Polychloramide Solution Properties on Bacterial Disinfection Kinetics

To predict linkages between polymer properties and biocidal activity, polymer-modified Chick-Watson (PCW) was proposed to account for bacterial disinfection kinetics of nonadsorbing polychloramides. This model focused on the nonadsorbing polychloramide concentration below the overlap concentration, C^* in the stamping regime. C^* can be experimentally determined as $C^* \cong 1/[\eta]$. In addition, Cl_{coil} (mol/L) is defined as the mols of chlorine atoms attached to an isolated, single polymer chain, divided by the volume occupied by that chain, V_{coil} . The polychloramide properties in the solution are estimated from the overlap concentration, C^* , and chlorine mass fractions. PCW model predicts the impacts of molecular weight (MW), oxidative chlorine mass fraction (Cl_{mf}), and polymer configuration.

In this chapter, PCW model was proposed and developed by Dr. Robert Pelton. Experimental data was collected and summarized by me. Dr. Robert Pelton wrote the modeling part, and I finished the experimental part of the first draft.

This chapter is allowed to reprint as they appear on Biomacromolecules with permission from ACS.

Modeling the Impact of Polychloramide Solution Properties on Bacterial Disinfection Kinetics

Robert H. Pelton, Gaoyin He, Lei Tian, Chaochen Song, and Zeinab Hosseinidoust
Biomacromolecules 2022, 23, 3919–3927

<https://doi.org/10.1021/acs.biomac.2c00736>

Modeling the Impact of Polychloramide Solution Properties on Bacteria Disinfection Kinetics

Robert Pelton,* Gaoyin He, Lei Tian, Chaochen Song and Zeinab Hosseinidou,

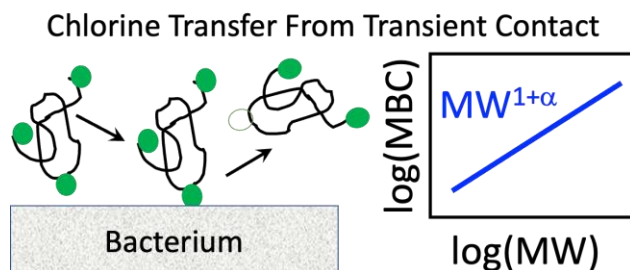
Keywords:

Chick-Watson, disinfection kinetics, polymer configuration, antimicrobial polymers,

Abstract

Anionic water-soluble polychloramide biocides are of interest because, compared to conventional cationic antimicrobial polymers, anionic biocides are less likely to be sequestered or deactivated by contact with non-microbial soil. Although electrostatics can prevent anionic polymers from adsorbing on microbes, water-soluble polychloramides appear to transfer oxidative chlorine during transient contacts between polymer chains and microbe surfaces. The Chick-Watson model of disinfection kinetics has been modified to account for the contributions of polychloramide molecular weight (MW) and the polychloramide configuration in solution estimated from the overlap concentration, C^* , below which dilute polymer chains exist as discrete objects in solution. The key assumption in the modeling was the transfer rate of oxidative chlorine from polychloramide chains to microbe surfaces impacts the disinfection kinetics. Because both C^* and MW are measurable, the polymer-modified Chick-Watson (PCW) model has one less unknown parameter than the two-parameter Chick-Watson equation. The PCW model predicts that lower molecular weight polymers are more effective biocides compared with high molecular weight counterparts. Additionally, polymers with more compressed configurations in solution are more effective biocides. Experimental evidence supports these conclusions. Based on the estimated timescale of bacteria/polymer collisions compared with disinfection kinetics, arguments are made that bacteria surfaces must be contacted many times by polychloramide chains to achieve sufficient Cl transfer to deactivate bacteria.

Graphical Abstract



Introduction

Many publications describe synthetic, [1-3] and biological [4] antimicrobial polymers. Those targeting surface treatments tend to be water-insoluble [5, 6] or grafted to insoluble supports, [7] whereas most of the water-soluble polymers are cationic. For example, less than 3% of antimicrobial peptides have a net negative charge. [4] We are interested in anionic (negatively charged), water-soluble polychloramide biocides because anionic polymers are less likely to be sequestered and thus neutralized by non-microbial anionic surfaces or soluble material in dirty systems. The killing agent in polychloramides is oxidative chlorine atoms that are present as N-Cl bonds. [8, 9] The literature suggests that when the N is present as an amide group, the primary pathway for oxidative chlorine transport to microbes is through direct contact between polymer chains and microbe surfaces. [10-12] Upon contact oxidative chlorine is either transferred to surface nitrogen atoms or reduced by surface reducing agents such as disulfide moieties.

In dilute aqueous solutions most linear, high molecular weight polymers exist as expanded configurations called coils. The genesis of this contribution was the realization that high concentrations of oxidative chlorine fixed to polymer coils, separated by essentially chlorine-free water, differ greatly from a uniform aqueous solution of hypochlorous acid or any other soluble, low molecular weight biocide. **Figure 3-1** shows four situations whereby a biocide contacts a bacterium in solutions. In **Figure 3-1A**, the green spheres represent low molecular weight, water-soluble biocides such as hypochlorous acid. The solution has a uniform distribution of biocide molecules that contact bacteria surfaces.

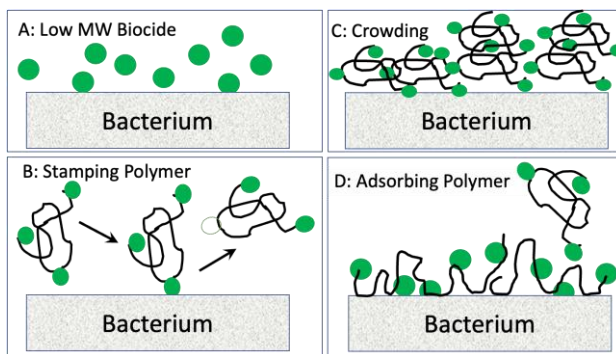


Figure 3-1 A- a low molecular weight oxidative chlorine such as hypochlorous acid. B – a nonadsorbing polychloramide concentration below the overlap concentration, C^* . C – a nonadsorbing polychloramide above C^* . D – an adsorbing polychloramide.

Figure 3-1B, the stamping regime, shows a dilute solution of polymer-bound biocide. The polymer chains are present as discrete entities in the solution. Non-adsorbing polymers do not adsorb (bind) to the bacterium surface, but instead, undergo transient contacts which can result in the transfer of oxidative chlorine.

Figure 3-1C, the crowding regime, shows a more concentrated solution of the same polymer. As one increases the concentration of a water-soluble polymer, a concentration is reached where the polymer coils fill the available space. This concentration is called the overlap concentration, C^* . Above C^* , the polymer molecules must undergo a combination of coil size shrinking and intermingling with neighboring polymer molecules to squeeze into the available volume. The polymer concentration is below C^* in the stamping regime, whereas the crowding regime is above C^* .

Finally, **Figure 3-1D** shows a polymeric biocide that can adsorb onto bacteria surfaces. Usually adsorbing polymers are cationic because the strong electrostatic interactions with negatively charged surfaces produce monolayers of adsorbed polymers that likely do not desorb. [13, 14] Adsorbing polychloramides can be very efficient biocides because both the cationic groups and the oxidative chlorine have biocidal activity. On the other hand, cationic polymers are easily sequestered by binding to non-microbial surfaces or forming irreversible complexes with waterborne anionic polymers.

The focus of this contribution is the stamping regime for non-adsorbing polychloramides. We hypothesize that it is useful to build measurable polymer solution characteristics into disinfection models, accounting for the impacts of polymer molecular weight and the extent to which the polymer configuration in solution is extended. Presented below is what we believe to be the first attempt to incorporate polymer solution properties into kinetic models of biocidal activity.

Experimental Section

Polychloramides. Two commercial (Vertellus) parent poly(ethylene-alt-maleic anhydride)s, PEMAs, with number-average molecular weights of 40.5 kDa and 214 kDa [15] were converted to polychloramides. Detailed characterization including NMR, conductometric titration, elemental analysis, and redox titrations were used to characterize the products. The synthesis and characterization of the polychloramides are reported, in detail, in our previous publication, [16] and the polychloramide structure is shown in **Figure 3-2**.

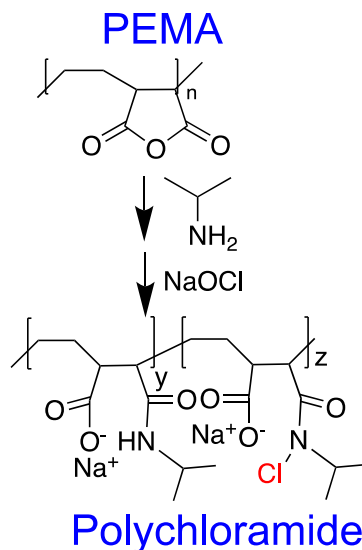


Figure 3-2 Polychloramide structure prepared by derivatizing poly(ethylene-alt-maleic anhydride), PEMA, with 2-propylamine, followed by chlorination. [16]

Disinfection Kinetics. Gram-negative *E. coli* and Gram-positive *Staphylococcus aureus* were grown in LB medium at 37 °C, overnight and then washed three times by suspension in sterile phosphate-buffered saline (PBS), followed by centrifugation at 6000g for 10 min at 4 °C in Eppendorf (EP) tubes. Finally, bacterial suspensions were re-suspended in 1×, 0.1×, or 0.01× PBS buffer.

Fixed polymer concentration, variable contact time. Typically, 10 µL of bacteria suspension in buffer was added to 0.99 mL of polychloramide in a sterilized buffer in a 1.5 mL microcentrifuge tube giving ~ 10⁷ CFU/mL in typically 0.2 g/dL polychloramide. The suspensions were agitated with a SCILOGEX SK-D1807-E Rocker at a frequency of 80 min⁻¹ at room temperature. 10 µL samples were taken at time intervals over 30 min and immediately added to 190 µL of 0.1 M Na₂S₂O₃ solution to quench the remaining oxidative chlorine. Thereafter, serial dilutions were carried out and transferred to LB agar plates, which are incubated at 37 °C overnight for titer count. The detection limits were 400 CFU/mL. Control experiments were performed without polymer to ensure no loss in viability over 30 min. Samples were plated in triplicate and standard deviations were less than 10% of the mean.

Fixed contact time, variable polymer concentration. Bacteria and polychloramide in PBS buffer were mixed at room temperature for one hour. The viable bacteria concentration was measured as described above. The minimum bactericidal concentrations (MBC) of polychloramide for log reduction of -5 in one-hour were determined by several experiments over a range of polychloramide concentrations.

Results and Discussion

Presented first is the modeling. Our approach is to combine elementary models of polymer solution behaviors with the Chick-Watson model [17, 18] of bacterial disinfection kinetics to give what we call the Polymer-modified Chick-Watson model, PCW. Following the derivations, model predictions are shown and comparisons with experimental results are used to support the modeling.

Polymer Solution Behaviors

The configuration (shape) of linear polymers in solution fall somewhere between three extremes – a compact sphere, a fully stretched out chain (rod), or an expanded coil. Compact spheres, by definition, are at or very near precipitation conditions. Extended rods have a high entropy penalty if the polymer chain is flexible. Therefore, most water-soluble polymers are present as swollen coils. In the dilute regime the polymer concentration is less than C^* and isolated water-swollen coils each occupy a volume of V_{coil} and the polymer concentration within that coil is C^* . The size of a polymer coil is described in terms of the “equivalent sphere” which occupies the same volume as the polymer coil. The polymer coil volume is related to the overlap concentration and molecular weight by **Equation 3-1** where N_A is Avogadro’s number.

$$V_{coil} = mw / (C^* N_A) \quad \text{Equation 3-1}$$

C^* is an important parameter in our modeling below because it is linked to V_{coil} . C^* can be experimentally determined as $C^* \cong 1/[\eta]$ [19] where $[\eta]$ is the intrinsic viscosity which is an easily measured parameter. For simulations, the intrinsic viscosity can be expressed as a function of polymer molecular weight by the empirical Mark-Houwink (MH) expression. **Equation 3-2** summarizes the resulting expressions for C^* where Da is the unit g/mol added to convert molecular weight, MW, to a dimensionless number. K_{mh} , and α are the MH coefficients and are fixed for a specific polymer and solvent combination at a given temperature and ionic strength. Expressing C^* by the MH equation allows simulations to probe the influences of polymer MW and swelling, via α .

$$C^* \approx \frac{1}{[\eta]} = \frac{1}{K_{mh} \left(\frac{mw}{Da} \right)^\alpha} \quad \text{Equation 3-2}$$

Table 3-1 shows typical low and high values for MW and for α . $HMW^{0.5}$ is an example of the notation used below. $HMW^{0.5}$ corresponds to a MW of 400 kDa with a Mark-Houwink expansion factor of $\alpha = 0.5$. Of the property combinations in **Table 3-1**, $LMW^{0.5}$ is the most compact polymer coil with a coil diameter of 13 nm whereas $HMW^{0.6}$ is the largest coil with a diameter of 63 nm. Therefore, the polymer coils are 1-2 orders of magnitude smaller than the characteristic dimension of many bacteria.

Table 3-1 Polymer solution parameters used for modeling.

	Lower value	Higher value
Molecular weight	LMW = 40 kDa	HMW = 400 kDa
MH exponent *	$\alpha = 0.5$	$\alpha = 0.6$
MH prefactor*	$K_{mh} = 8.5 \times 10^{-4}$ dL/g	-
Polymer concentration	pc = 0.25 g/dL	pc = 0.5 g/dL,
Chlorine mass fraction	$Cl_{mf} = 0.045$	$Cl_{mf} = 0.09$

*The Mark-Houwink parameters are for poly(ethylene-alt-maleic acid). [20]

The polychloramides of interest are usually prepared by first synthesizing the polyamide followed by a chlorination step. [16] A series of polychloramides can be prepared from a given polyamide by varying the extent of chlorination. [21] Thus chlorine mass fraction, Cl_{mf} , is an independent parameter. The modeling below employs Cl_{coil} (mol/L) defined as the mols of chlorine atoms attached to an isolated, single polymer chain, divided by the volume occupied by that chain, V_{coil} . The polymer concentration within V_{coil} is equal to C^* . Multiplying C^* by Cl_{mf} gives the corresponding Cl concentration, wt/vol. Dividing by AM_{Cl} , the Cl atomic mass, gives Cl_{coil} (mol/L) – see **Equation 3-3**. Substituting the Mark-Houwink expression for C^* shows how MW and the extent of chain expansion (α), influence Cl_{coil} (mol/L). The chlorine molarity within a polymer coil increases with decreasing molecular weight and/or α . This expression is valid when the polymer concentration, pc (g/dL), is less than C^* .

$$Cl_{coil} = \frac{C^* Cl_{mf}}{AM_{Cl}} = \frac{1}{K_{mh} \left(\frac{mw}{Da}\right)^\alpha} \frac{Cl_{mf}}{AM_{Cl}} \quad pc \quad \text{Equation 3-3}$$

$$\leq C^*$$

Some implications of **Equation 3-3** are illustrated in

Figure 3-3. Two x-axis scales are shown. Along the bottom is the total chlorine atom molarity, $Cl_T = pc Cl_{mf}/AM_{Cl}$. Across the top of the figure is the corresponding polymer concentration. The y-axis gives the Cl_{coil} values. The diagonal black line represents two identities $Cl_{coil} = Cl_T$, and $pc = C^*$. The dilute solution regime called the stamping regime herein, is to the left of the diagonal black line whereas the overlap or crowding regime is to the right. The Cl_{coil} values for three polymers are mapped onto the plot as three dashed lines. The polymer lines are horizontal as they are independent of polymer concentrations $< C^*$.

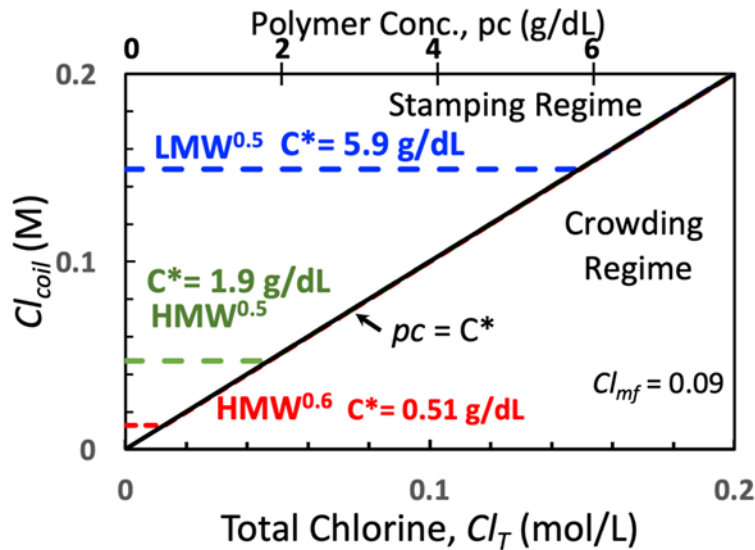


Figure 3-3 Comparing Cl_{coil} , the Cl concentration within polymer coils, corresponding to the total Cl atom concentration, $Cl_T = pc Cl_{mf}/AM_{Cl}$ where pc is polymer concentration (g/dL) and AM_{Cl} is the atomic mass of Cl.

The significance of concentrating Cl on polymer chains is illustrated in

Figure 3-3. When the total Cl concentration of $LMW^{0.5}$ is only 0.02 M, the Cl concentration within the polymer coil is $Cl_{coil} = 0.15$ M, nearly an order of magnitude higher. We propose that the high local concentration within the polymer coils drives the transfer of oxidative chlorine transfer to bacteria surfaces during transient contacts. The next section applies the above descriptions of polymer characteristics to modify the Chick-Watson disinfection model.

Chick-Watson Bacteria Disinfection Kinetics

Since Chick's pioneering work [17] in 1908, there has been interest in modeling bacteria disinfection kinetics by biocides or radiation. Beyond scientific interest, good models help address practical issues around the design and operation of disinfection schemes. The Chick-Watson differential equation for a chlorine biocide is given in **Equation 3-4** where Cl (mol/L) is the biocide concentration in solution and B is the concentration of viable bacteria. In the integral form, B_0 is the initial bacteria concentration when the biocide is introduced. The Chick-Watson model has two parameters, k_{cw} , and n . The rate constant k_{cw} accounts for Cl transport to the bacteria surfaces, possibly diffusion inside, and the kinetics of lethal chemical reactions. The exponent n is called the coefficient of dilution. [22] The integrated version of **Equation 3-4** makes the usual assumption that the biocide concentration is constant. Linear plots of log survival ratios versus time are the hallmark of the Chick-Watson predictions. Herein the slopes of such lines are called disinfection rates.

$$\frac{dB}{dt} = -k_{cw} Cl_T^n B \quad \text{and} \quad \log\left(\frac{B}{B_0}\right) = -2.303 k_{cw} Cl_T^n t \quad \text{Equation 3-4}$$

Experimental results often deviate from the log-linear straight lines predicted by Chick-Watson. There are excellent articles discussing mechanisms and summarizing modeling approaches that account for deviations from Chick-Watson behaviors. [22-24] Our model, described below, takes a slightly different approach as it incorporates polychloramide solution properties into the Chick-Watson equation to predict linkages between polymer properties and biocidal activity. To minimize the number of parameters, our modeling does not account for deviations from log-linear plots.

PCW Model

The following modeling starts with the assumption that the bacteria are planktonic with no exocellular polymer. Also, we assume that the low levels of Cl released from the hydrolysis of chloramide groups, do not contribute to disinfection. [10, 11] In other words, we assume contact killing. [12] We acknowledge that polychloramides can hydrolyze, converting N-Cl to N-H + HOCl. Using Akad's [25] dissociation constant (10^{-9}) for chloramides, we estimated the concentration of HOCl in equilibrium with 0.5 g/dL of polychloramide with, Cl_{mf} equal to 0.09. The estimated HOCl concentration in a demand-free solution was in the nanomolar concentration range whereas the chloramide concentration was 0.013 M. In other words, highly chlorinated polymer chains are dispersed in essentially chlorine-free water.

Envisioned are two kinetic events. First, polymer coils collide with microbe surfaces due to some combination of diffusion and fluid flow with a rate constant k_{col} . The second kinetic event is the chemical transfer of oxidative chlorine from a polymer chain segment to sites on the microbe with a rate constant k_{tr} . The probability of chain/microbe contact at the sub-nanometer distance scale depends upon many factors including polymer chain flexibility, interaction potentials, and fluid flow. These complex and poorly characterized events are now collapsed to a simple expression employing levels of approximation consistent with the Chick-Watson equation.

Equation 3-5 gives the polymer-modified Chick-Watson (PCW) differential rate equation. The collision rate between polymer coils and microbe surfaces is assumed proportional to the concentration of polymer chains, (the terms in brackets) and the bacteria concentration, B. The contribution of chlorine is introduced as Cl_{coil} , the molar concentration Cl within the volume occupied by a polymer coil in dilute solution (see **Equation 3-3**). B, the concentration of viable bacteria, is assumed to be the only time-dependent term in the righthand side of **Equation 3-5**. Cl_{coil} captures the properties of the polymer coil contacting a bacterium surface.

$$\frac{dB}{dt} = -k_{col} k_{tr} \left(\frac{pc}{mw} N_A\right) B \cdot Cl_{coil} \quad pc < C^* \quad \text{Equation 3-5}$$

The Chick-Watson equation has a single rate constant, k_{cw} in **Equation 3-4**, whereas we have defined the product $k_{col} k_{tr}$ where all the complexities of chlorine interactions with microprobes are accounted for by k_{tr} . This was done because we needed the collision rate

constant, k_{col} , for the Poisson analysis in the next section. Smoluchowski derived the expression in **Table 3-2** for k_{smol} , the rate constant for the diffusion-driven collision of uniform spheres. [19] Herein k_{col} is expressed as a product of the constant k_{smol} with β as a dimensionless collision rate – see **Equation 3-6**. For most of the calculations below, β was set to 10 to account for the contribution of agitation to collision frequency.

$$k_{col} = \beta k_{smol} \quad \text{Equation 3-6}$$

Table 3-2 Base case parameters for the Polymer-modified Chick-Watson (PCW) model.

Overall PCW rate constant, base case	$k_{pcw} = 0.0196 \text{ m}^6/(\text{kg}\cdot\text{s}\cdot\text{mol})$, Equation 3-7A
The transfer rate constant	$k_{tr} = 4.06 \times 10^{-12} \text{ m}^3 / \text{mol}$, Equation 3-5
Smoluchowski collision rate constant	$k_{smol} = \frac{8kT}{3\eta} = 1.2 \times 10^{-17} \frac{\text{m}^3}{\text{s}}$ at 25 °C
Base case beta value	$\beta = 10$, Equation 3-6
Poisson Intensity	$q = 1$, Equation 3-13
Microbe equivalent radius	$r_b = 250 \text{ nm}$, Equation 3-10

η is viscosity, k is Boltzmann's constant, and T is temperature.

In the following paragraphs, two equivalent versions of the integrated PCW model are shown. One version uses the Mark-Houwink parameters to calculate C^* as a function of MW and α , **Equation 3-2**. This leads to analytical expression whereby the influences of MW and polymer configuration are mathematically probed. In the second version, C^* is present as a parameter like MW or polymer concentration. When fitting experimental results, the C^* versions are more useful because C^* is easier to measure compared to the two Mark-Houwink coefficients. C^* can be calculated from experimental intrinsic viscosity, **Equation 3-2**. For low ionic strength cases (potable water for example) where intrinsic viscosity data for charged polymers is problematic, C^* can be estimated from viscosity versus polymer concentration curves. By contrast, Mark-Houwink coefficients require intrinsic viscosity data from a homologous series of polymers spanning a range of molecular weights.

Equation 3-7A gives two equivalent forms of the integrated PCW model, giving the log survival ratio ($\log\text{SR} = \log(B/B_0)$) as functions of time. In A) the Mark-Houwink equation is used to calculate C^* - see **Equation 3-2**, whereas in B) C^* is directly used as a parameter. All terms on the right-hand side are assumed to be independent of time except t, giving linear log survival ratio vs contact time predictions. Compared to the beautiful simplicity of the Chick-Watson equation, both forms of the PCW model have more terms. However, p_c , MW, C^* , and Cl_{mf} are known or independently measurable by standard techniques in polymer technology. The overall rate constant k_{pcw} ($\text{m}^6/(\text{kg}\cdot\text{s}\cdot\text{mol})$) captures the unknown kinetic rate constant product βk_{tr} , plus a group of known constants in a single term. k_{pcw} must be determined from experimental disinfection data.

$$\begin{aligned} \text{A)} \quad \log\left(\frac{B}{B_0}\right) &= \log SR && \text{Equation 3-7} \\ &= -k_{pcw} \frac{pc}{mw} \frac{1}{K_{mh} \left(\frac{mw}{Da}\right)^\alpha} Cl_{mf} t \end{aligned}$$

or

$$\begin{aligned} \text{B)} \quad \log\left(\frac{B}{B_0}\right) &= \log SR = -k_{pcw} \frac{pc}{mw} C^* Cl_{mf} t \\ \text{where } k_{pcw} &= \ln(10) k_{smol} \frac{N_A}{AM_{Cl}} \beta k_{tr} \end{aligned}$$

Inspection of **Equation 3-7A** reveals $\log SR \propto mw^{-(1+\alpha)}$ where the MH α value is 0.5-0.7. Therefore lower molecular weight polymers are predicted to be more effective biocides. Similarly decreasing polymer coil expansion by lowering α , increases biocidal activity. Before getting to more specific model predictions and the comparisons between theory and experimental results, the stamping process is considered in a little more detail. Specifically, we now compare the estimated time scale of bacteria/polymer collisions with disinfection times scales.

Poisson Stamping Time Scales

Consider first a macroscopic physical model. Imagine an ink-coated rubber ball contacting (stamping) a paper surface at a fixed frequency but in random locations. Each impact would leave behind some ink in a circular pattern (i.e., a footprint) reflecting the contact area during impact. The fraction of the paper surface area impacted at least once increases with time as does the density of ink increases reflecting multiple impacts on a specific site. Random stamping is a Poisson process and the probability of a specific point on the paper experiencing n impacts is given by **Equation 3-8** where λ is the total area of footprints divided by the area of the paper. λ is a function of time as it is proportional to the total number of impacts. λ values can be greater than 1. However, because the stamping is in random positions, surface coverage with ink is not uniform with a finite probability of bare spots, $p(0,\lambda)$.

$$p_{(n,\lambda)} = \frac{\lambda^n}{n!} \exp(-\lambda) \quad \text{Equation 3-8}$$

The collision of a polymer coil with a bacterium surface (**Equation 3-1B**) is analogous to the stamping process and the transfer of ink shares parallels the transfer of oxidative chlorine. The number of coil/bacteria impacts at time t , IN_V (m^{-3}), is given by the following equation where k_{col} (m^3/s) is the collision rate constant, PC_{coil} is the number concentration of polymer chains and B_0 is the initial viable bacteria concentration. For non-adsorbing polymers, PC_{coil} is independent of time. Assuming dead and live bacteria

have similar collision characteristics, the total viable and non-viable bacteria concentrations is approximately B_o .

$$IN_V = k_{col} PC_{coil} B_o t \quad \text{Equation 3-9}$$

To apply the Poisson statistics, we need the number of impacts per unit bacteria surface area, IN_A (m^{-2}) which is given by **Equation 3-10** where r_b is the radius of a sphere with the same surface area as the bacterium.

$$IN_A = \frac{k_{col} PC_{coil}}{4\pi r_b^2} t \quad \text{Equation 3-10}$$

The λ function for Poisson stamping is given in **Equation 3-11** where A_{es} is the projected area of a polymer coil - **Equation 3-12**. A_{es} is the area of the footprint when a polymer chain contacts a bacterium. Note $\lambda_{ps} \propto mw^{\frac{2}{3}(\alpha+1)-1}$ and when MH exponent $\alpha = 0.5$, the MW exponent is zero indicating λ has no MW dependence whereas for $\alpha > 0.5$ the MW exponent is a positive number.

$$\lambda_{ps} = IN_A A_{es} = \frac{\beta k_{smol}}{4\pi r_b^2} \frac{pc}{mw} N_A \pi^{\frac{1}{3}} \left(\frac{3 Da K_{mh}}{4 N_A} \right)^{\frac{2}{3}} \left(\frac{mw}{Da} \right)^{\frac{2}{3}(\alpha+1)} t \quad \text{Equation 3-11}$$

or

$$\lambda_{ps} = IN_A A_{es} = \frac{\beta k_{smol}}{4\pi r_b^2} \frac{pc}{mw} N_A \left(\frac{3mw}{4\pi C^* N_A} \right)^{\frac{2}{3}} t$$

The projected area of the equivalent sphere on a plane, A_{es} , is given as follows which is based on V_{coil} given in **Equation 3-1**.

$$\begin{aligned} A_{es} &= \pi \left(\frac{3 mw}{4 \pi C^* N_A} \right)^{\frac{2}{3}} \\ &= \pi^{\frac{1}{3}} \left(\frac{3 Da K_{mh}}{4 N_A} \right)^{\frac{2}{3}} \left(\frac{mw}{Da} \right)^{\frac{2}{3}(\alpha+1)} \end{aligned} \quad \text{Equation 3-12}$$

The Poisson stamping function f_{ps} is defined as the fraction of microbial surface area that has been stamped at least q times where q is a positive integer. Application of the Poisson probability function, **Equation 3-8**, leads to the mathematical formulation of f_{ps} shown in **Equation 3-13**.

$$\begin{aligned} f_{ps(q, \lambda_{ps})} &= 1 - \sum_{n=0}^{n=q-1} p(n, \lambda_{ps}) = 1 - \sum_{n=0}^{n=q-1} \left(\frac{\lambda_{ps}^n}{n!} \exp(-\lambda_{ps}) \right) \\ f_{ps}(1, \lambda_{ps}) &= 1 - \exp(-\lambda_{ps}) \quad \text{when } q = 1 \end{aligned} \quad \text{Equation 3-13}$$

The time scale of the Poisson stamping is determined by β in λ_{ps} . Note the rate constant k_{ir} does appear in **Equation 3-11**. A β value of 1 corresponds to k_{col} equaling the Smoluchowski collision rate constant, k_{smol} . Our experimental disinfection studies

involved agitating the mixtures of bacteria and polychloramide. Therefore the mixing should give higher collision rates compared to the Smoluchowski diffusion-controlled rate. We propose $\beta = 10$ would be a reasonable guess for modeling. **Figure 3-4** shows three plots of f_{ps} ($q=1$) versus time. When $\beta = 10$, the time required for f_{ps} to approach a value of 1 is in the range of 10^{-4} to 10^{-5} min for a typical polymer concentration and molecular weight. This is approximately six orders of magnitude faster than the timescale for bacteria inactivation in our laboratory investigations. In other words, the bacteria surfaces experience thousands to millions of polymer impacts before inactivation. This suggests that chlorine transfer from polymer to microbe surfaces is inefficient. In addition, Gottardi and Nagl reported that *Escherichia coli* takes up 2×10^8 Cl atoms per CFU while having a high survival ratio of 74% - it takes the transfer of many Cl atoms to deactivate bacteria. [26]

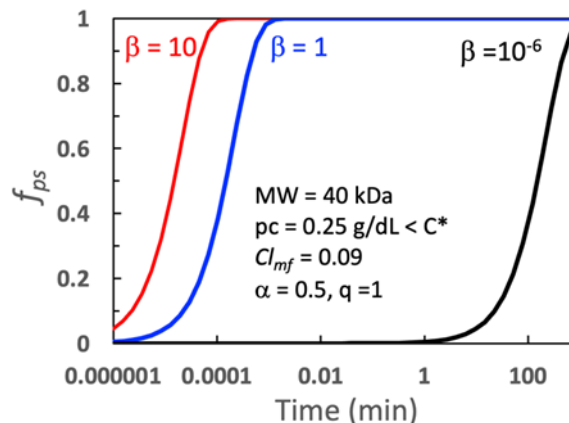


Figure 3-4 The stamping function f_{ps} (**Equation 3-13**) versus time shows the fraction of microbe surfaces stamped at least 1 time for three β values. The microbe equivalent radius for **Equation 3-11** was $r_b = 250$ nm

Shown in the following sections are predictions of the PCW model. **Equation 3-7A** and **7B** are used to predict either log survival ratios, $\log SR$, versus time, or the minimum biocidal concentrations, MBC, for a given log reduction of survival ratio after a given contact time.

Molecular Weight. Predictions of the PCW model are now presented. The assignment of model parameters was based on these steps: 1) we assumed the Mark-Houwink parameters in **Table 3-1** which are the MH parameters for poly(ethylene-alt-maleic acid) [20]; and 2) we set $k_{pcw} = 0.0196 \text{ m}^6/(\text{kg}\cdot\text{s}\cdot\text{mol})$, a value that gave reasonable log survival ratios versus time curves for the 4 combinations of MW and α shown in **Figure 3-5A**. Like the Chick-Watson equation, the PCW model always gives linear log survival ratios as functions of contact times. The highest concentration of the lowest molecular weight (LMW, 40 kDa) gave the fastest disinfection rate. At the other extreme, the lowest concentration of the larger polymer (400 kDa) gave a nearly horizontal line.

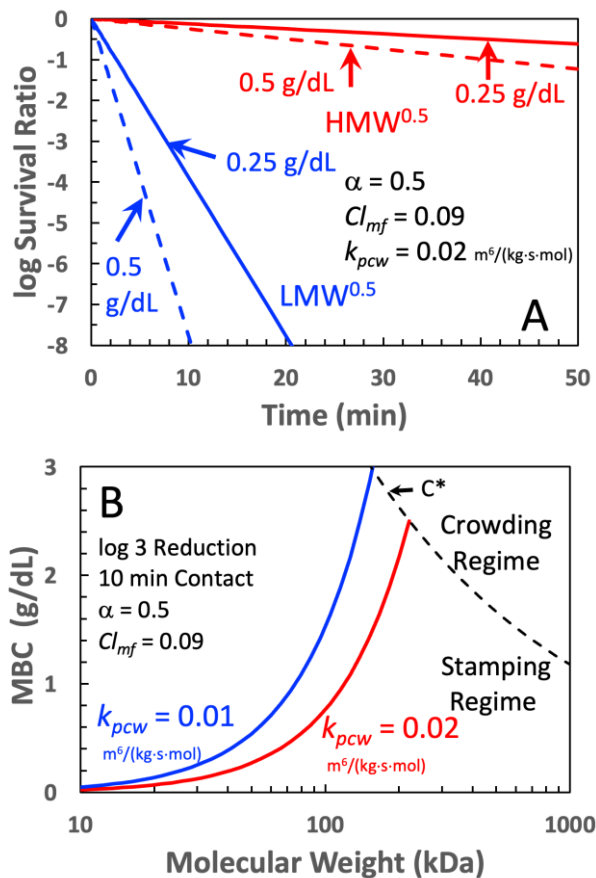


Figure 3-5 The influence of polymer molecular weight on log survival ratio versus time curves and MBC versus molecular weight. HMW = 400kDa, LMW = 40 kDa, and $K_{mh} = 8.5 \times 10^{-4} \text{ dL/g}$.

Equation 3-7A and **7B** can be rearranged to give a minimum biocidal concentration, MBC, for a specified log decrease in the survival ratio after a specified microbe/biocide contact time. **Figure 3-5B** shows MBCs (log 3 reduction, 10 min contact time) as functions of polymer molecular weight. The two curves illustrate the role of the PCW model rate constant, k_{pcw} - defined in **Equation 3-7A** and **7B**. Faster collision rates give lower MBC values. The curves are linear when plotted on a log/log axis, indicating a powerlaw relationship of $MBC \propto MW^{1+\alpha}$. The main message either from inspection of **Equation 3-7A** and **7B** or **Figure 3-5** is that lower molecular weight non-adsorbing polymeric biocides should be the most effective.

The MBC values in **Figure 3-5B** increase with MW until hitting the C* limit, above which the model is not valid. When calculating MBC values from **Equation 3-7A** or **7B**, there is no mathematical lower MW limit to the equations. However, when trying to apply the model to experimental data, the Mark-Houwink parameters or C* values cannot be

measured for small molecules. Indeed, the concept of overlap concentration does not apply to small molecules.

Figure 3-2 shows the structure of the polychloramide polymers used to probe the model predictions. The purified polymers were then exposed to NaOCl giving chloride mass fractions of 2 or 9%. Details of purification and characterization are given in our previous publication. [16] **Table 3-3** summarizes both polymer properties and some minimum biocidal concentrations (MBCs). The polymer properties include experimental chlorine mass fractions and overlap concentrations based on intrinsic viscosity measurements.

Table 3-3 Comparisons of experimental MBC values with PCW model predictions.

Polychloramide Properties						MBC (-5 log reduction, 1h contact)		
Row #	Name	Cl_{mf}	Mw ¹ kDa	PBS Conc.	C* ² g/dL	<i>E. coli</i> g/dL	<i>S. aureus</i> g/dL	PCW ³ g/dL
1	H0	0	346	1x	0.38	No killing	No Killing	
2	H9.2	9.2%	379	1x	6.92	-	-	-
3	H2.3	2.3%	354	1x	1.942	1.75 ± 0.25	1.75 ± 0.25	1.88
4	H2.3	2.3%	354	0.1x	0.83	1.5 ± 0.5*	2.5 ± 0.5*	4.39*
5	L2.5	2.5%	67	1x	1.938	0.3 ± 0.2	0.075 ± 0.025	0.092
6	H9.2	9.2%	379	0.01x	5.65	-	-	-

¹ MWs based on the parent PEMA number average degree of polymerization.

² Values determined in PBS buffer.

³ Calculated by **Equation 3-7B** using experimental C* values and setting $k_{pcw} = 0.0587 \text{ m}^6/(\text{kg}\cdot\text{s}\cdot\text{mol})$.

* The experimental and calculated MBC values are $> C^*$, where the PCW model does not apply.

Row #3 and #5 in **Table 3-3** compare experimental MBC values with PCW predictions for two molecular weight polychloramide polymers applied to *E. coli* and *S. aureus* bacteria. Both experimental and model results showed an order of magnitude decrease in MBC values when going from high to low polychloramide molecular weights. Recall that the classic Chick-Watson equation does not speak to biocide MW.

Buffer Concentration

Rows #3 and #4 in **Table 3-3** compare the impacts of buffer concentration (1x vs 0.1x PBS) on MBC values. However, because the polymer MW was high and the Cl content was only 2.3%, the corresponding C* values were low. For 1x PBS in Row 3, the calculated MBC value was slightly less than C*, which satisfies the $pc < C^*$ requirement. Whereas both the experimental and calculated MBC values in Row 4, far exceeded the corresponding C* and thus were in the crowding regime where the model does not apply. Comparing Rows #2 and #6 shows that C* was lower in 0.1x PBS compared to 1x PBS indicating the polymer was more expanded in lower ionic strength conditions. In

summary, the MBC values and the C^* values were not very sensitive to buffer concentration over the ranges in **Table 3-3**.

Polymer Configuration

The volume occupied by one polymer chain in the solution, V_{coil} , increases with the MH α value. **Figure 3-6A** shows dramatic decreases in the disinfection rates when increasing α from 0.4 to 0.7. **Figure 3-6B** shows MBC versus α curves at two contact times. As expected, the longer the polymer/microbe contact time, the lower the MBC. α is a sensitive parameter indicating the more expanded the polymer coils, the higher the MBC. However, polychloramides are more hydrophobic than the parent polyamides. [21] Furthermore the measures to increase oxidative stability such as using nitrogen heterocycles and replacing backbone hydrogen with methyl groups, tend to increase hydrophobicity. Thus α values of water-soluble polychloramides are likely to be near 0.5.

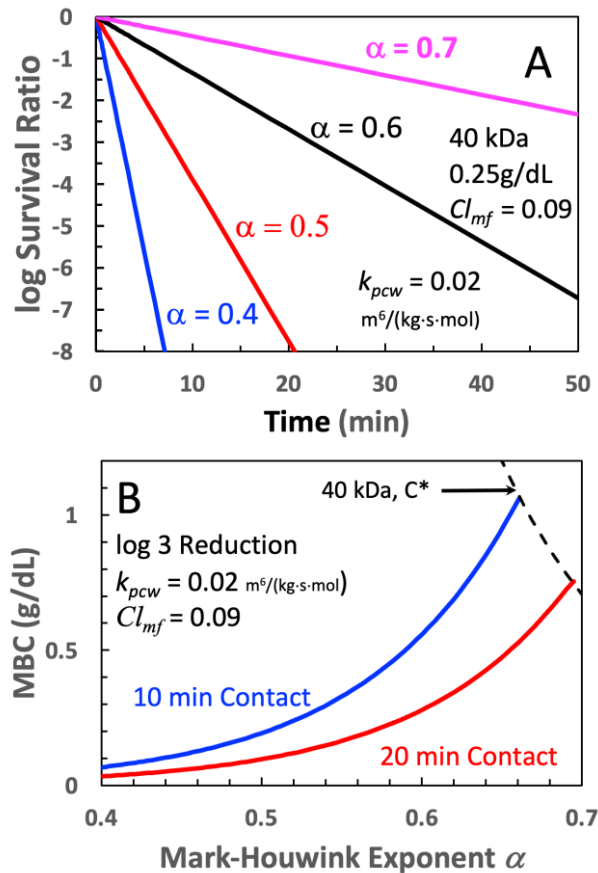


Figure 3-6 The influence of Mark-Houwink exponent α on log survival ratio and MBC behaviors. $k_{pcw} = 0.02 \text{ m}^6/(\text{kg}\cdot\text{s}\cdot\text{mol})$, $K_{mh} = 8.5 \times 10^{-4} \text{ dL/g}$.

Figure 3-6 is a simulation – it does not verify the model. The molecular weight results in **Table 3-3** (Row 3 versus Row 5) suggest the PCW model has some validity. More support for the model is shown in the next section.

Influence Oxidative Chlorine Mass Fraction, Cl_{mf}

The influence of chlorine content is subtle. Inspection of **Equation 3-7A** and **7B** gives the impression that disinfection rates (i.e., the slope of the log survival ratio vs time plots) have a linear dependence on Cl_{mf} . However C^* also depends on Cl_{mf} because chlorination increases the hydrophobicity of water-soluble polyamides. **Figure 3-7A** shows C^* in 1x PBS is a linear function of the Cl wt%, based on the H0, H2.3, and H9.2 data in **Table 3-3**. A similar linear relationship has been reported for the influence of Cl contents on the cloud point temperatures of poly(N-isopropylacrylamide). [21]

Applying the experimental linear relationship between C^* and Cl_{mf} along with $k_{pcw} = 0.0587 \text{ m}^6/(\text{kg}\cdot\text{s}\cdot\text{mol})$ from **Table 3-3**, the PCW model was used to simulate the influence of the chlorine mass fraction in the polychloramides. **Figure 3-7B** shows MBC values and the disinfection rates as a function of chlorine content. Neither curve is linear with Cl_{mf} . The Cl_T^n term in the Chick-Watson **Equation 3-4**, anticipates nonlinear biocide rate dependencies; perhaps the PCW model gives insight into the mechanistic origin of $n > 1$ for polymeric, soluble biocides.

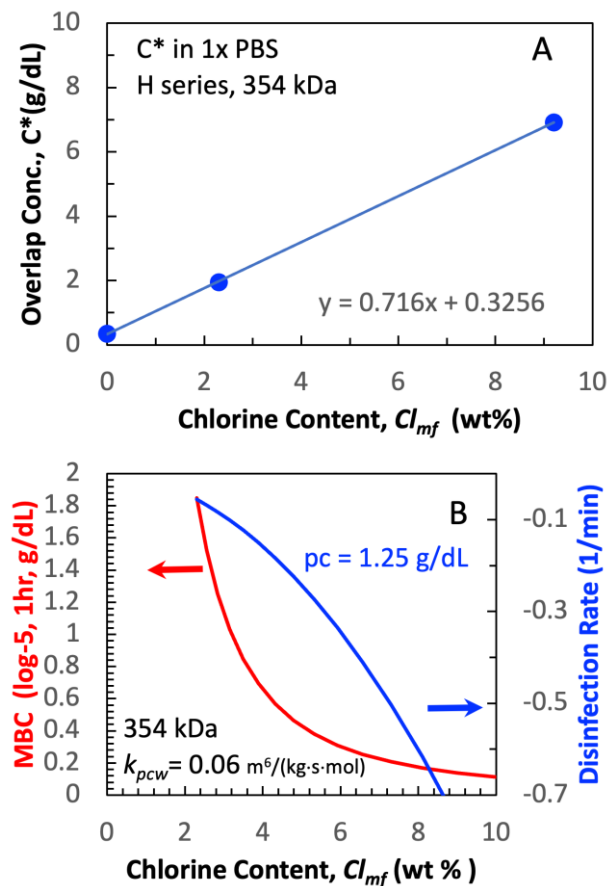


Figure 3-7 The influence of chloride content on A: C* for the H series polychloramide in 1x PBS, and, B: the corresponding disinfection rates ($pc = 1.25 \text{ g/dL}$) and MBC (log -5, 1 hr), assuming $k_{pcw} = 0.0587 \text{ m}^6/(\text{kg}\cdot\text{s}\cdot\text{mol})$.

Shown next is a comparison of two polychloramides, one with a low Cl content (Cl_{mf}) and the other with a high Cl_{mf} . When applied to a bacteria suspension the total Cl concentration was kept constant by using different concentrations of the two polymers. This comparison addresses the question - which is the more effective biocide, a low concentration of the highly chlorinated polymer or a high concentration of the low Cl polymer? The Chick-Watson equation says the two cases should give the same result. **Figure 3-8** shows that AP9.2, applied at a low concentration, is more effective than AP2.3 applied at a high concentration. The higher chlorine content polymer is more collapsed, giving a bigger C*.

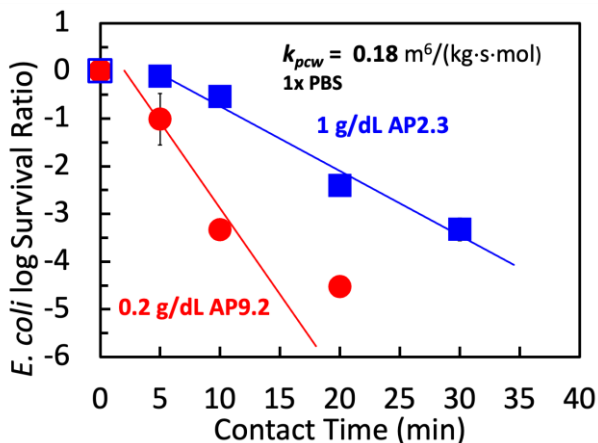


Figure 3-8 Comparing low (2.3%) chloride and high (9.2%) chloride at approximately the same total chlorine concentrations.

Both sets of experimental data in **Figure 3-8** have an induction period, about 2 min for AP9.2 and 5 min for AP2.3. Neither the Chick-Watson equation nor the PCW model accounts for induction periods. The blue line is the best fit through the AP2.3 data, excluding the zero-time point. The slope of linear fit was used to calculate the corresponding $k_{pcw} = 0.1789 \text{ m}^6/(\text{kg}\cdot\text{s}\cdot\text{mol})$ from **Equation 3-7B**, using the AP2.3 concentration, chlorine content, C^* , and MW. Therefore, the blue line through the AP2.3 also corresponds to the PCW fit. The red line through the AP9.2 data was calculated using the same value for k_{pcw} , while offsetting the contact time by 5 minutes to account for the induction period. Note that when applying the model, because of the differences in chlorine contents, the two polymers in **Figure 3-8** have different concentrations, slightly different molecular weights and more than a three-fold difference in C^* - see **Table 3-3**. Summarizing, the two model curves in **Figure 3-8** were based on 1 value of 1 adjustable parameter, k_{pcw} . All other terms (p_c , MW, C^* , and Cl_{mf}) in **Equation 3-7B** were populated with experimentally determined values. We propose that the results are a good demonstration of the utility and validity of the PCW model.

Concluding Remarks

When non-adsorbing, water-soluble polymer chloramides are employed in dilute solution, oxidative chlorine is concentrated on isolated polymer chains in water. Transient collisions between polymer chains and microbe surfaces result in the transfer of chlorine to the microbe surfaces in what we call a stamping process, illustrated in **Figure 3-1B**. In dilute solutions, individual flexible water-soluble polymer chains are isolated and with each chain occupying an average volume, V_{coil} , that depends on the molecular weight and hydrophilicity of the polymer backbone. We believe that the PCW model is the first to consider the local concentration of Cl in the volume occupied by polymer chains that are impacting bacteria surfaces. In addition to predicting the well-known benefits of low

molecular weight and high Cl contents, the model emphasizes the impacts of polymer hydrophilicity on V_{coil} and biocidal activity leading to the predictions listed below.

The PCW model, **Equation 3-7A** and **7B**, assumes that chlorine transfer rates from stamping are reflected in the overall kinetics of bacteria deactivation. The classic Chick-Watson classic deactivation model has been modified to include four measurable polymer properties. They are pc , Cl_{mf} , C^* , and MW, where pc is the polymer concentration, Cl_{mf} is the mass fraction of chlorine in the polymer, C^* is the overlap concentration below which polymer chains are present as discrete entities in solution, and MW is the average molecular weight. Like the original Chick equation, the PCW model has one adjustable parameter, k_{pcw} , which is a rate constant. The main predictions of the model are:

The PCW model predicts that low MW polychloramides are more effective than longer polymer chains with the same composition. Low MW polymers have a high C^* meaning they are likely to be applied at concentrations in the stamping regime. Two effects make low MW polymers more effective below C^* . First, the lower the MW, the higher the concentration of Cl within the volume occupied by one polymer coil (compare horizontal sections in **Figure 3-3**). Second, comparing low and high MW polymers at the same mass concentration, the stamping frequency is higher for low MWs because the number concentration of polymer chains is higher.

The PCW model predicts that for a given polymer chain length, the more the polymer configuration in the solution is expanded, the lower the disinfection rate. Increased expansion lowers C^* and decreases the Cl concentration within the polymer coil.

Because chlorination increases the hydrophobic character of polychloramides, the polymer coils shrink with increasing Cl_{mf} . The PCW model predicts that the disinfection rates have a non-linear dependence on Cl_{mf} because both increased Cl content and coil shrinkage contribute to enhanced disinfection rates.

An analysis based on Poisson statistics suggests that a random position on bacteria surfaces will experience as many as 10^6 collisions with polymer chains in the timescale of bacteria inactivation. We propose this reflects a combination of the inefficiency of Cl transfer from polymer chains to microbe surfaces and the large number of transferred Cl atoms required to deactivate a bacterium.

The model predictions imply two suggestions to those developing and testing water-soluble polychloramide antimicrobials. First, it is of value to determine if a candidate polymeric biocide adsorbs onto microbe surfaces – there are significant kinetic differences between adsorbing versus stamping water-soluble polymers. Second, the polymer overlap concentration should be measured under pH and ionic strength conditions used in the bacteria-killing assays and the final application. Matching testing solution pH and ionic strengths to end-use conditions is important. For example, laboratory results from testing in high ionic strength buffer when ionic polymers are compressed, may not be relevant to applications involving low ionic strength where charged polymers are highly expanded and much less effective. The PCW model is easy to apply given experimental Cl_{mf} , MW, and C^* values. Irrespective of a detailed model,

it seems obvious that the stamping and crowding regimes, illustrated in **Figure 3-1**, likely have different kinetic characteristics and one should know if experimental MBC values are below or above C^* .

Acknowledgments

We thank the Natural Sciences and Engineering Research Council of Canada (NSERC) and Suncor Energy for funding this project. Dr. Michael Fefer, and Jun Liu both from Suncor, and Professor Carlos Filipe from McMaster are thanked for stimulating discussions.

References

1. Kenawy, E.-R., Worley, S., and Broughton, R., The chemistry and applications of antimicrobial polymers: a state-of-the-art review. *Biomacromolecules*, **2007**, 8(5): 1359-1384.
2. Ganewatta, M.S. and Tang, C., Controlling macromolecular structures towards effective antimicrobial polymers. *Polymer*, **2015**, 63: A1-A29.
3. Steinman, N.Y., Hu, T., Dombrovsky, A., Reches, M., and Domb, A.J., Antiviral polymers based on N-halamine polyurea. *Biomacromolecules*, **2021**, 22(10): 4357-4364.
4. Ergene, C., Yasuhara, K., and Palermo, E.F., Biomimetic antimicrobial polymers: recent advances in molecular design. *Polymer Chemistry*, **2018**, 9(18): 2407-2427.
5. Demir, B., Broughton, R., Huang, T., Bozack, M., and Worley, S., Polymeric antimicrobial N-halamine-surface modification of stainless steel. *Industrial & Engineering Chemistry Research*, **2017**, 56(41): 11773-11781.
6. Nazi, N., Humblot, V., and Debiemme-Chouvy, C., A new antibacterial N-halamine coating based on polydopamine. *Langmuir*, **2020**, 36(37): 11005-11014.
7. Tavakolian, M., Munguia-Lopez, J.G., Valiei, A., Islam, M.S., Kinsella, J.M., Tufenkji, N., and van de Ven, T.G., Highly absorbent antibacterial and biofilm-disrupting hydrogels from cellulose for wound dressing applications. *ACS Applied Materials & Interfaces*, **2020**, 12(36): 39991-40001.
8. Hui, F. and Debiemme-Chouvy, C., Antimicrobial N-halamine polymers and coatings: A review of their synthesis, characterization, and applications. *Biomacromolecules*, **2013**, 14(3): 585-601.
9. Product performance test guidelines OCSPP 810.2000: general considerations for testing public health antimicrobial pesticides guidance for efficacy testing. **2018**, Environmental Protection Agency.
10. Williams, D.E., Elder, E.D., and Worley, S.D., Is free halogen necessary for disinfection? *Applied and Environmental Microbiology*, **1988**, 54(10): 2583-2585.
11. Gutman, O., Natan, M., Banin, E., and Margel, S., Characterization and antibacterial properties of N-halamine-derivatized cross-linked polymethacrylamide nanoparticles. *Biomaterials*, **2014**, 35(19): 5079-5087.
12. Kaur, R. and Liu, S., Antibacterial surface design – Contact kill. *Progress in Surface Science*, **2016**, 91(3): 136-153.
13. Chatellier, X., Bottero, J.Y., and Le Petit, J., Adsorption of a cationic polyelectrolyte on *Escherichia coli* bacteria: 1. Adsorption of the polymer. *Langmuir*, **2001**, 17(9): 2782-2790.

14. Chatellier, X., Bottero, J.Y., and Le Petit, J., Adsorption of a cationic polyelectrolyte on Escherichia coli bacteria: 2. Interactions between the bacterial surfaces covered with the polymer. *Langmuir*, **2001**, 17(9): 2791-2800.
15. Johnson, D.W., New applications for poly(ethylene-alt-maleic anhydride). **2010**, Durham University.
16. He, G., Tian, L., Fatona, A., Wu, X., Zhang, H., Liu, J., Fefer, M., Hosseinidoust, Z., and Pelton, R.H., Water-soluble anionic polychloramide biocides based on maleic anhydride copolymers. *Colloids and Surfaces, B: Biointerfaces*, **2022**, 215: 112487.
17. Chick, H., An investigation of the laws of disinfection. *Journal of Hygiene*, **1908**, 8(1): 92-158.
18. Watson, H.E., A note on the variation of the rate of disinfection with change in the concentration of the disinfectant. *Epidemiology & Infection*, **1908**, 8(4): 536-542.
19. Evans, D.F. and Wennerström, H., The colloidal domain: where physics, chemistry, biology, and technology meet. **1999**, New York: Wiley-VCH. 374.
20. Semenova, A.S., Leitman, M.I., Stefanovich, L.G., and Shalayeva, L.F., The copolymerization of ethylene with maleic anhydride. *Polymer Science U.S.S.R.*, **1972**, 14(10): 2470-2473.
21. Wang, Z. and Pelton, R., Chloramide copolymers from reacting poly (N-isopropylacrylamide) with bleach. *European Polymer Journal*, **2013**, 49(8): 2196-2201.
22. Gyürék, L.L. and Finch, G.R., Modeling Water Treatment Chemical Disinfection Kinetics. *Journal of Environmental Engineering*, **1998**, 124(9): 783-793.
23. Haas, C.N. and Joffe, J., Disinfection under dynamic conditions: modification of Hom's model for decay. *Environmental science & technology*, **1994**, 28(7): 1367-1369.
24. Jensen, J.N., Disinfection model based on excess inactivation sites: implications for linear disinfection curves and the Chick-Watson dilution coefficient. *Environmental Science & Technology*, **2010**, 44(21): 8162-8168.
25. Akdag, A., Okur, S., McKee, M.L., and Worley, S., The stabilities of N-Cl bonds in biocidal materials. *Journal of Chemical Theory and Computation*, **2006**, 2(3): 879-884.
26. Gottardi, W. and Nagl, M., Chlorine covers on living bacteria: the initial step in antimicrobial action of active chlorine compounds. *Journal of Antimicrobial Chemotherapy*, **2005**, 55(4): 475-482.

Chapter 4

Impacts of Non-microbial Soils on Polychloramides Disinfectants

To investigate the impacts of organic soils on the biocidal activity of an anionic polychloramide, a cationic polychloramide, and a cationic quaternary ammonium polymer, a series of model soils such as polyacrylic acid (PAA), cellulose nanocrystals (CNCs), bovine serum albumin (BSA), ammonium chloride, glycine, and (1-(hydroxymethyl)-5,5-dimethylhydantoin (HDMH), were applied. Possible impact mechanisms of various soils were discussed and identified with sequestration, extraction of oxidative chlorine, and enhancement.

The data within this chapter were collected and summarized by me with the assistance of Mr. Chaochen Song, who worked as a summer student. The cationic polymer was prepared by Dr. Fatona. The GPC measurements of polymers were performed by Mr. Alexander Jesmer. Dr. Tian and Dr. Hosseinidoust provided laboratory facilities and advice on microbiological work. I wrote the first draft and Dr. Robert Pelton re-wrote the manuscript as necessary.

Impacts of Non-microbial Soils on Polychloramides Disinfectants

Gaoyin He, Ayodele Fatona, Lei Tian, Chaochen Song, Jun Liu, Michael Fefer, Zeinab Hosseinidoust, and Robert H. Pelton

This chapter is in preparation for publication.

Impacts of Non-microbial Soils on Polychloramides Disinfectants

Gaoyin He ^a, Ayodele Fatona ^a, Lei Tian ^a, Chaochen Song, ^a Jun Liu ^b, Michael Fefer ^b, Zeinab Hosseinidoust ^a, and, Robert H. Pelton ^{a,*}

^a Department of Chemical Engineering, McMaster University, Hamilton, Ontario, Canada, L8S 4L7

^b Suncor AgroScience, 2489 North Sheridan Way, Mississauga, ON L5K 1A8, Canada

*Corresponding author: *peltonrh@mcmaster.ca

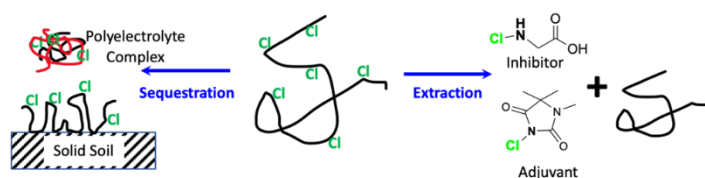
Keywords:

soil load, organic burden, polychloramide charge, soil mechanisms

Abstract

Nonmicrobial chemicals, herein called “soils”, are known to degrade the performance of biocides, and biocidal assays often include mixtures of materials to mimic the effects of soils. The relationships between soil composition and antimicrobial polymer biocidal activity were compared for an anionic polychloramide, a cationic polychloramide, and a cationic poly(quaternary ammonium) biocide. Pure one-component model soils were employed. The nanoscale soil models individually investigated were polyacrylic acid (PAA), cellulose nanocrystals (CNCs), and bovine serum albumin. The low molecular weight model soils were ammonium chloride, glycine, and (1-(hydroxymethyl)-5,5-dimethylhydantoin (HDMH), a cyclic low molecular weight imide. Three types of soil impacts were identified: 1) sequestration whereby the soil physically inhibited the biocide interaction with microbes; 2) extraction whereby the soil reduced or extracted oxidative chlorine decreasing or eliminating the oxidative chlorine strength; and, 3) enhancement whereby the biocidal activity increases in the presence of a soil acting as an adjuvant. PAA and CNCs inhibit cationic biocides by sequestration but have little impact on anionic polychloramide. Glycine and BSA extract oxidative chlorine, lowering the biocidal activity of the anionic and cationic polychloramides while not impacting the poly(quaternary ammonium) biocide. Finally, HDMH increased bacteria deactivation of both anionic and cationic polychloramides. We propose that HDMH is an adjuvant that extracts oxidative chlorine from the polychloramides and transports it to the bacteria.

Index Graphic



Introduction

Aqueous chlorine bleach (NaOCl) is an important disinfectant for potable water treatment, swimming pools, and as a constituent of cleaning products for floors and other surfaces. [1] However, dilute bleach treatment provides little residual protection once a cleaned surface dries because the bleach residuals are volatile. [2, 3] Consumer products exist that leave an antimicrobial polymer film on a cleaned surface. In one case, a mixture of low molecular weight biocides embedded in the polymer provides residual antimicrobial activity. [4] A polymer film providing extended antimicrobial protection is a good idea. However, low molecular weight organic biocides may not be ideal. As stated by Worley, polymeric biocides are not volatile, do not pass through skin, and should be less challenging to the environment compared to low molecular weight biocides. [5] Therefore, we have been exploring using one-component polychloramides [6] as post-cleaning treatments for surfaces cleaned with bleach-based products. Polychloramides are obvious choices for bleach-treated surfaces because, like bleach, the active component in polychloramides is oxidative chlorine, which is present as N-Cl moieties. [7] This paper explores the hypothesis that negatively charged (anionic) polychloramides could be more effective than their positively charged (cationic) counterparts. With more than 1000 publications [8] describing almost exclusively cationic synthetic polymers and antimicrobial proteins, our hypothesis is controversial.

Our hypothesis developed from the supposition that in contaminated samples, non-microbial materials will negatively impact cationic water-soluble antimicrobial polymers more than anionic polymers. The non-microbial chemical materials that can consume biocides are called “soil load” or “organic burden” [9] – for brevity, “soil” is used herein. The US Environmental Protection Agency proposes 5% (v/v) blood serum as a soil additive in biocidal assays. [9] Compared in this contribution are the influences of a series of model soils on the biocidal activity of an anionic polychloramide, a cationic polychloramide, and a cationic quaternary ammonium polymer. All are water soluble with similar molecular weights and structures.

One-component, well-defined materials have been chosen as model soils. Our water-soluble model soils were further subdivided as low molecular weight molecules or nano-sized polymers. The negative impacts of specific soil types on polychloramide disinfection presented are explained by one or both of two broad mechanisms: 1) sequestration – the partial or complete capture of polychloramide chains inhibiting transport to and/or adsorption on bacteria surfaces; and 2) extraction of oxidative chlorine either by reduction to chloride or transfer of Cl^+ to other molecules.

Sequestration of polychloramides includes adsorption at solid/water interfaces or by forming polyelectrolyte complexes with oppositely charged water-soluble polymers. The polymer adsorption literature is rich [10], and the most important forces driving adsorption are electrostatic and hydrophobic interactions. Polymer adsorption tends to be irreversible. Polyelectrolyte complexation has been extensively studied. [11, 12] The main conclusions from the literature are: 1) like adsorption on a solid surface,

complexation is driven by the entropy gain afforded by the release of counterions; 2) complexation is irreversible; 3) complexes are usually present somewhere in the continuum between colloidal microgels and low water-content nanoparticles; [13] 4) polyelectrolyte complexes are always accompanied by excess polymer in solution; and 5) the charge of the polymer in excess dictates the net charge of the complexes.

Extracting oxidative chlorine from polychloramides can follow multiple pathways, including hydrolysis in water, giving HOCl/NaOCl, [14] direct exchange following contact with soil nitrogen, [15] or by reducing oxidative chlorine by species such as disulfide moieties. [16] The hydrolysis equilibrium constants follow the order chlorimide>chloramide>chloramine [14]. Finally, chlorimides are more effective biocides than chloramides which, in turn, are more effective than chloramines. [17]

Experimental

Materials. N-Isopropylacrylamide (NIPAM, 99%), purchased from Thermo Fisher Scientific (New Jersey, NJ), was purified by recrystallization with hexane. Glycine, ammonium chloride (ACS reagent, $\geq 99.5\%$), Isopropylamine ($\geq 99\%$), diallyldimethyl ammonium chloride solution (DADMAC, 65 wt% in H₂O), and tetramethylethylenediamine ($\geq 99.5\%$), bovine serum albumin (BSA, lyophilized powder, >96%, ~66 kDa), poly(ethylene-alt-maleic anhydride) (PEMA, average Mw 100–500 kDa), poly(acrylic acid) (PAA, average Mw ~450 kDa), Luria-Bertani (LB) broth, LB agar, sodium thiosulfate (Na₂S₂O₃, >99%), N, N-dimethylformamide anhydrous (DMF, 99.8%), and sodium hypochlorite (NaOCl, 10–15%) were purchased from Sigma-Aldrich (Canada). 0.001 N potassium polyvinyl sulfate (PVSK) and 0.001 N poly(diallyldimethyl ammonium chloride) (PDADMAC) were obtained from BTG Americas Inc. (US). 1-(hydroxymethyl)-5,5-dimethylhydantoin (HDMH, >98.0%) was purchased from TCI America.

The *Escherichia coli* (*E. coli* 13127) was purchased from the German Collection of Microorganisms and Cell Cultures GmbH. *Staphylococcus aureus* (*S. aureus* MZ100) was obtained from stocks held within Dr. Michael Surette, McMaster University. 12.2 wt % cellulose nanocrystals (CNC) containing 0.85 wt % sulfur were produced by the U.S. Forest Products Laboratory (FPL) and provided by the University of Maine Process Development Center (batch number 2015-FPL-CNC-071).

Mütek Polyelectrolyte Titrations. The net charge of soluble polymers was measured by polyelectrolyte titration with 0.001 N PVSK for cationic polymers or 0.001 N PDADMAC titrants for anionic polymers. The titration endpoints were detected with a Mütek PCD 03 (BTG, Switzerland) streaming current detector. The polyelectrolytes were dissolved into 1 mM pH=7.4 phosphate buffer. The PCD LabX software gave the titrant volumes corresponding to zero streaming potential. The net charge results were reported as meq/g of dry polymer.

Overlap Concentrations, C^* . The C^* values of the polymers were estimated as the reciprocal of the intrinsic viscosity. The viscosities were measured with an Ubbelohde viscometer (CUC-75 Cannon Company), suspended in a 25 °C bath. Polymer solutions were prepared $\times 1$ PBS buffer in concentrations varying from 5 to 20 mg/mL, and the flow time of the buffer solution was 105 s. Both the Huggins [18] and Kraemer plots are shown in **Figure S4-4**. In most cases, the two extrapolations gave similar results.

CNC Dispersions. 45 mg/mL CNC dispersions were prepared by redispersion in deionized water and sonicated 3 times for 5 min and were then passed through a VWR® glass microfiber filter (pore size 1.1 μm) to remove trace aggregates.

Electrophoretic Mobility. Typically, 1 mL of $\sim 10^9$ CFU/mL Gram-negative *E. coli* in the nutrient-rich bacterial suspensions were washed twice with 1 mM pH 7.4 KCl solution through centrifugation at 6000g for 10 min at 4 °C in sterile 1.5 mL microcentrifuge tubes. Then, the resulting bacteria pellet *E. coli* were mixed with 1 mL antimicrobial polymer (1 mg/mL) in sterile 1.5 mL microcentrifuge tubes and were placed in a shaker (SCIOGEX SK-D1807-E Rocker) at a frequency of 80 1/min at room temperature for 20 min. Then, the bacteria were isolated by centrifugation at 6000 g for 5 min and washed twice with 1 mL of 1 mM KCl solution. The resulting bacteria pellets were resuspended in 5 mL of 1 mM KCl solution,[19] giving a final bacteria concentration of $\sim 2 \times 10^8$ CFU/mL. Samples were placed in disposable folded capillary cells (DTS1070) and measured in triplicate. Electrophoretic mobilities of bacteria with and without the addition of polychloramides in 1 mM pH 7.4 KCl solution were determined using a Zetasizer Nano ZSP (Brookhaven Instruments, US).

Bactericidal Concentration (BC). In a typical experiment, a series of sterile 1.5 mL microcentrifuge tubes were filled with 990 μL 1xPBS buffer containing a range of polychloramide concentrations. 10 μL of bacteria suspension in buffer was added, giving bacteria concentrations around 10^7 CFU/mL. The sealed tubes were placed in a SCIOGEX SK-D1807-E Rocker at a frequency of 80 1/min at room temperature for 1 h. After that, 10 μL of bacteria suspension quenched by 190 μL 0.1 M $\text{Na}_2\text{S}_2\text{O}_3$ solution was transferred to LB agar plates. The number of bacterial colonies was recorded after LB agar plates were incubated at 37 °C overnight. The BC results are reported as a range, x-y, where x is the largest biocide concentration with viable bacteria after 1 h, and y is the lowest biocide concentration giving no growth for a detection limit of 100 CFU/mL.

Bacterial Killing in the Presence of Model Soils. The antibacterial efficacies of the three polymeric biocides were measured individually in the presence of each of the model soils. For example, 0.5 mL of 1 wt/vol% CP0 was added to 0.25 mL 1 wt/vol% BSA and 0.24 mL $\times 1$ PBS buffer in a sterile 1.5 mL microcentrifuge tube at room temperature. It was shaken in a SCIOGEX SK-D1807-E Rocker at a frequency of 80 min^{-1} for 1 h at room temperature. Then, 10 μL *E. coli* or *S. aureus* suspension was added to 0.99 mL of the soil/polymer mixture, giving a total volume of 1 mL with approximately 10^7 CFU/mL bacteria. After 1 h shaking at room temperature, 10 μL suspensions were quenched by adding 190 μL of $\text{Na}_2\text{S}_2\text{O}_3$ solution. Serial dilutions with sterile PBS buffer were carried

out, and 50 μL aliquots were transferred to LB agar plates, which were incubated at 37 $^{\circ}\text{C}$ overnight. The detection limits were 400 CFU/mL.

Results and Discussion

Polychloramides. Three types of polyamides were employed, and their structures are shown in **Figure 4-1**. CP0, a copolymer of N-isopropylacrylamide and diallyldimethyl ammonium chloride, was synthesized, [20] and the experimental details, including NMR characterization, are given in the supporting information. CP2.5 was prepared by chlorinating CP0 with NaOCl. The preparation and characterization of AP2.3 were described in detail in a previous publication. [6] The three polymers are soluble in water and PBS buffer. CP0 and AP0 have the same chlorinated isopropylamine moieties. CP0 also has quaternary ammonium groups, whereas AP0 has carboxylic acid groups.

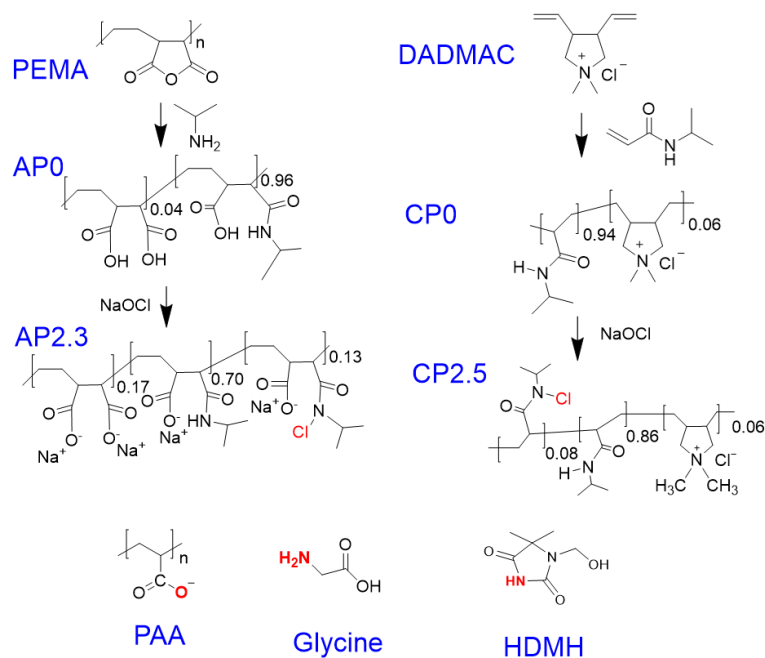


Figure 4-1 Structures of cationic polychloramide CP2.5, cationic polyquat CP0, and anionic AP polychloramide AP2.3, where the numbers are the oxidative chlorine mass fraction. PAA (polyacrylic acid), HDMH (1-(hydroxymethyl)-5,5-dimethylhydantoin), and glycine are model soil components.

Table 4-1 summarizes some properties of the polymers used herein. The weight-average molecular weight of CP0 was 1.6 times greater than the MW of AP0. C^* is the overlap concentration estimated from intrinsic viscosity measurements, $C^* \cong 1/[\eta]$. [21] The larger C^* , the more compact the polymer coils. Additionally, C^* is an estimate of the polymer concentration within the volume occupied by an isolated polymer chain in a dilute solution. We have argued previously that disinfection rates in the presence of water-soluble anionic polychloramides increase with C^* . [22] A comparison of C^* values for CP0 and AP0 is interesting. Although CP0 has a higher molecular weight than AP0, CP0 is far more compact, as evidenced by a higher C^* . This difference reflects the net charge contents. AP0 has ten times more charge than CP0, and intramolecular electrostatic repulsion drives chain expansion, reducing C^* . We have reported before that chlorinating a water-soluble polychloramide increases the polymer hydrophobicity, causing chain collapse (i.e., an increase in C^*) and precipitation if the Cl content is high. [23] With the transition of CP0 to CP2.5, there is a doubling of C^* , whereas the AP0 transition to AP2.3 gave a 5 times increase in C^* . It is, therefore, a lucky coincidence that C^* for CP2.5 is equal to that of AP2.3, thus making this polychloramide polymer pair ideal for comparison of the role of electrical charge in disinfection.

Table 4-1 Properties of the polymeric reagents.

Polymer	Name	MW _m (kDa)	Cl Mass Fraction	C* in PBS (mg/mL)	Net Charge Structure (meq/g)	Net Charge Titration ^d (meq/g)
Cationic polyamide	CP0	190 (PDI 2.1)	0	11.9±0.6	+0.50	+0.6
Cationic polychloramide	CP2.5	194	2.5	19.9±1.2	+0.50	+0.7
Anionic Polyamide	AP0	118 ^c	0	3.8±0.1 ^b	-5.0 ^a	-5.0
Anionic Polychloramide	AP2.3	121	2.3	19.5±1.1 ^b	-5.0 ^a	-5.1
Poly(acrylic acid)	PAA	450	0	1.9±0.1	-11.6 ^a	-12.9
Bovine Serum Albumen	BSA	66.5	0	-	-	-0.93

^a Assuming carboxylic acid groups are present as sodium salts.

^b From reference [22]

^c From reference [6]

^d Measured in 1 mM phosphate buffer at pH 7.4.

The net charge content of the polymers was estimated from the polymer structures in **Figure 4-1** and measured by polyelectrolyte titration; [24] the two analyses gave good agreement. The anionic polymers AP0 and AP 2.3 had ten times more negatively charged groups than the cationic charge contents of CP0 and CP2.5. PAA, a model soil, had a very high charge density.

Soil-free Disinfection. The literature suggests that both polymeric chloramides [7, 15, 25, 26] and quats [27] require direct contact with microbe surfaces for biocidal activity. Upon contact, polychloramides transfer oxidative chlorine atoms to nitrogen atoms on the bacteria, or oxidative chlorine is reduced by contacting thiol groups. By contrast, chemically inert quaternary ammonium groups quats fixed to the polymer and are not consumed. The biochemical mechanisms by which oxidative chlorine [7] [28] [29] or quats [27] deactivate bacteria have been discussed by many others, and we have nothing to add.

Table 4-2 summarizes the results of two experiments with soil-free mixtures of bacteria and polymers. First, electrophoretic mobilities measured in 1 mM KCl solution at pH 7.4 were used to determine if polymer adsorbed onto bacteria surfaces. The anionic AP0 and AP2.3 did not influence the electrophoretic mobility of *E. coli* and *S. aureus*, indicating no polymer adsorption on either bacteria type. Whereas exposure to cationic CP0 or CP2.5 reversed the sign of the net charge on both types of bacteria, indicating adsorption.

Table 4-2 Summary of electrophoretic mobilities and bactericidal concentrations in soil-free conditions.

	Electrophoretic Mobility ($\text{MU} = 10^{-8} \text{ m}^2 \text{ V}^{-1} \text{ s}^{-1}$)				
	Bactericidal Concentration (BC) for 5 log Reduction in 1 h Incubation ^c				
	No polymer	CP0 ^b	CP2.5 ^b	AP0 ^b	AP2.3 ^b
<i>E. coli</i> ^a	-3.2±0.2 MU -	0.5±0.1 MU 10-15 mg/mL	1.2±0.1 MU 2-5mg/mL	-3.2±0.2 MU No killing	-3.3±0.1 MU 15-20 mg/mL
<i>S. aureus</i> ^a	-2.2±0.2 MU -	0.5±0.1 MU 2-5 mg/mL	0.6±0.1 MU 2-5 mg/mL	-2.4±0.1 MU No killing	-1.9±0.1 MU 15-20 mg/mL

^a The initial bacteria concentration was $\sim 10^9$ CFU/mL for the adsorption experiments. ^b 1 mg/mL polymer. ^c The initial bacterial concentration was $\sim 10^7$ CFU/mL for determining the BC values.

Below each mobility value is the corresponding biocidal concentration (BC). The unchlorinated CP0 had a BC of 10-15 mg/mL, reflecting the biocidal properties of the quaternary ammonium groups. The chlorinated CP2.5 was more effective (2-5 mg/mL). The anionic AP2.3 was much less effective than CP2.5, and AP0 has no biocidal activity. These results explain the popularity of cationic biocidal polymers.

Model Soils. Presented in the following sections are results showing the influence of model soil materials, chosen to span a range of properties: water-insoluble cellulose nanocrystals (CNCs); water-soluble high molecular weight macromolecules, polyacrylic acid (PAA) and bovine serum albumin (BSA); and, soluble low molecular weight soils (glycine, HDMH, and ammonium chloride). The structures of PAA and HDMH are shown in **Figure 4-1**. The polymeric biocides were first mixed with the model soil in PBS buffer for 1 h, after which the bacteria were added. The concentration of viable bacteria was measured after 1 h of exposure to the biocide/soil mixtures. The impacts of the model soils on bacteria viability were modest in the absence of polymeric biocides – see **Table S4-(3-5)** and **Table S4-1** in the supporting information file.

Insoluble soil. **Table 4-3** summarizes the impacts of CNC particles on the activities of three polymeric biocides. The CNCs are cellulose particles colloidally stabilized by surface sulfate ester groups, typically giving a surface charge density of 0.06-0.1 C/m². [30] The product specification of our material included a characteristic CNC dimension of 150x50x5 nm³. CNC particles have no nitrogen atoms to accept Cl⁺ and very limited ability to reduce active chlorine. Summarizing, CNCs provide an inert, anionic surface. Without biocide, CNC slightly reduced bacteria concentration – compare R#1 with #2 in **Table 4-3**. CNC interfered with the cationic poly(quaternary ammonium), CP0, and with the chlorinated CP2.5, whereas the presence of CNC particles did not impact the anionic AP2.3. The obvious explanation is that CP2.5 polymers adsorbed onto CNC surfaces, presumably forming large, water-swollen aggregates, inhibiting polymer transport to the bacteria surfaces. Both types of bacteria gave similar responses.

Table 4-3 The influence of cellulose nanocrystals (CNC) on antimicrobial polymers.

R#	CNC (mg/mL)	Biocide Type	Biocide Conc. (mg/ml)	<i>E. coli</i> (CFU/mL)	<i>S. aureus</i> (CFU/mL)
1	0	-	-	1.7×10 ⁷	4.3×10 ⁶
2	23	-	-	3.9×10 ⁶	1.7×10 ⁶
3	0	CP0	10	<DL*	<DL*
4	23	CP0	10	1.4×10 ⁵	2.7×10 ⁵
5	0	CP2.5	10	<DL*	<DL*
6	23	CP2.5	10	3.3×10 ⁶	3.2×10 ⁴
7	0	AP2.3	10	<DL*	<DL*
8	23	AP2.3	10	<DL*	<DL*

*Detection Limit 4×10² CFU/mL.

Soluble High Molecular Weight Soils. We have employed polyacrylic acid (PAA) and bovine serum albumin (BSA) as high MW, water-soluble model soils. Polyacrylic acid is a linear, hydrophilic polymer with a carboxylic acid group on every other backbone carbon – see **Figure 4-1**. Fully ionized PAA is highly negatively charged (11 meq/g), a value 20 times greater than the positive charge density of CP0. **Table 4-4** summarizes the influence of PAA on the three polymeric biocides. Without biocide, PAA did not influence the bacteria concentrations (compare row #1 with #2). Also, PAA did not influence the biocidal activity of anionic AP2.3, which was expected because polyelectrolyte complexes do not usually form between like-charged polymers. Both cationic biocides, CP0 and CP2.5, were inhibited by PAA. However, the adverse effects of PAA were overcome when the CP2.5 concentration was doubled (compare rows #6 with #7). The ability to overcome adverse soil effects by excess biocide addition is predicted by both polychloramide sequestration and oxidative chlorine extraction mechanisms.

Table 4-4 Influence of polyacrylic acid (PAA) on antimicrobial polymers.

R#	PAA (mg/mL)	Biocide Type	Biocide Conc. (mg/ml)	E. coli (CFU/mL)	S. aureus (CFU/mL)
1	0	-	-	1.7×10^7	4.3×10^6
2	5	-	-	1.8×10^7	3.4×10^6
3	0	CP0	10	<DL*	<DL*
4	5	CP0	10	1.0×10^6	3.9×10^6
5	0	CP2.5	10	<DL*	<DL*
6	5	CP2.5	10	1.0×10^6	3.3×10^6
7	5	CP2.5	20	<DL*	<DL*
8	0	AP2.3	10	<DL*	<DL*
9	5	AP2.3	10	<DL*	<DL*
10	5	AP2.3	20	<DL*	<DL*

*Detection Limit 4×10^2 CFU/mL.

BSA, a common model soil in biocide assays, is a water-soluble protein that can extract oxidative chlorine from polychloramide by both the transfer and reduction mechanisms. About 50 N-Cl moieties are formed per BSA molecule (chlorine transfer), as well as sulfonyl chloride groups ($-\text{SO}_2\text{Cl}$). [16] The anionic and cationic polychloramides were inhibited by the presence of BSA - see **Table 4-5**. BSA forms polyelectrolyte complexes with the cationic polymer PDADMAC. [31, 32] Presumably, BSA also complexes with cationic polychloramides

We could not measure valid dynamic light scattering results when mixing BSA with AP2.3, suggesting no formation of colloids by complexation. Therefore we propose that Cl^+ extraction was the primary mechanism by which BSA interacts with anionic polymer. Finally, with BSA, there is more of a dependence on the type of bacteria compared to the other solid or high molecular weight soils.

Table 4-5 The influence of BSA on polymeric biocide activities.

R#	BSA (mg/mL)	Biocide Type	Biocide Conc. (mg/mL)	E. coli (CFU/mL)	S. aureus (CFU/mL)
1	0	-	-	1.7×10^7	4.3×10^6
2	2.5	-	-	2.2×10^7	2.5×10^6
3	0	CP0	5	5.1×10^5	<DL*
4	2.5	CP0	5	1.3×10^6	1.0×10^6
5	0	CP2.5	5	<DL*	<DL*
6	2.5	CP2.5	5	2.6×10^5	2.0×10^5
7	0	AP2.3	10	<DL*	<DL*
8	2.5	AP2.3	10	<DL*	3.1×10^6
9	2.5	AP2.3	20	<DL*	5.1×10^5

*Detection Limit 4×10^2 CFU/mL.

Soluble Low MW Soil. Glycine, HDMH, and ammonium chloride were evaluated as model soils. The structures of glycine and HDMH are shown in **Figure 4-1**. Low molecular weight molecules are unlikely to sequester the large polychloramide molecules leaving Cl^+ extraction as a potential interaction mechanism. The results are summarized in **Figure 4-2**. The HDMH gave the most dramatic results. In every case, premixing HDMH with polychloramide for 60 min improved disinfection. This implies the transfer of oxidative chlorine from polyamide to the low molecular weight HDMH. Chlorimides are known to be effective biocides, [33] and the small nonionic molecule could rapidly diffuse to and possibly into bacteria. One might expect that chlorine transfer from chloramide to an HDMH would not be favored compared to the reverse reaction. Qian

and Sun reported slow chlorine transfer from chloramine amine to succinimide [33], suggesting that transfer from chloramide to HDMH is possible. To summarize, HDMH appears to act as an effective shuttle transferring oxidative chlorine to the bacteria.

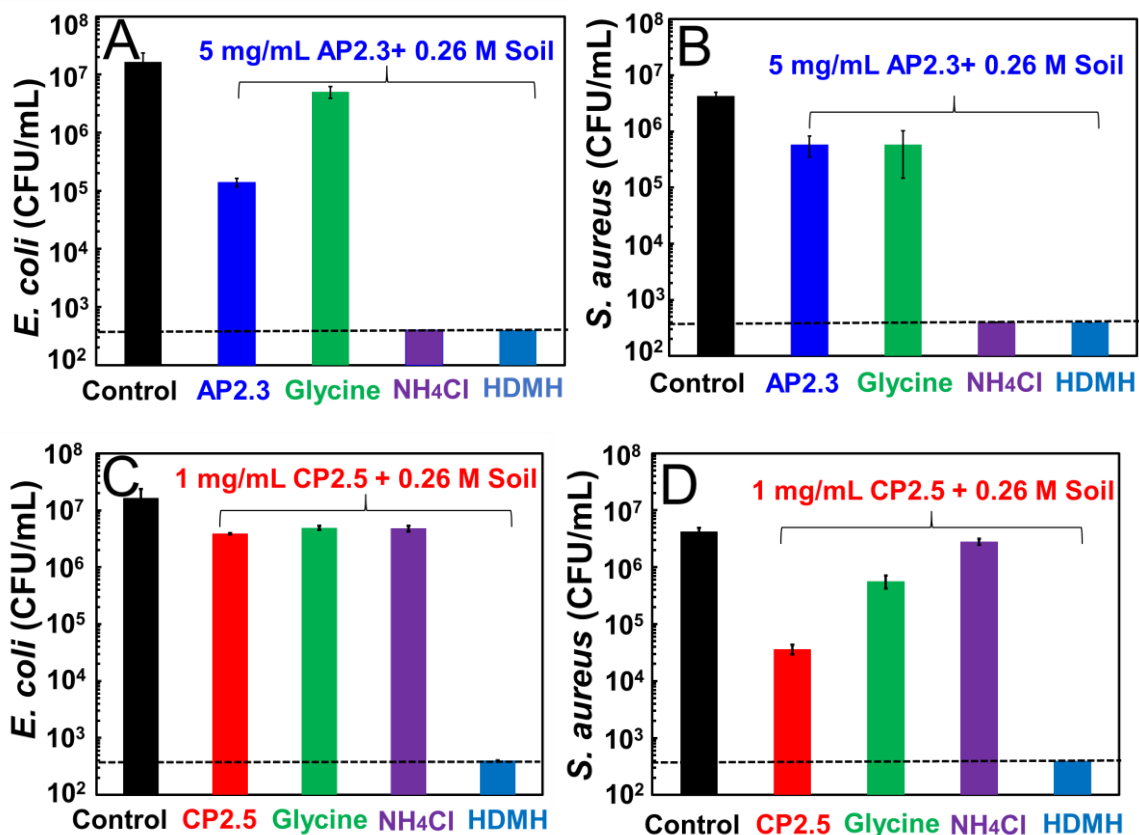


Figure 4-2 The influence of low molecular weight model soils (0.26 M) on the activity of cationic and anionic polychloramides in 1x PBS buffer. “HDMH” is 1-(Hydroxymethyl)-5,5-dimethylhydantoin. The horizontal dashed line is the detection limit.

Glycine inhibits polychloramide function for most cases in **Figure 4-2**, suggesting that N-chloroglycine is not a potent biocide. More results showing the influence of glycine on AP2.3 as a function of polychloramide concentration are shown in **Figure S4-3**. Ammonium chloride enhanced AP2.3 performance, whereas it inhibited CP2.5 performance.

Conclusions

Non-microbial materials, which we call soils, are present in most disinfection applications, and some soils can impact the efficiencies of biocides. Reported are the impacts of model soils on the antimicrobial performance of three polymers, a cationic quaternary ammonium polyamide (CP0), a cationic polychloramide (CP2.5), and an anionic polychloramide (AP2.3). Model soil components, individually investigated, were dispersed cellulose nanocrystals (CNC), soluble PAA (polyacrylic acid), BSA (bovine serum albumen), ammonium chloride, glycine, and 1-(hydroxymethyl)-5,5-dimethylhydantoin (HDMH). The main conclusions were:

1. The negative impacts of specific soil types on polychloramide disinfection can be explained by one or both of two mechanisms: 1) sequestration – the partial or complete capture of polychloramide chains inhibiting transport to and adsorption on bacteria surfaces; and 2) extraction of oxidative chlorine either by reduction or transfer of Cl^+ to other molecules.
2. Soils that can sequester polychloramides include macroscopic solids, dispersed solids, and soluble polymers. Electrostatic interactions drive adsorption onto solid interfaces and polyelectrolyte complexation with oppositely charged water-soluble soil polymers. Since most surfaces and water-soluble polymers in the environment are negatively charged, cationic polychloramides are more susceptible to sequestration than are anionic polychloramides.
3. Low molecular weight, water-soluble soils that extract oxidative chlorine from polychloramides can inhibit or enhance disinfection. Glycine extracts chlorine from polychloramide to give N-chloroglycine that has low biocidal activity and thus degrades the performance of polychloramides. By contrast, HDMH increases the biocidal activity of both anionic and cationic polychloramides. We propose that HDMH is an adjuvant that extracts oxidative chlorine from the polymers and transports chlorine to the bacteria more efficiently than direct polymer/bacteria contact.
4. BSA, a commonly used surrogate for soil in biocide assays, deactivates cationic polychloramides by two mechanisms sequestration (complex formation) and chlorine extraction, whereas only extraction is operative with anionic polychloramide.
5. The performance of both cationic and anionic polychloramides can be degraded by soils that extract oxidative chlorine, whereas only cationic polychloramides are particularly susceptible to sequestering soils.

There are two important implications from our results. Anionic antimicrobial polymers could have advantages over cationic counterparts, particularly in highly soiled applications. In addition, when adding model soils to antimicrobial assays, a separate assessment of pure sequestering soils and extractive soils may offer enhanced mechanistic insights into inhibition mechanisms compared to results from experiments using complex soil mixtures.

Supporting Information

The file includes descriptions of the synthesis and characterization of CP0 and CP2.5, additional *E. coli* results with glycine and AP2.3, and the viscosity curves for intrinsic viscosity and C^* of the polymers.

Acknowledgments

We thank the Natural Sciences and Engineering Research Council of Canada (NSERC) and Suncor Energy for funding this project. We thank Mr. Alexander Jesmer for performing the GPC measurements. Prof. Ryan Wylie is thanked for giving access to his GPC. R. H. Pelton holds the Canada Research Chair in Interfacial Technologies, and Zeinab Hosseinidoust holds the Canada Research Chair in Bacteriophage Bioengineering.

References

1. Rutala, W.A. and Weber, D.J., Guideline for disinfection and sterilization in healthcare facilities, 2008 Update: May 2019. **2019**, Centers for Disease Control (CDC) p. 1-163.
2. Wojtowicz, J.A., Dichlorine monoxide, hypochlorous acid, and hypochlorites. *Kirk-Othmer Encyclopedia of Chemical Technology*, **2004**, 8: 544-581.
3. Wong, J.P.S., Carslaw, N., Zhao, R., Zhou, S., and Abbatt, J.P.D., Observations and impacts of bleach washing on indoor chlorine chemistry. *Indoor Air*, **2017**, 27(6): 1082-1090.
4. Procter&Gamble. *Microban 24 Ingredients List*. 2020 [cited 2020 Nov. 1, 2020]; Available from: <https://smartlabel.pg.com/00037000474159.html>.
5. Kenawy, E.-R., Worley, S., and Broughton, R., The chemistry and applications of antimicrobial polymers: a state-of-the-art review. *Biomacromolecules*, **2007**, 8(5): 1359-1384.
6. He, G., Tian, L., Fatona, A., Wu, X., Zhang, H., Liu, J., Fefer, M., Hosseinidoust, Z., and Pelton, R.H., Water-soluble anionic polychloramide biocides based on maleic anhydride copolymers. *Colloids and Surfaces, B: Biointerfaces*, **2022**, 215: 112487.
7. Dong, A., Wang, Y.-J., Gao, Y., Gao, T., and Gao, G., Chemical Insights into Antibacterial N-Halamines. *Chemical Reviews*, **2017**, 117(6): 4806-4862.
8. Ergene, C., Yasuhara, K., and Palermo, E.F., Biomimetic antimicrobial polymers: recent advances in molecular design. *Polymer Chemistry*, **2018**, 9(18): 2407-2427.
9. anon, Product Performance Test Guidelines OCSPP 810.2000: General Considerations for Testing Public Health Antimicrobial Pesticides Guidance for Efficacy Testing. **2018** Environmental Protection Agency.
10. Fler, G., Stuart, M.C., Scheutjens, J.M., Cosgrove, T., and Vincent, B., *Polymers at interfaces*. **1993**: Springer Science & Business Media.
11. Philipp, B., Dautzenberg, H., Linow, K.J., Koetz, J., and Dawydoff, W., Polyelectrolyte complexes - recent developments and open problems. *Progress in Polymer Science*, **1989**, 14(1): 91-172.
12. Meka, V.S., Sing, M.K.G., Pichika, M.R., Nali, S.R., Kolapalli, V.R.M., and Kesharwani, P., A comprehensive review on polyelectrolyte complexes. *Drug Discovery Today*, **2017**, 22(11): 1697-1706.
13. Bohidar, H., Dubin, P.L., Majhi, P.R., Tribet, C., and Jaeger, W., Effects of protein-polyelectrolyte affinity and polyelectrolyte molecular weight on dynamic

- properties of bovine serum albumin-poly(diallyldimethylammonium chloride) coacervates. *Biomacromolecules*, **2005**, 6(3): 1573-1585.
14. Qian, L. and Sun, G., Durable and regenerable antimicrobial textiles: Synthesis and applications of 3-methylol-2,2,5,5-tetramethyl-imidazolidin-4-one (MTMIO). *Journal of Applied Polymer Science*, **2003**, 89(9): 2418-2425.
 15. Williams, D.E., Elder, E.D., and Worley, S.D., Is free halogen necessary for disinfection? *Applied and Environmental Microbiology*, **1988**, 54(10): 2583-2585.
 16. Debiemme-Chouvy, C., Haskouri, S., and Cachet, H., Study by XPS of the chlorination of proteins aggregated onto tin dioxide during electrochemical production of hypochlorous acid. *Applied Surface Science*, **2007**, 253(12): 5506-5510.
 17. Hui, F. and Debiemme-Chouvy, C., Antimicrobial N-halamine polymers and coatings: A review of their synthesis, characterization, and applications. *Biomacromolecules*, **2013**, 14(3): 585-601.
 18. Huggins, M.L., The viscosity of dilute solutions of long-chain molecules. IV. Dependence on concentration. *Journal of the American Chemical Society*, **1942**, 64(11): 2716-2718.
 19. Polaczyk, A.L., Amburgey, J.E., Alansari, A., Poler, J.C., Propato, M., and Hill, V.R., Calculation and uncertainty of zeta potentials of microorganisms in a 1:1 electrolyte with a conductivity similar to surface water. *Colloids and Surfaces A: Physicochemical and Engineering Aspects*, **2020**, 586: 124097-124097.
 20. Deng, Y. and Pelton, R., Synthesis and solution properties of poly (N-isopropylacrylamide-co-diallyldimethylammonium chloride). *Macromolecules*, **1995**, 28(13): 4617-4621.
 21. Evans, D.F. and Wennerström, H., *The colloidal domain: where physics, chemistry, biology, and technology meet*. **1999**, New York: Wiley-VCH. 374.
 22. Pelton, R.H., He, G., Tian, L., Song, C., and Hosseinidoust, Z., Modeling the Impact of Polychloramide Solution Properties on Bacterial Disinfection Kinetics. *Biomacromolecules*, **2022**, 23: 3919-3927.
 23. Wang, Z. and Pelton, R., Chloramide copolymers from reacting poly (N-isopropylacrylamide) with bleach. *European Polymer Journal*, **2013**, 49(8): 2196-2201.
 24. Pelton, R., Cabane, B., Cui, Y., and Ketelson, H., Shapes of Polyelectrolyte Titration Curves. 1. Well-Behaved Strong Polyelectrolytes. *Analytical Chemistry*, **2007**, 79(21): 8114-8117.
 25. Gutman, O., Natan, M., Banin, E., and Margel, S., Characterization and antibacterial properties of N-halamine-derivatized cross-linked polymethacrylamide nanoparticles. *Biomaterials*, **2014**, 35(19): 5079-5087.

26. Kaur, R. and Liu, S., Antibacterial surface design – Contact kill. *Progress in Surface Science*, **2016**, 91(3): 136-153.
27. Murata, H., Koepsel, R.R., Matyjaszewski, K., and Russell, A.J., Permanent, non-leaching antibacterial surfaces—2: How high density cationic surfaces kill bacterial cells. *Biomaterials*, **2007**, 28(32): 4870-4879.
28. Hawkins, C.L., Pattison, D.I., and Davies, M.J., Hypochlorite-induced oxidation of amino acids, peptides and proteins. *Amino Acids*, **2003**, 25(3): 259-274.
29. Fukuzaki, S., Mechanisms of actions of sodium hypochlorite in cleaning and disinfection processes. *Biocontrol Science*, **2006**, 11(4): 147-157.
30. Reid, M.S., Villalobos, M., and Cranston, E.D., Benchmarking Cellulose Nanocrystals: From the Laboratory to Industrial Production. *Langmuir*, **2017**, 33(7): 1583-1598.
31. Li, Y.J., Mattison, K.W., Dubin, P.L., Havel, H.A., and Edwards, S.L., Light scattering studies of the binding of bovine serum albumin to a cationic polyelectrolyte. *Biopolymers*, **1996**, 38(4): 527-533.
32. Wen, Y.P. and Dubin, P.L., Potentiometric studies of the interaction of bovine serum albumin and poly(dimethyldiallylammonium chloride). *Macromolecules*, **1997**, 30(25): 7856-7861.
33. Qian, L. and Sun, G., Durable and Regenerable Antimicrobial Textiles: Chlorine Transfer among Halamine Structures. *Industrial & Engineering Chemistry Research*, **2005**, 44(4): 852-856.

Supporting Information

Impacts of Non-microbial Soils on Polychloramides Disinfectants

Gaoyin He ^a, Ayodele Fatona ^a, Lei Tian ^a, Chaochen Song, ^a Jun Liu ^b, Michael Fefer ^b, Zeinab Hosseinidoust ^a, and, Robert H. Pelton ^{a,*}

^a Department of Chemical Engineering, McMaster University, Hamilton, Ontario, Canada, L8S 4L7

^b Suncor AgroScience, 2489 North Sheridan Way, Mississauga, ON L5K 1A8, Canada

*Corresponding author: [*peltonrh@mcmaster.ca](mailto:peltonrh@mcmaster.ca)

Table S4-1 The influence of model soils in 1 × PBS on the concentration of colony-forming bacteria after 1 h contact time in the absence of polychloramides

Soil Types	<i>E. coli</i> (CFU/mL)	<i>S. aureus</i> (CFU/mL)
1x PBS only	1.7×10^7	4.3×10^6
Glycine	5.3×10^6	4.7×10^5
NH ₄ Cl	6.2×10^6	4.8×10^5
HDMH	1.7×10^6	3.4×10^5

Synthesis and Characterization of Poly(NIPAM-co-DADMAC) (CP0). The copolymerization was carried out using a previously reported synthetic method with some modifications. [1] The recipe and final composition are summarized **Table S4-2**. Specifically, 2 g (17.7 mmol) of recrystallized NIPAM and 1.1 g (6.8 mmol) of DADMAC were dissolved in 40 mL of degassed MilliQ water in a 250 mL two-neck flask fitted with a nitrogen bubbling tube and a vent. After the system was purged with nitrogen for 30 min while stirring with a magnetic stirrer, 0.001 g of potassium persulfate (KPS) and 0.002 g of tetramethylethylenediamine (TEMED) in 2 mL of degassed MilliQ water were injected into the system, and the reaction was allowed to proceed for 24 h at room temperature. The copolymer was precipitated by adding NaCl at ~50 °C (× 3). The precipitated copolymer was dissolved in water and dialyzed against MilliQ water for 3 days using a Spectra/Por2 regenerated cellulose tubing with a molecular weight cut-off of 12-14 kDa to give a final product which was freeze-dried and stored at room temperature until use.

Table S4-2 CP0 recipe and resulting polymer composition.

Sampl e	Tem p (°C)	KPS (g)	TEME D (g)	Fraction in feed ^a (mol %)		Fraction in polymer ^b (mol %)		M _w (×10 ⁵ Da) ^c
				NIPAM	DADMA C	NIPAM	DADMA C	
CP0 1	23	0.00	0.002	72.3	27.7	94	6	1.88

^a Based on the total monomers. ^b Based on NMR analysis. ^c Based on GPC analysis.

¹H NMR spectra of CP0 in D₂O were measured with a Bruker NEO 600 spectrometer (600 MHz), and chemical shifts were reported in δ (ppm). The proton NMR spectrum of CP0 is illustrated in **Figure S4-1**. These resonance peak assignments are based on the proton peaks of polyDADMAC [2] and poly(diallyl dimethylammonium chloride)-co-poly(N- isopropylacrylamide) (PDDA-co-PNIPAM). [3] For ¹H NMR of polyDADMAC in D₂O, peaks of DADMAC are assigned to c(1.3-1.9 ppm), e(3.6-3.9 ppm), f(3.0-3.4 ppm), g(2.3-2.8 ppm). [4] As for the ¹H NMR of PDDA-co-PNIPAM in D₂O, peaks of NIPAM are a(3.8-4.0 ppm), b(1.0-1.3 ppm), c(1.3-1.9 ppm), and d(1.9-2.3 ppm).

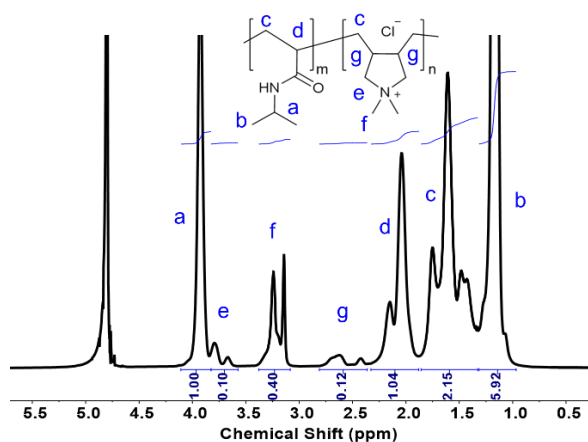


Figure S4-1 Proton NMR spectra of CP0 in D₂O. *m* in CP0 was determined from the peak areas of the peak (a) relative to the peak (a and f/6).

The CP0 molecular weight distribution was measured by Gel Permeation Chromatography (GPC) analysis using an Agilent 1260 infinity RI detector and a GE healthcare Superose 6 Increase 10/300 GL column. A 0.5 N acetic acid/0.2 N sodium nitrate solution was used as the eluent. SEC conditions were as follows: CP0 was dissolved in 1×PBS with 0.5 mg/mL sodium azide and filtered through a 0.45 μm PTFE

disposable membrane before use. After that, 100 μL 1 mg/mL CP0 was injected with a flow rate of 0.5 mL/min. The column temperature was 23 $^{\circ}\text{C}$. The RI detector cell was kept at ambient temperature. The resulting molecular weight distribution is shown in **Figure S4-2**.

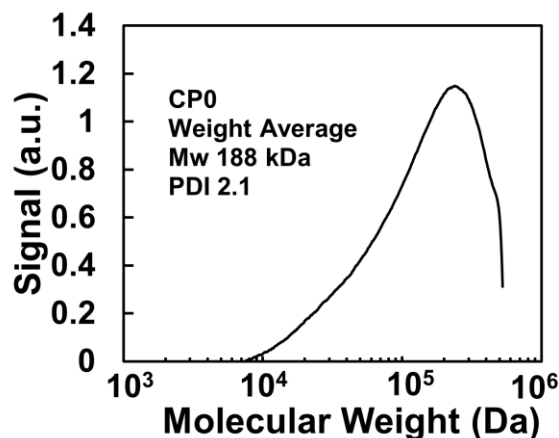


Figure S4-2 Molecular weight distribution of CP0 based on GPC measurements.

Polyamide Chlorination.

CP0 was chlorinated with an aqueous NaOCl. Typically, 5 mL of CP0 solution (3 g/L) and 10 mL of 60 mM NaOCl were combined in a vial, and the solution pH was adjusted to 10.5. Thereafter, the vials were kept at room temperature for 2 h. After a 2 h reaction, the chlorinated polymer was dialyzed against 4 L water for 5 hours to remove unbonded chlorine. The chlorinated polymers were freeze-dried and stored at 4 $^{\circ}\text{C}$.

The oxidative chlorine (Cl^+) contents of AP2.3 and CP2.5 were measured by a standard KI/starch/thiosulfate titration method. [5] An excess amount of KI (around 0.1 g) was added to 5 mL of 1 mg/mL polychloramides (~5 mg) solution, and the solution pH was adjusted to about 3. The solution was titrated with sodium thiosulfate after adding 2 mL of 1% starch indicator.

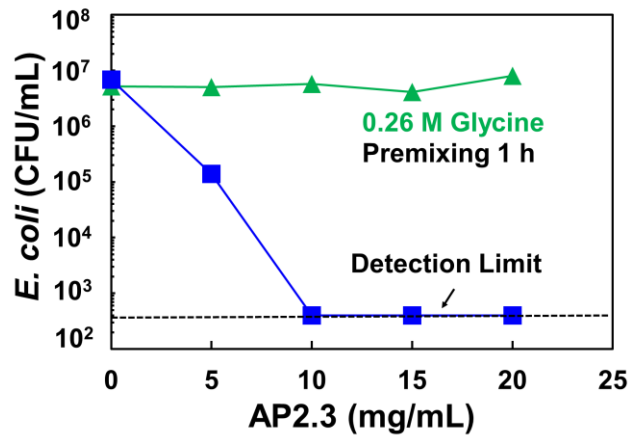
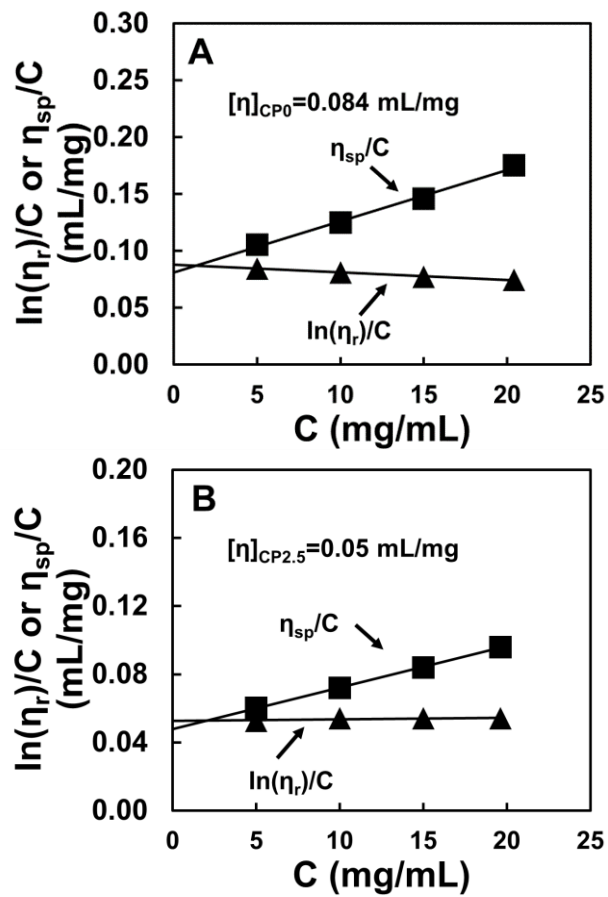


Figure S4-3 Influence of AP2.3 exposure to glycine on antimicrobial activity.



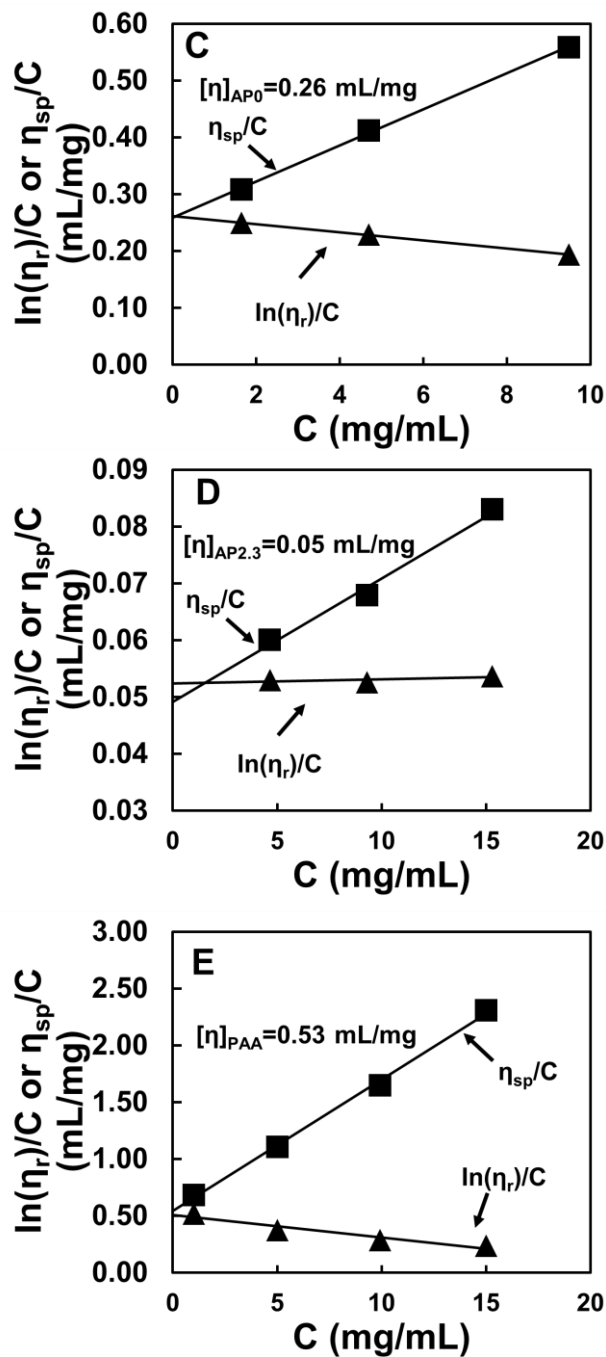


Figure S4-4 Reduced and inherent viscosity for CP0 (A), CP2.5 (B), AP0 (C), AP2.3 (D), and PAA (E) in $1\times$ PBS at $T = 25$ °C. η is the intrinsic viscosity of the polymer.

References

1. Deng, Y. and Pelton, R., Synthesis and solution properties of poly (N-isopropylacrylamide-co-diallyldimethylammonium chloride). *Macromolecules*, **1995**, 28(13): 4617-4621.
2. Donovan, S., Atkinson, A.J., Fischer, N., Taylor, A.E., Kieffer, J., Croue, J.P., Westerhoff, P., and Herckes, P., Nuclear magnetic resonance enables understanding of polydiallyldimethylammonium chloride composition and N-nitrosodimethylamine formation during chloramination. *Environmental Science: Water Research & Technology*, **2021**, 7(6): 1050-1059.
3. Xiang, Y., Banks, M.K., Wu, R., Xu, W., and Chen, S., Synthesis of thermo-sensitive PDDA-co-PNIPAM/graphene hybrid via electrostatic interactions and its thermal modulated phase transition. *Materials Chemistry and Physics*, **2018**, 220: 58-65.
4. Timofeeva, L.M., Kleshcheva, N.A., Moroz, A.F., and Didenko, L.V., Secondary and tertiary polydiallylammonium salts: novel polymers with high antimicrobial activity. **2009**.
5. He, G., Tian, L., Fatona, A., Wu, X., Zhang, H., Liu, J., Fefer, M., Hosseinidoust, Z., and Pelton, R.H., Water-soluble anionic polychloramide biocides based on maleic anhydride copolymers. *Colloids and Surfaces, B: Biointerfaces*, **2022**, 215: 112487.

Chapter 5

Low Molecular Weight Imide Shuttle Molecules Enhance Polychloramide Antimicrobial Activity

To enhance the biocidal property of polychloramides, shuttle chemicals were applied to accelerate the chlorine transfer from polychloramides to bacteria. In this chapter, the synthesis and chlorination of water-soluble, anionic model polyamides (PSC3) were from the reaction of poly(styrene-*alt*-maleic anhydride and primary amine. Three model compounds of small imide shuttle molecules, including 1-(hydroxymethyl)-5,5-dimethylhydantoin (HDMH), 5,5-dimethylhydantoin (DMH), and succinimide (SI), were selected to investigate the chlorine transfer and biocidal influence on polychloramides. In addition, chlorine transfer kinetics between shuttle chemicals and polychloramides were evaluated by centrifugal filter experiment.

The data within this chapter were collected and summarized by me. The chlorination of polymer was prepared by summer student Mr. Chaochen Song. Dr. Tian and Dr. Hosseinidoust provided laboratory facilities and help with the microbiological work. I wrote the first draft and Dr. Robert Pelton re-wrote the manuscript as necessary.

Low Molecular Weight Imide Shuttle Molecules Enhance Polychloramide Antimicrobial Activity

Gaoyin He ^a, Lei Tian ^a, Ayodele Fatona ^a, Chaochen Song ^a, Jun Liu ^b, Michael Fefer ^b, Zeinab Hosseinidoust ^a, and, Robert H. Pelton ^{a,*}

^a Department of Chemical Engineering, McMaster University, Hamilton, Ontario, Canada, L8S 4L7

^b Suncor AgroScience, 2489 North Sheridan Way, Mississauga, ON L5K 1A8, Canada

*Corresponding author: [*peltonrh@mcmaster.ca](mailto:peltonrh@mcmaster.ca)

This chapter is in preparation for publication.

Low Molecular Weight Imide Shuttle Molecules Enhance Polychloramide Antimicrobial Activity

Gaoyin He ^a, Lei Tian ^a, Ayodele Fatona ^a, Chaochen Song ^a, Jun Liu ^b, Michael Fefer ^b, Zeinab Hosseinidoust ^a, and, Robert H. Pelton ^{a,*}

^a Department of Chemical Engineering, McMaster University, Hamilton, Ontario, Canada, L8S 4L7

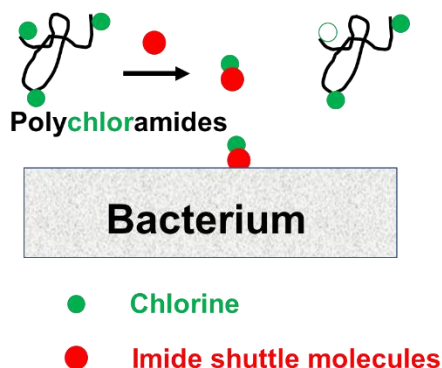
^b Suncor AgroScience, 2489 North Sheridan Way, Mississauga, ON L5K 1A8, Canada

*Corresponding author: [*peltonrh@mcmaster.ca](mailto:peltonrh@mcmaster.ca)

Abstract

An intermolecular chlorine transfer between chloramide and imide groups may impact the antibacterial activity of polychloramides. The key assumption is that low molecular weight imide shuttle molecules can accelerate the oxidative chlorine transfer from polychloramide chains to microbe surfaces. Three model compounds of imide shuttle molecules, including 1-(hydroxymethyl)-5,5-dimethylhydantoin (HDMH), 5,5-dimethylhydantoin (DMH), and succinimide (SI), were employed to investigate chlorine transfer and biocidal influence of polychloramides. The synthesis of polyamides (PSC3) was prepared by the maleic anhydride groups and primary isopropylamine and then chlorinated with bleach to give antimicrobial property. Furthermore, the experimental results reveal that the oxidative chlorine of polychloramides can be transported to small imide shuttle molecules. The oxidative chlorine transfer reaction is the pseudo-first-order rate constant (k_{obs}) to polychloramides, with the order of 10^{-3} min^{-1} . Chlorine shuttle from polychloramides to low molecular weight, water-soluble imides increases the biocidal activity of polychloramides.

Index Graphic



Introduction

Compared to cationic antimicrobial polymers, anionic polychloramides perform advantages in the presence of highly soiled systems such as non-microbial anionic surfaces or soluble materials. [1] The active component of anionic, water-soluble polychloramide biocides is oxidative chlorine in chloramide moieties. [2, 3] Considered now are the oxidative chlorine transports from the polymers with N-Cl moieties to the bacteria surfaces. They include direct transfer, hydrolytic transfer, and shuttle transfer (see **Figure 5-1**). Direct transfer refers to oxidative chlorine from N-Cl molecules to bacterial surfaces directly. Williams et al. [4] found 3-chloro-4,4-dimethyl-2-oxazolidinone (compound 1) prefers to transport chlorine directly to bacteria and this is the primary chlorine transfer path.

The hydrolytic transfer is the release of HOCl from N-Cl molecules reacting with water, following diffusion to bacteria. Most chlorine-containing compounds experience hydrolysis in water and the hydrolysis equilibrium constants are in the order chlorimide>chloramide>chloramine. [5]

Shuttle transfer is the oxidative chlorine transport of a chloramide molecule to a shuttle chemical which then moves to the bacteria. In general, oxidative chlorine from chlorimides to amides or amines can easily be transported due to the electron effect. [6-8] Because the chlorine transfer of chlorimide to amide or amine is a thermodynamically spontaneous process. [9, 10] Antelo et al. [8] found N-chlorosuccinimide and amine reaction were in the forward direction and the direct chlorination reaction step was the rate-controlling step. Similarly, Ahmed et al. [11] confirmed chlorine exchange between the nutrient broth and chlorimides. The components of nutrient broth include peptones and beef extracts with amide groups.

On the other hand, it is also possible with the oxidative chlorine transport of chloramides or chloramines to imide compounds. For example, Higuchi and coworkers verified that the chlorine exchange between succinimide and dimethylchloramine [12] or chloramine-T [13] was not from the hydrolysis of intermediate formation of HOCl but direct chlorine transport. In Qian and coworkers' work [10], the oxidative chlorine of 1-chloro-2,2,5,5-tetramethylimidazolidin-4-one (MC, chloramine) can transport to succinimide in both water and chloroform solutions. However, the reaction rate is very low with the order of 10^{-4} - 10^{-5} mmol/min. In this regard, intermolecular chlorine transfer is possible between nitrogen-containing components. Hypothesized herein is that low molecular weight imide chemicals act as shuttles carrying oxidative chlorine from polychloramides to bacteria.

The biocidal mechanisms of chlorinated polymers may combine two or three oxidative chlorine transport processes. [3] For example, Ahmed et al. [14] found the antimicrobial actions of polychlorimides are based on the direct chlorine transfer to bacteria, hydrolyzed chlorine, and shuttle transfer of chlorine to medium components. Also, the literature suggests that the primary chlorine transport pathway of polychloramides to microbes is through direct contact transport. [15, 16]

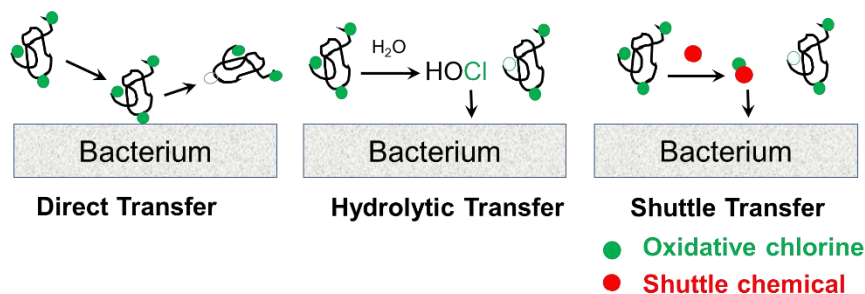


Figure 5-1 The possible oxidative chlorine transfer from polymers with N-Cl moieties to bacteria surfaces, including direct transfer, hydrolytic transfer, and shuttle transfer.

In our previous report, the addition of 1-(hydroxymethyl)-5,5-dimethylhydantoin (HDMH, imide) increased the bactericidal activity of both anionic and cationic polychloramides. Thereafter, the goal of this paper included ensuring that other low molecular weight imides showed the same behavior and strengthening the experimental support for the shuttle transfer mechanism. In this work, one negatively charged polychloramide model was prepared from the reaction of maleic anhydrides and primary amines, followed by chlorination with bleach. Thereafter, the biocidal property of polychloramides with shuttle chemicals was evaluated. In addition, the transfer kinetics of oxidative chlorine between polychloramides and shuttle chemicals were investigated.

Experimental

Materials. Poly(styrene-alt-maleic acid) sodium salt solution (13 wt% in H_2O , weight average Mw 350 kDa), isopropylamine ($\geq 99\%$), N, N-dimethylformamide anhydrous (DMF, 99.8%), hydrochloric acid (1 mol/L HCl), sodium hydroxide solution (1 mol/L NaOH), sodium thiosulfate ($Na_2S_2O_3$, $>99\%$), 5,5-dimethylhydantoin (DMH), succinimide, sodium dichloroisocyanurate dihydrate (NaDCC) and sodium hypochlorite (NaOCl, 10–15%) were obtained from Sigma-Aldrich (Canada) and used without further purification. 1-(hydroxymethyl)-5,5-dimethylhydantoin (HDMH, $>98.0\%$) was obtained from TCI America. The *Escherichia coli* (*E. coli* 13127) was purchased from the German Collection of Microorganisms and Cell Cultures GmbH. The *Staphylococcus aureus* (*S. aureus* MZ100) was obtained from stocks held within Dr. Michael Surette, McMaster University.

Chlorine Transfer Kinetics in Shuttle Chemicals. Shuttle chemicals include 1-(hydroxymethyl)-5,5-dimethylhydantoin (HDMH), 5,5-dimethylhydantoin (DMH), and succinimide (SI). These chemicals are individually dissolved in 10 mM pH 7 phosphate buffer. As one example, 1.2 mL of 10 mg/mL PSC14 was dissolved in 10.4 mL of 3 mM shuttle chemical and 0.4 mL buffer solution at room temperature, giving 12 mL of 1

mg/mL PSCI4 and 2.6 mM shuttle chemical in a 20 mL vial. Thereafter, 2 mL of mixture solution was delivered to a centrifugal filter unit (3 kDa MWCO, Amicon® Ultra-15) at a specific incubation time at room temperature and then the solution was centrifugated in Allegra® 25R Centrifuge (Beckman Coulter®) with 4000 rpm for 10 min. Unless otherwise stated, experiments were conducted under the same procedures. Finally, the chlorine contents of the filtrate were measured by 0.2 mM TNB assay which is based on the consumption of TNB which adsorbs light at 412 nm. [17] Chlorine test of each sample was repeated 3 times. The chlorine concentration was obtained from the standard plot of absorbance versus the known chlorine concentration from NaDCC solutions – see **Figure S5-1A**.

Bactericidal Concentration (BC). The BC results are reported as a range, x-y, where x is the largest biocide concentration with viable bacteria after 1 h, and y is the lowest biocide concentration giving no growth for a detection limit of 100 CFU/mL. Typically, 10 μ L of around 10^7 CFU/mL bacteria suspension in the polychloramides solution, quenched by 190 μ L 0.1 N $\text{Na}_2\text{S}_2\text{O}_3$ solution, was transferred to LB agar plates. The number of bacterial colonies was recorded after LB agar plates were incubated at 37 °C overnight.

Bacterial Killing in the Presence of Shuttle Chemicals. The antibacterial efficacies of the PSCI4 were measured individually in the presence of imide shuttle molecules. In one typical experiment, 100 μ L of 10 mg/mL PSCI4 was added to 866 μ L of 3 mM HDMH and 24 μ L \times 1 PBS buffer in a sterile 1.5 mL microcentrifuge tube at room temperature. Then, the tube was shaken in a SCIOLOGEX SK-D1807-E Rocker at a frequency of 80 min^{-1} for 1 h at room temperature. Thereafter, 10 μ L *E. coli* or *S. aureus* suspension was added to 0.99 mL of the polymer/HDMH mixture, giving a total volume of 1 mL with approximately 10^7 CFU/mL bacteria. After 1 h shaking at room temperature, 10 μ L suspensions were quenched by adding 190 μ L of $\text{Na}_2\text{S}_2\text{O}_3$ solution. Serial dilutions with sterile PBS buffer were carried out, and 50 μ L aliquots were transferred to LB agar plates, which were incubated at 37 °C overnight. The detection limits were 400 CFU/mL.

Results and Discussion

Polymer Modification and Characterization. The structures of polyamides are shown in **Figure 5-2**. The synthesis of PSC3 was from poly (styrene-alt-maleic anhydride) (PSMA) and isopropylamine, followed by chlorination with NaOCl (see **Figure S5-2**). Characterizations of polymers such as ^1H NMR, ATR-FTIR spectra, and solubility are presented in the supporting information. Chlorine contents of PSC1 and PSCI4 were determined by iodometric titration. [18] 4.4 % chlorine content of PSCI4 was obtained at 90 °C and 0.8 % chlorine content of PSC1 was obtained at 30 °C (see **Figure S5-6**). The final numbers of PSC1 and PSCI4 denote the chlorine mass fraction on chlorinated polymer. PSC3, PSC1, PSCI4, and shuttle chemicals (HDMH, DMH, and SI) are water-

soluble both in 1x PBS and in 10 mM phosphate buffer at pH 7. In this work, PBS buffer and phosphate buffer are used for bacterial killing and chlorine transport experiments.

As to the stability of PSCI4 in dry storage, chlorinated samples are stored in a 4 °C fridge and the remaining chlorine contents are determined by titration method. **Figure S5-7** shows less than 5% loss of chlorine in a 4 °C storage over 130 days. However, the gradual degradation behavior of PSCI was observed in an aqueous solution (see **Figure S5-8**).

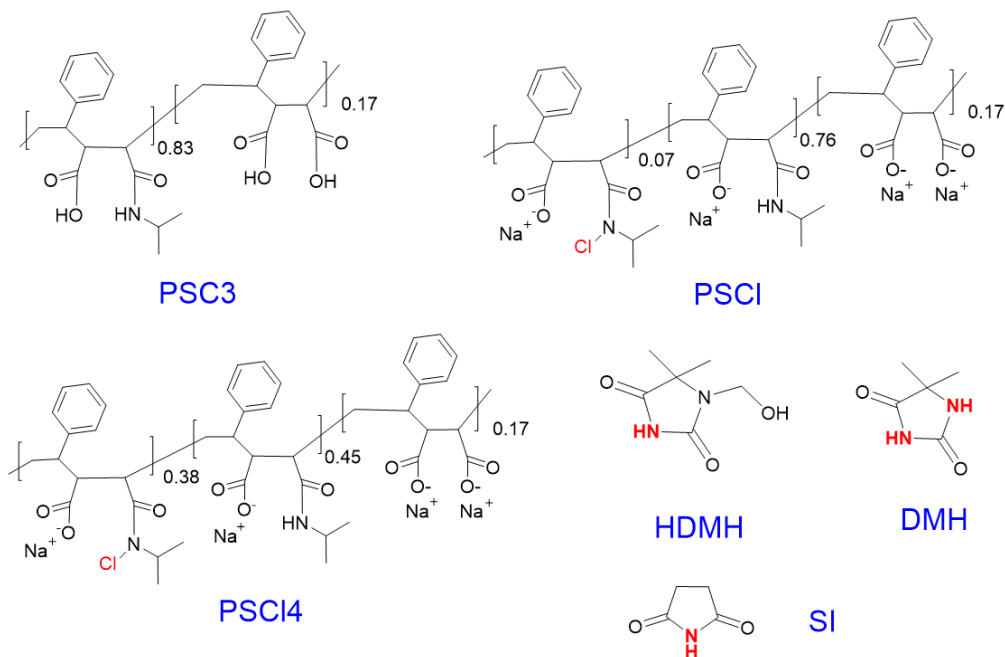


Figure 5-2 Structures of anionic polyamide PSC3, and anionic polychloramide PSCI and PSCI4, where the numbers are the oxidative chlorine mass fraction. (1-(hydroxymethyl)-5,5-dimethylhydantoin) (HDMH), 5,5-dimethylhydantoin (DMH), and succinimide (SI) are shuttle chemicals.

Antimicrobial Activities of Polychloramides. The antimicrobial activities of polychloramides and polymeric properties are given in

Table 5-1. For water-soluble polymers, the overlap concentration (C^*) is a concentration where the polymer coils fill the available space. The Huggins and Kraemer plots of polymers are applied to determine C^* values of PSC3, PSCI, and PSCI4 (see **Figure S5-9**). [19] As seen in

Table 5-1, C^* of polymers increases from 0.7 to 20 g/dL with chlorine content increase. The collapse of polychloramides comes from the hydrophobic chloramide groups.[18] In addition,

Table 5-1 shows that chlorinated polymers can kill bacteria, and higher chlorine contents on polymers decrease the bactericidal concentrations.

Table 5-1 Polymeric properties and antibacterial activities.

Polymers	C* in $\times 1$ PBS (g/dL)	Chlorine Mass Fraction (wt%)	Bactericidal Conc. (mg/mL)	
			<i>E. coli</i>	<i>S. aureus</i>
PSC3	0.7	0	No Killing	No killing
PSC1	2.0	0.8	15-20	20-30
PSC14	20	4.4	2-5	5-10

Shuttle Chemical Influence on biocidal activity of Polychloramides. For control groups, 1mg/mL PSC14 does not give effective biocidal activity with 1 h contact (see **Table S5-1**). In pure 0.26 M shuttle chemical solution, there is no bacterial reduction. Premixing refers to the incubation time between shuttle chemicals and PSC14. The addition of shuttle chemicals with imide groups can enhance the biocidal activity of PSC14-See **Figure 5-3**.

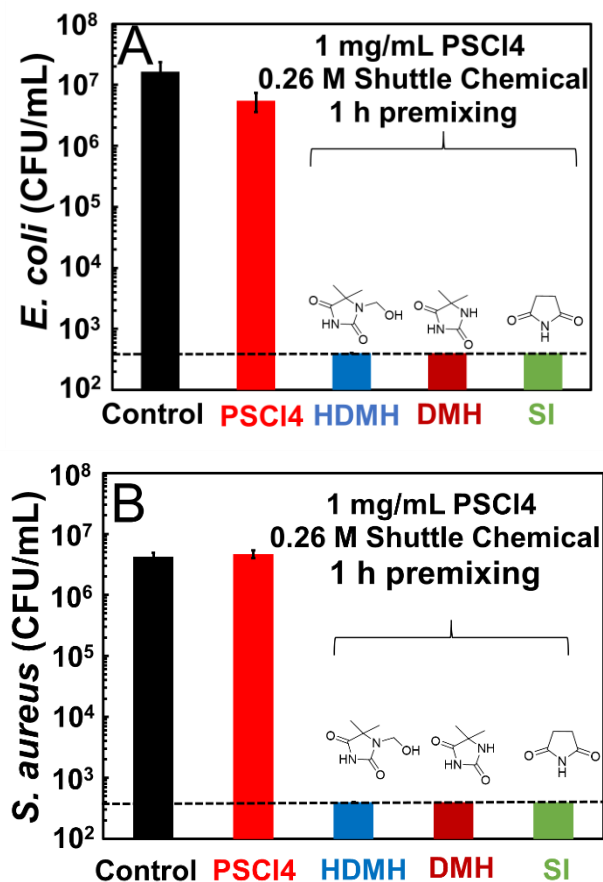


Figure 5-3 The influence of low molecular weight adjuvants (0.26 M) on the activity of anionic polychloramides for 1 h premixing in 1x PBS buffer. The plates were analyzed after 1 h inoculation. “HDMH” is 1-(hydroxymethyl)-5,5-dimethylhydantoin, “DMH” is 5,5-dimethylhydantoin, and “SI” is succinimide. The horizontal dashed line is the detection limit.

Chlorine Transport from Polychloramides to Imides. Polychloramides and shuttle chemical solutions were mixed for a specific incubation time, after which the shuttle chemical solution was isolated by a cellulose membrane in a centrifuge tube. Chlorine contents in the shuttle chemical solution were measured by TNB assay and the calibration curve of the TNB assay was shown in **Figure S5-1A**. **Figure S5-1B** gives the UV-Vis spectra of pure HDMH solution and the TNB buffer with filtrate solution of PSCI4 or PSCI4+HDMH. Results confirm that HDMH in PSCI4 accelerates the free chlorine release from PSCI4. Similarly, **Figure 5-4A** demonstrates that the addition of imide shuttle chemicals accelerates oxidative chlorine transport from polychloramides to imide shuttle chemicals. **Figure 5-4B** describes the oxidative chlorine contents change in HDMH +PSCI4 and pure PSCI4 systems with varying incubation times. For the alone

PSCl₄ system, free oxidative chlorine contents increase gradually. Only 1.4% of chlorine (0.017 mM) in the polymer liberates into the water without HDMH at 1 h. This illustrates the hydrolysis reaction of PSCl₄ gives a very small amount of free chlorine remaining in the solution. However, 0.08 mM Cl⁺ exists in 2.6 mM HDMH solution, giving 6.7% of chlorine on the polymer to HDMH for 1 h incubation. This gives direct evidence of chlorine transfer from polymer to shuttle chemicals.

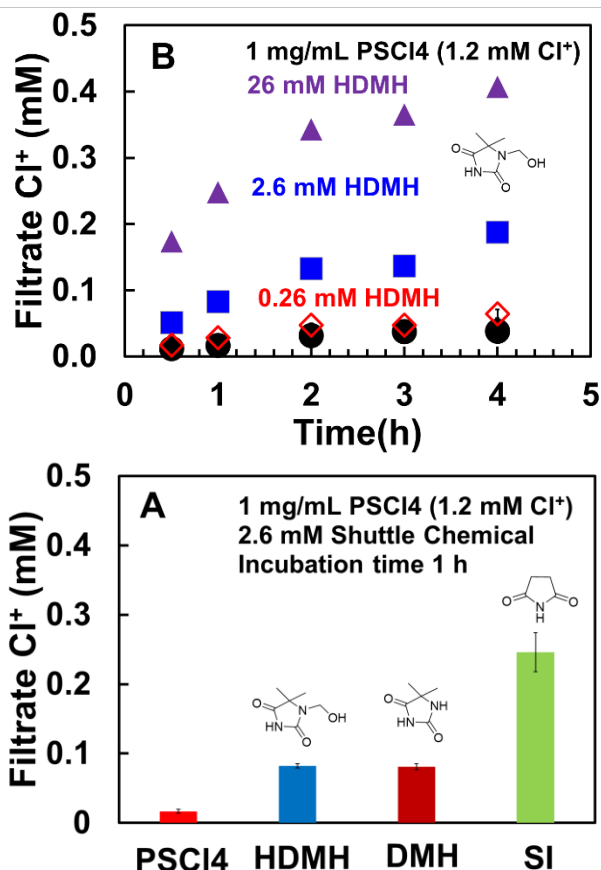


Figure 5-4 The oxidative chlorine contents in filtrate solution after separation of 1 mg/mL PSCl₄ with HDMH, DMH, and succinimide (SI) in 10 mM pH 7 phosphate buffer for 1 h incubation (A). Chlorine contents change with varying incubation time in different HDMH concentration (B). The purple triangles (▲) are 26 mM HDMH +PSCl₄ system, the blue squares (■) are 2.6 mM HDMH +PSCl₄ system, the red open diamonds (◇) is 0.26 mM HDMH +PSCl₄, and full circles (●) are pure 1 mg/mL PSCl₄.

The influence of HDMH concentration on the biocidal activity of PSCl₄ was given in **Figure 5-5** and results perform no visible bacteria colony when the HDMH concentration is more than 2.6 mM. According to the results in **Figure 5-4B**, imide shuttle chemicals can extract oxidative chlorine from chloramides. In detail, 0.08 mM free oxidative

chlorine in 1 mg/mL PSCI4+2.6 mM HDMH was obtained for 1 h incubation. Thereafter, low molecular chlorimides demonstrates more effective biocidal activity in both *E. coli* and *S. aureus*. [20] However, 0.017 mM Cl^+ exists in the HDMH-free system for 1 hour of incubation. They cannot deactivate bacteria because of the low amount of chlorine transfer to bacteria. In addition, release of formaldehyde may occur in the HDMH solution [21], which may result in bacterial reduction.

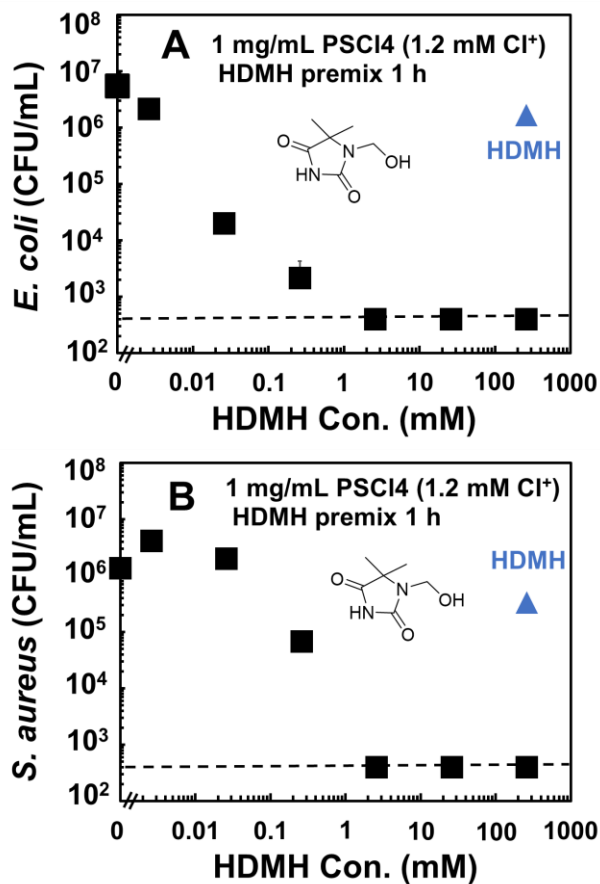


Figure 5-5 The influence of HDMH concentration on the antimicrobial activity of 1 mg/mL PSCI4 for 1 h contact. Blue triangles are bacteria in the HDMH solution.

To further investigate the incubation time influence of HDMH with PSCI4, the direct mixture of HDMH +PSCI4 +bacteria, or premixing HDMH +PSCI4 for 1 h were compared. The direct mixing of HDMH +PSCI4 +bacteria solution can cause a gradual reduction of bacteria within 30 min in both *E. coli* and *S. aureus* (**Figure 5-6**). After 30 min contact, there is no visible bacteria colony in the HDMH +PSCI4 +bacteria system. However, *E. coli* and *S. aureus* experience a faster bacteria reduction within 10 min in the

premixing system of HDMH +PSCl₄. In this case, HDMH resembles the chlorine transporter from the PSCl₄ system to bacteria and this process is a rate-limiting step.

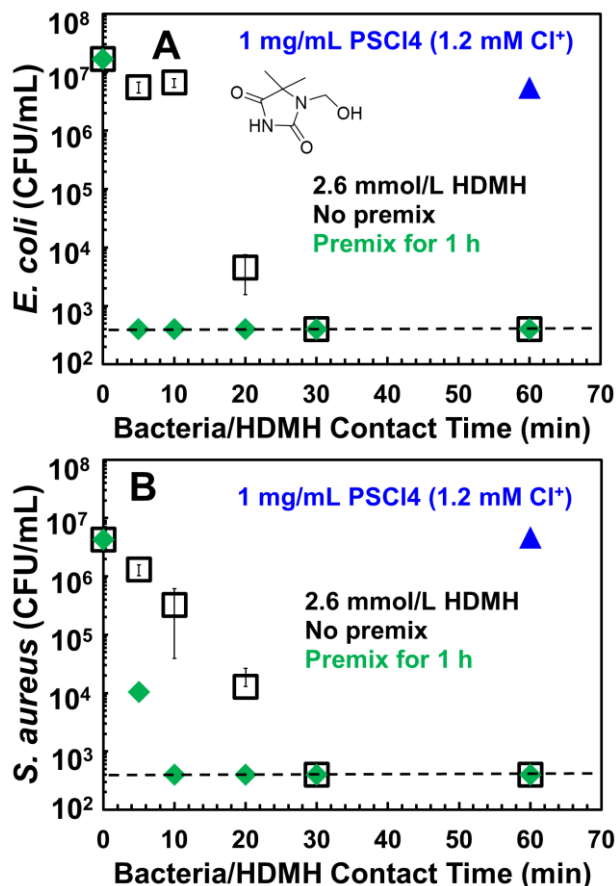


Figure 5-6 The influence of bacteria/HDMH contact time on the antimicrobial activity of 1 mg/mL PSCl₄. Black open squares denote the direct mixture of HDMH +PSCl₄ +bacteria system. Green diamonds are a 1 h incubation of HDMH +PSCl₄ before adding bacteria. Blue triangles are only PSCl₄.

Reaction Kinetics to Succinimide (SI). To simplify the chlorine transfer kinetics, one simple model molecule succinimide (SI) was applied to model oxidative chlorine transfer. The Cl⁺ concentration in filtrate solution was measured with varying incubation time in PSCl₄ + SI system (see **Figure 5-7A**). Increasing the incubation time with SI results to the higher oxidative chlorine in filtrate solution. Furthermore, when fixing incubation time at 10 min, the Cl⁺ concentration increases with the increase of SI in lower SI concentrations (see **Figure 5-7B**). However, the Cl⁺ concentration shows independence on SI concentration when SI concentrations is over 52 mM.

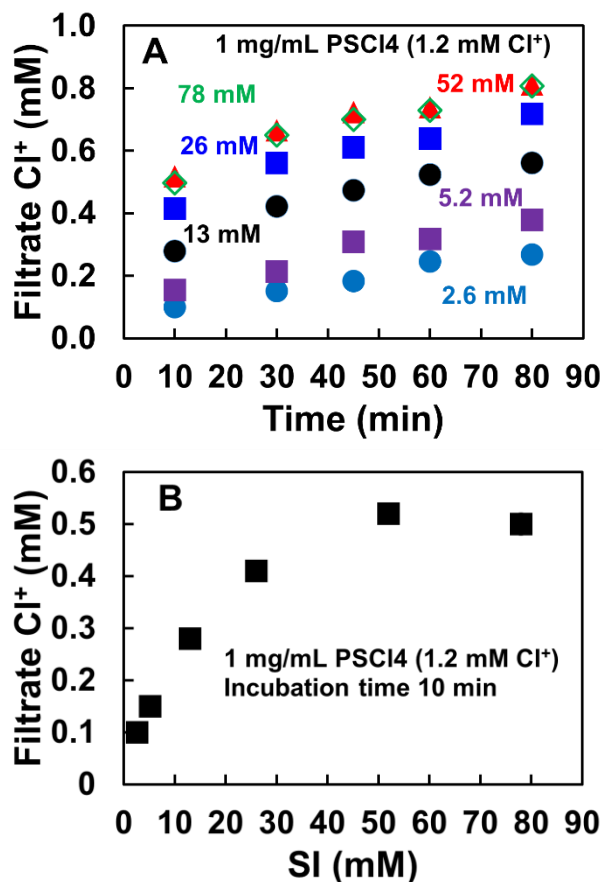


Figure 5-7 The oxidative chlorine contents in filtrate solution in different succinimide concentrations (SI) with varying incubation time (A). The oxidative chlorine contents in filtrate solution as a function of the total SI concentrations at 10 min incubation (B). Experiments were prepared in 1 mg/mL PSCI4 + SI in 10 mM pH 7 phosphate buffer.



where SI is succinimide, NCS is N-chlorosuccinimide, PCL is chloramide concentration, and P is amide group concentration.

$$v = -\frac{d[\text{PCL}]}{dt} = k_{obs}[\text{PCL}]^a \quad (2)$$

Where v is the reaction rate, k_{obs} is the pseudo constant rate, and a is the reaction order. $[\text{PCL}]$ is the concentration of PCL, $[\text{SI}]$ is the concentration of succinimide ($[\text{SI}] \gg 10 [\text{PCL}]$), and t is the reaction time.

All kinetic studies were performed with the succinimide in excess. The concentrations of succinimides are at least 10 times greater than that of chloramides. Therefore, the

succinimide concentration can be considered practically constant in kinetic reaction, and it can be included in the rate constant (k_{obs}).

To verify the order of reaction to the [PCI] concentration, the data ($\ln[\text{PCI}]$ versus t) were fitted to the first-order equation, and the good fit of the data to equation (2) allows us to confirm the pseudo-first-order reaction to the PCI concentration ($a=1$). k_{obs} with varying succinimide concentrations were shown in **Table 5-2** and the reaction rate constant is in the order of 10^{-3} min^{-1} .

Table 5-2 k_{obs} with varying succinimide concentrations in 10 mM pH 7 phosphate buffer and [PCI]=1.2 mM.

[SI]/mM	13	26	52	78
$k_{obs} / \text{min}^{-1}$	0.005	0.006	0.007	0.007

Conclusions

In summary, this work demonstrates a specific adjuvant mechanism whereby low molecular weight, water-soluble imides shuttle active chlorine from soluble anionic, polychloramides, to bacteria increasing the biocidal activity. Specific conclusions include:

- Water-soluble imides extract Cl^+ from polychloramides despite chlorimide hydrolysis equilibrium constants being 10^4 times greater than corresponding chloramide constants. [5]
- The chlorimide produced by mixing imides with polychloramides are more effective biocides compared to the polymer alone. For example, 2.6 mM HDMH extracted 0.08 mM Cl^+ from 1 mg/mL PSC14 (**Figure 5-4**) and decreased bacteria to the detection limit (**Figure 5-5**) whereas without HDMH, 2-5 mg/mL PSC14 carrying 2.5-6.2 mM Cl^+ was required to reach the detection limit of *E. Coli*. Presumably, the transport of low molecular weight, nonionic chloramides to bacteria surfaces is rapid compared to the transport of large, negatively charged, polychloramides.
- One water-soluble, anionic, and antimicrobial platform polychloramide (PSC1) was developed from poly(styrene-alt-maleic acid) sodium salt. Purified polychloramides show dry storage stability over 150 days with less than 5% chlorine loss. However, polychloramides face degradation in an aqueous solution within the day's range.

Supporting Information

The file includes descriptions of the calibration curve for the TNB, UV-Vis absorbance curve of chlorine contents in polymer and shuttle chemicals filtrate with TNB, the synthesis and characterization of PSC3 and chlorinated polymer, the stability of chlorinated polymer, the viscosity curves for intrinsic viscosity and C^* of the polymers, and additional bacterial results with shuttle chemicals.

Acknowledgments

We thank the Natural Sciences and Engineering Research Council of Canada (NSERC) and Suncor Energy for funding this project. R. H. Pelton holds the Canada Research Chair in Interfacial Technologies, and Zeinab Hosseinidoust holds the Canada Research Chair in Bacteriophage Bioengineering.

Supporting Information

Low Molecular Weight Imide Shuttle Molecules Enhance Polychloramide Antimicrobial Activity

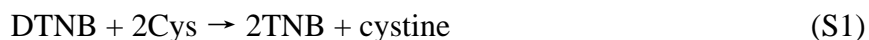
Gaoyin He ^a, Lei Tian ^a, Ayodele Fatona ^a, Chaochen Song ^a, Jun Liu ^b, Michael Fefer ^b, Zeinab Hosseinidoust ^a, and, Robert H. Pelton ^{a,*}

^a Department of Chemical Engineering, McMaster University, Hamilton, Ontario, Canada, L8S 4L7

^b Suncor AgroScience, 2489 North Sheridan Way, Mississauga, ON L5K 1A8, Canada

*Corresponding author: [*peltonrh@mcmaster.ca](mailto:peltonrh@mcmaster.ca)

TNB Assay. The oxidative chlorine of filtrate from PSCI4 and shuttle chemical solution was measured by the TNB method. Fresh TNB solution was produced before each experiment via the addition of 2 equivalents of 4 mM cysteine (Cys) to 1 equivalent of 2 mM 5,5'-dithiobis(2-nitrobenzoic acid) (DTNB) in 10 mM phosphate buffer solution at pH 7 following the reaction (S3). A highly colored yellow solution (TNB) was diluted 10 times and stored at a 4 °C fridge overnight after cysteine and DTNB were mixed. Thereafter, this stock solution was mixed with filtrate in equal volumes to measure the oxidative chlorine concentration. The standard curve of TNB UV-vis absorbance as a function of oxidative chlorine concentration is presented in **Figure S2-2 A**.



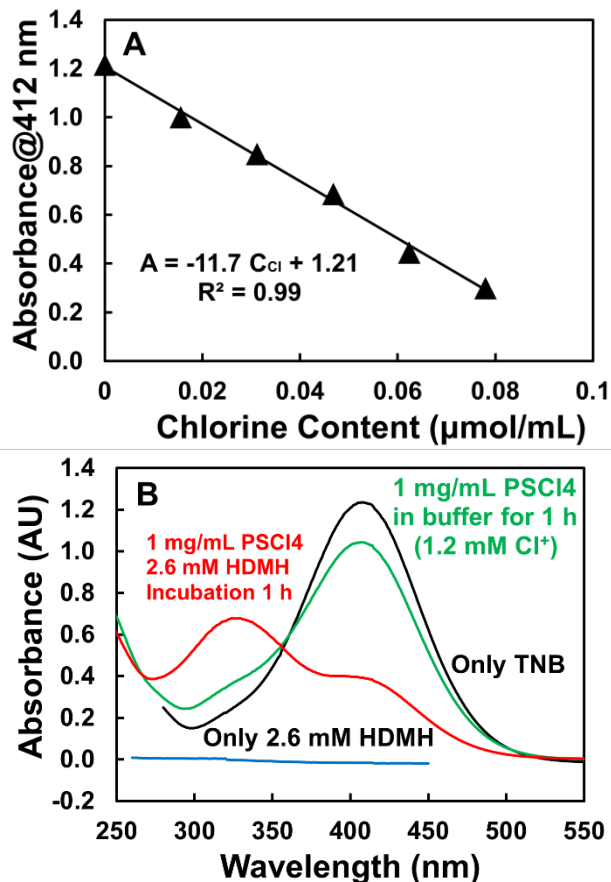


Figure S5-1 The standard UV-Vis absorbance curve of the TNB vs oxidative chlorine contents of NaDCC solution in 10 mM phosphate buffer (A). UV-Vis absorbance curve for the filtrate Cl^+ in different solutions (B). Only TNB means pure TNB in 10 mM phosphate buffer, PSCI4 in buffer means TNB + filtrate solution of polymer, and PSCI4+ HDMH means all three TNB + filtrate solution of polymer +HDMH. Only HDMH is the pure HDMH solution.

Synthesis of PSMA. The starting material poly (styrene-alt-maleic acid) sodium salt solution was acidified with pH=2 HCl and soaked in the solution overnight. Afterward, poly (styrene-alt-maleic acid) was filtered and heated overnight in 160 °C vacuum oven to obtain poly (styrene-alt-maleic anhydride) (PSMA). The anhydride groups of poly (styrene-alt-maleic anhydride) were confirmed by infrared spectroscopy.

Synthesis of PSC3. In one typical experiment, 1 g (4.3 mmol) of PSMA was dissolved into 20 mL of anhydrous DMF. Then, 0.29 g (4.9 mmol) of isopropylamine in 2 mL of DMF was added dropwise to the PSMA solution. The reaction mixture was stirred overnight at 60 °C. Thereafter, 10 mL of 0.01 M HCl was added to stop the reaction, and the solution was transferred to 12-14 kDa dialysis tube against deionized water for 8 h and the solution was then adjusted to pH 7-8. Thereafter, a static adsorption experiment of

polymer solution (~0.5 g) was performed with 10 g Dowex® 50WX8 in Na form exchange resin for 4 h at room temperature to remove excess amine. Finally, the pH of the polymer solution was adjusted to 2 and the polymer solution was further dialyzed against deionized water for 2 days and then recovered by freeze-drying.

Preparation of PSCl. PSC3 polymers were chlorinated with an aqueous NaOCl solution. Typically, 15 mg of PSC3 and 15 mL of 267 mM NaOCl were mixed in a vial and the solution pH was adjusted to 10.5 by 1 mol/L standard HCl/NaOH solution. Thereafter, the solution was dialyzed in 12-14 kDa cellulose membrane tubes against 4 L water with stirring for 5 h to remove excess NaOCl and salt. The dry chlorinated polymers were obtained by freeze-drying. The conversion process is shown in **Figure S5-1**.

Characterization. Fourier transform infrared (FTIR) spectra of polymers were acquired with a Thermo Nicolet 6700 FTIR spectrometer in ATR mode over a wavelength range of 700 to 4000 cm^{-1} . The chemical structure of the compound was confirmed by ^1H NMR (Bruker AVANCE, 600 MHz) in methanol- d_4 and D_2O .

^1H NMR spectra of PSMA-H, PSC3, and PSCl are given in **Figure S5-3** in the supplementary material. ^1H NMR of PSC3 (600 MHz, methanol- d_4): 7.54-6.30 (br, PhH), 3.49-4.20 (br, NCHCH₃CH₃), 3.17-1.49 ppm (br, CHCH₂NH), CH₂ and CH in the main chain are at 3.17-1.49 ppm. The sharp peak at 1.3 ppm is the residual amine in PSC3.

ATR-FTIR spectra of poly (styrene-*alt*-maleic acid) (PSMA-H), PSMA, and PSC3 are presented in **Figure S5-4**. The band at 1705 cm^{-1} in IR spectra of PSMA-H may be assigned to C=O group of carbonyl acid. The maleic anhydrides (C=O) of PSMA display asymmetric and symmetric peaks in 1772 and 1853 cm^{-1} , and the low asymmetric band at 1772 cm^{-1} is stronger. A broad spectrum from 3000–3600 cm^{-1} is due to the hydroxyl groups of PSC3. The peaks of PSC3 at 1632 and 1552 cm^{-1} are corresponding to amide I ($\nu_{\text{C=O}}$) and amide II ($\nu_{\text{N-H}}$).

Chlorine Titration on Polymer. The oxidative chlorine content of the sample was determined by iodometric titration. The oxidative Cl content was calculated according to the formula: $35.45 \times (V_{\text{Cl}} - V_0) \times C_0 / 2m_0$, where V_{Cl} and V_0 are the volumes (L) of the iodine solution consumed in the titration of the chlorinated polymers and the control, C_0 is the $\text{Na}_2\text{S}_2\text{O}_3$ concentration (mol/L) in titration and m_0 is the weight (g) of the chlorinated polymers.

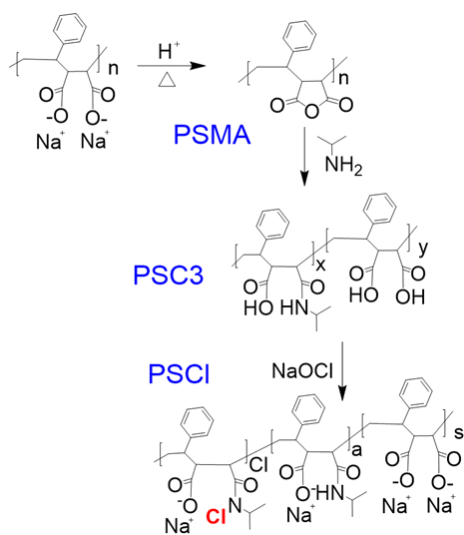


Figure S5-2 The conversion of poly (styrene-alt-maleic anhydride) sodium to PSC3 and PSCI.

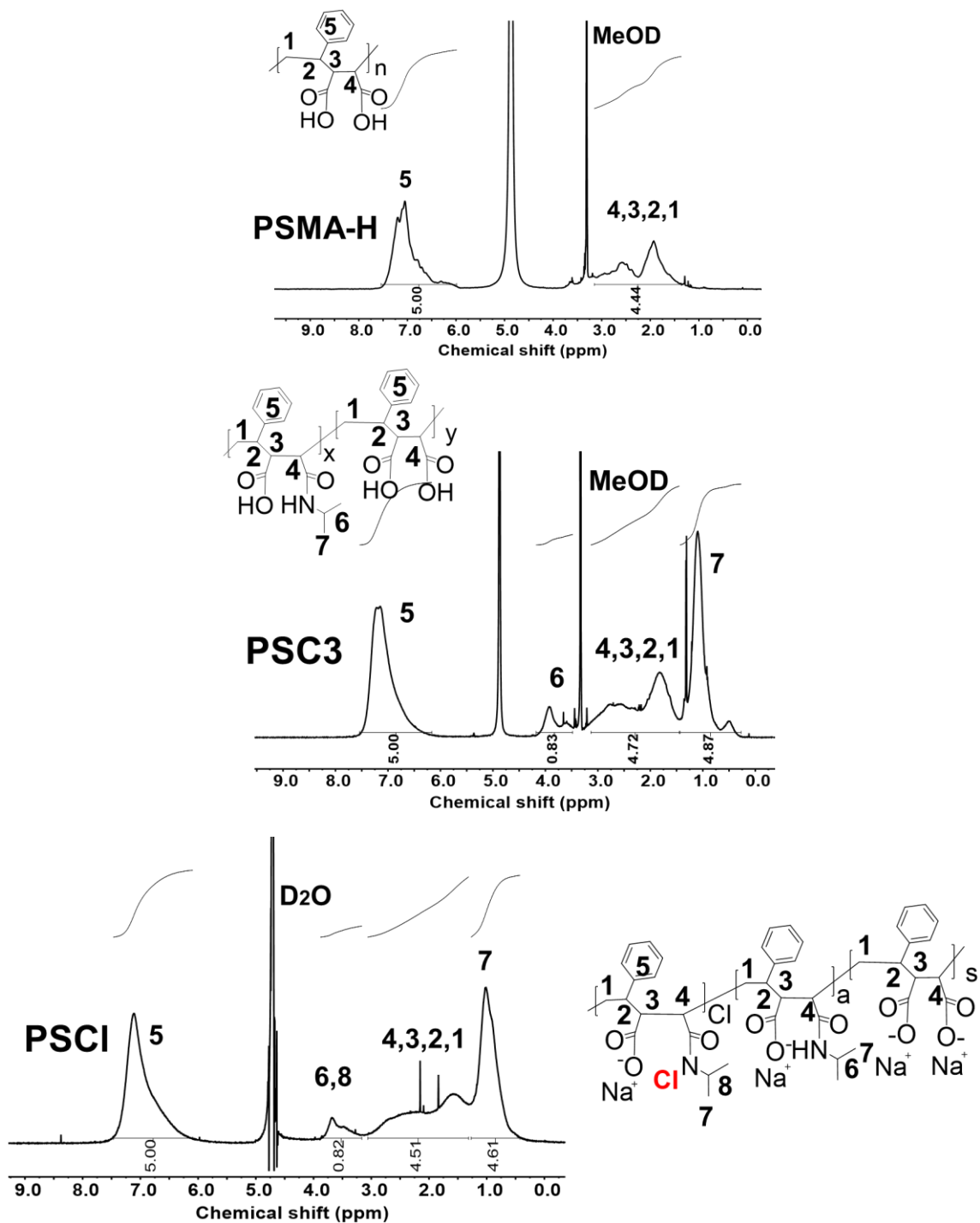


Figure S5-3 Proton NMR spectra of PSMA-H and PSC3 in methanol-d₄. $x=0.83$ in PSC3 was determined from the peak areas of peak 5 relative to peak 6.

Proton NMR spectra of PSCl was in D₂O, from the PSC3 chlorination at 30 °C, pH 10.5, and 2 h.

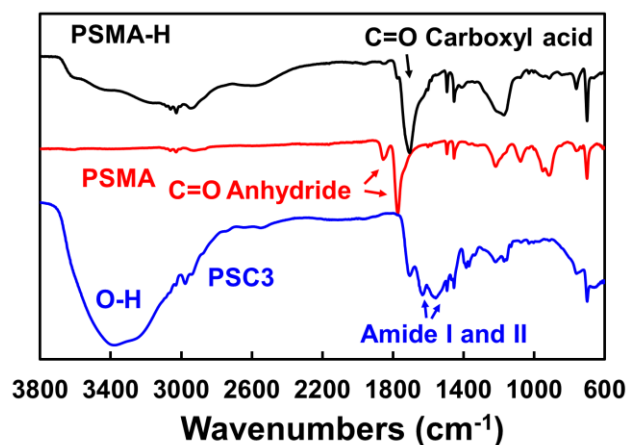


Figure S5-4 ATR-FTIR spectra of poly (styrene-alt-maleic acid) (PSMA-H), poly (styrene-alt-maleic anhydrides) (PSMA), and PSC3.

pH-Responsive Behavior of PSC3. PSC3 was dissolved and stirred for 1 h, and pH was adjusted by 1 mol/L standard HCl/NaOH solution to obtain 1 g/L polymer solution. Then, the PSC3 solution at different pHs was placed in polystyrene cuvettes. The transmittance of the PSC3 solution at 500 nm was recorded by a DU800 UV-Vis spectrophotometer (Beckman Coulter).

PSMA-H and PSC3 Solubility. The optical transmittance at 500 nm of PSC3 and PSMA-H solutions were measured as functions of pH in 1 mM NaCl solution—see **Figure S5-5**. pH-responsive behavior of PSMA-H was not observed even when the pendant hydrophilic carboxylic groups of PSMA-H were protonated at low pH. However, the transmittance of the PSC3 solution showed a dramatic decrease to 38% at pH= 2.6. The PSC3 solution remains soluble when pH is over 7.

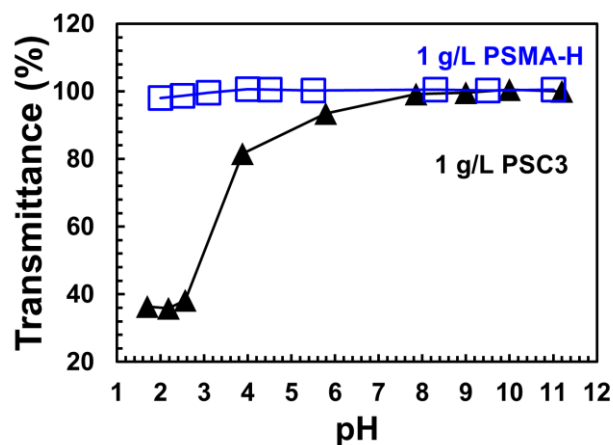


Figure S5-5 Transmittance of PSMA-H and PSC3 solutions in 1 mM NaCl solution at 500 nm as functions of pH.

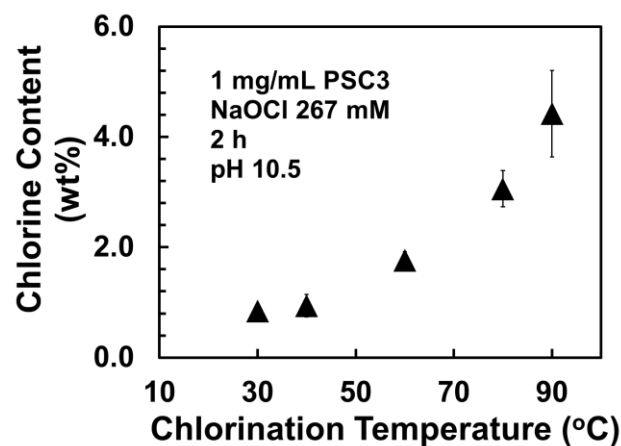


Figure S5-6 The influence of chlorination conditions on the mass fractions of Cl in PSCl. The error bars on the chlorine contents reflect the standard deviations of triplicate measurements.

Figure S5-6 demonstrates the temperature influence on the chlorination of PSC3, varying from 30 °C to 90 °C. Chlorine mass fractions on PSCl increase with increasing chlorination temperature.

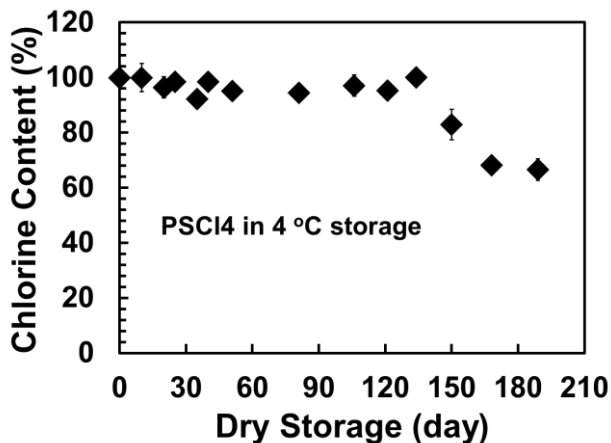


Figure S5-7 Chlorine contents of PSCI4 with the dry aging periods, as a percentage of the initial content at 4 °C.

The stability of PSCI in aqueous solution. PSCI was obtained by the chlorination of PSC3 at 30 °C, pH 10.5, and 2 h. The freeze-dried polymer was dissolved in D₂O and corresponding proton NMR spectra of PSCI were recorded to investigate the stability of PSCI in solution. There is a sharp peak that appeared at 1.1 ppm on the 1st and 3rd day, indicating the gradual degradation behavior of PSCI in solution (see **Figure S5-8**).

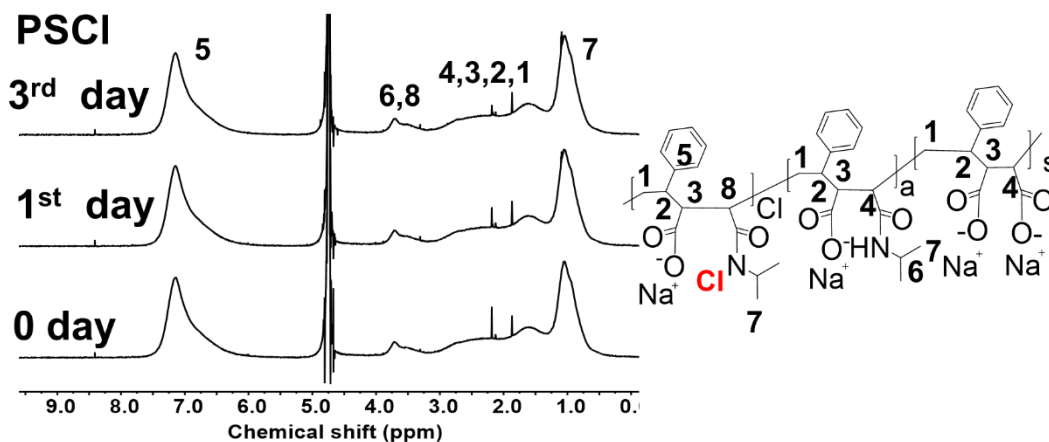


Figure S5-8 Proton NMR of PSCI at 30 °C, pH 10.5, and 2 h in D₂O solution for 3 days.

Overlap Concentrations (C^*) of Polymers. The C^* values of the polymers were from the reciprocal of the intrinsic viscosity, coming from the Huggins and Kraemer plots. The viscosities were measured with an Ubbelohde viscometer (CUC-75 Cannon Company), suspended in a 25 °C bath. Polymer solutions were prepared $\times 1$ PBS buffer in concentrations varying from 5 to 20 mg/mL, and the flow time of the buffer solution was 105 s.

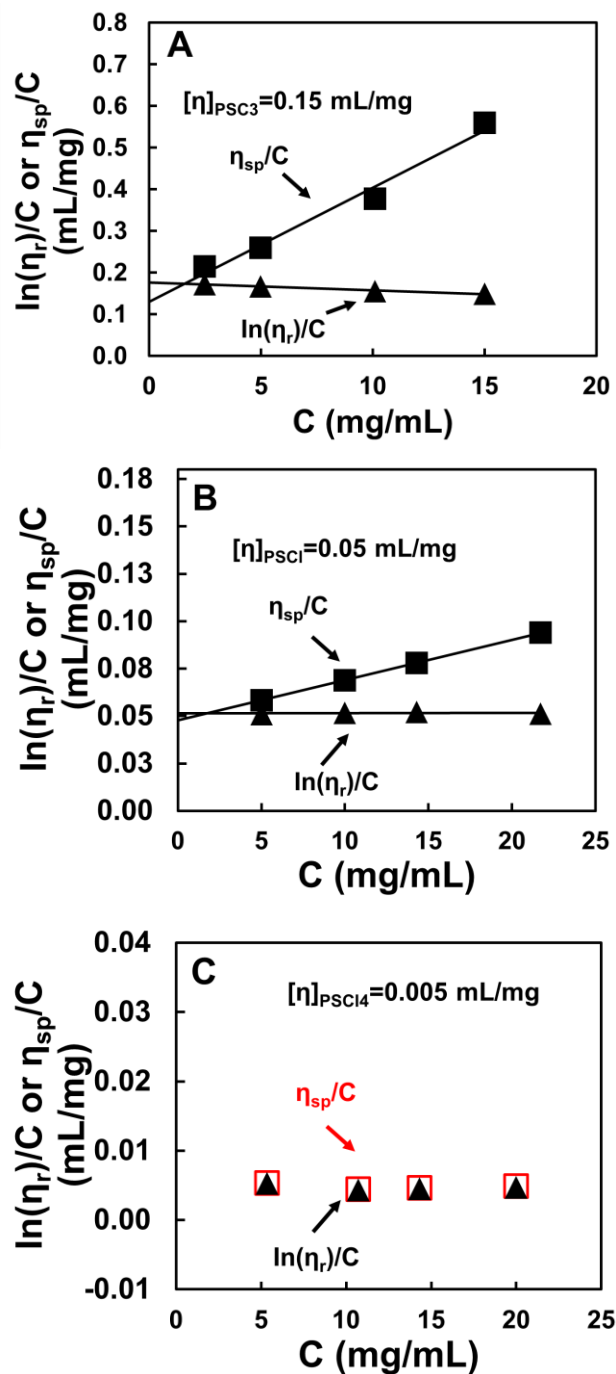


Figure S5-9 Reduced and inherent viscosity for PSC3 (A), PSC1 (B), and PSC14 (C) in 1x PBS at $T = 25$ °C. η is the intrinsic viscosity of the polymer.

Table S5-1 The influence of HDMH and PSCI4 in 1× PBS on the concentration of colony-forming bacteria after 1 h contact time.

Types	Concentration	<i>E. coli</i> (CFU/mL)	<i>S. aureus</i> (CFU/mL)
1x PBS only	---	1.7×10^7	4.3×10^6
DMH	0.26 M	5.6×10^6	4.5×10^6
SI	0.26 M	4.4×10^6	3.6×10^6

References

1. Pelton, R.H., He, G., Tian, L., Song, C., and Hosseini, Z., Modeling the impact of polychloramide solution properties on bacterial disinfection kinetics. *Biomacromolecules*, **2022**, 23(9): 3919-3927.
2. Hui, F. and Debiemme-Chouvy, C., Antimicrobial N-halamine polymers and coatings: A review of their synthesis, characterization, and applications. *Biomacromolecules*, **2013**, 14(3): 585-601.
3. Dong, A., Wang, Y.-J., Gao, Y., Gao, T., and Gao, G., Chemical insights into antibacterial N-halamines. *Chemical Reviews*, **2017**, 117(6): 4806-4862.
4. Williams, D., Elder, E., and Worley, S., Is free halogen necessary for disinfection? *Applied and Environmental Microbiology*, **1988**, 54(10): 2583-2585.
5. Qian, L. and Sun, G., Durable and regenerable antimicrobial textiles: Synthesis and applications of 3-methylol-2,2,5,5-tetramethyl-imidazolidin-4-one (MTMIO). *Journal of Applied Polymer Science*, **2003**, 89(9): 2418-2425.
6. Paine, M.R., Pianegonda, N.A., Huynh, T.T., Manfield, M., MacLaughlin, S.A., Rice, S.A., Barker, P.J., and Blanksby, S.J., Evaluation of hindered amine light stabilisers and their N-chlorinated derivatives as antibacterial and antifungal additives for thermoset surface coatings. *Progress in Organic Coatings*, **2016**, 99: 330-336.
7. Liu, Q., Zhang, Y., Liu, W., Wang, L.H., Choi, Y.W., Fulton, M., Fuchs, S., Shariati, K., Qiao, M., and Bernat, V., A broad-spectrum antimicrobial and antiviral membrane inactivates SARS-CoV-2 in minutes. *Advanced Functional Materials*, **2021**, 31(47): 2103477.
8. Antelo, J.M., Arce, F., Franco, J., Lopez, M.C.G., Sanchez, M., and Varela, A., Kinetics of the chlorination of secondary amines by N-chlorosuccinimide. *International Journal of Chemical Kinetics*, **1988**, 20(5): 397-409.
9. Naqib, I., Tsao, T.C., Sarathy, P.K., and Worley, S.D., Kinetic versus thermodynamic control in chlorination of imidazolidin-4-one derivatives. *Industrial & Engineering Chemistry Research*, **1991**, 30(7): 1669-1671.
10. Qian, L. and Sun, G., Durable and regenerable antimicrobial textiles: chlorine transfer among halamine structures. *Industrial & Engineering Chemistry Research*, **2005**, 44(4): 852-856.
11. Ahmed, A.E.-S.I., Hay, J.N., Bushell, M.E., Wardell, J.N., and Cavalli, G., Biocidal polymers (II): determination of biological activity of novel N-halamine biocidal polymers and evaluation for use in water filters. *Reactive and Functional Polymers*, **2008**, 68(10): 1448-1458.

12. Higuchi, T. and Hasegawa, J., Rate of exchange of chlorine between dimethylchloramine and succinimide. *The Journal of Physical Chemistry*, **1965**, 69(3): 796-799.
13. Higuchi, T., Ikeda, K., and Hussain, A., Mechanism and thermodynamics of chlorine transfer among organochlorinating agents. Part III. Autocatalytic pathway between N-chloro-succinimide and chloramine-T. *Journal of the Chemical Society B: Physical Organic*, **1968**: 1031-1036.
14. Ahmed, A.E.S.I., Hay, J.N., Bushell, M.E., Wardell, J.N., and Cavalli, G., Optimizing halogenation conditions of N-halamine polymers and investigating mode of bactericidal action. *Journal of Applied Polymer Science*, **2009**, 113(4): 2404-2412.
15. Gutman, O., Natan, M., Banin, E., and Margel, S., Characterization and antibacterial properties of N-halamine-derivatized cross-linked polymethacrylamide nanoparticles. *Biomaterials*, **2014**, 35(19): 5079-5087.
16. Kaur, R. and Liu, S., Antibacterial surface design – Contact kill. *Progress in Surface Science*, **2016**, 91(3): 136-153.
17. He, G., Tian, L., Fatona, A., Wu, X., Zhang, H., Liu, J., Fefer, M., Hosseinidoust, Z., and Pelton, R.H., Water-soluble Anionic Polychloramide Biocides Based on Maleic Anhydride Copolymers. *Colloids and Surfaces B: Biointerfaces*, **2022**, 215: 112487.
18. Wang, Z. and Pelton, R., Chloramide copolymers from reacting poly (N-isopropylacrylamide) with bleach. *European Polymer Journal*, **2013**, 49(8): 2196-2201.
19. Huggins, M.L., The Viscosity of Dilute Solutions of Long-Chain Molecules. IV. Dependence on Concentration. *Journal of the American Chemical Society*, **1942**, 64(11): 2716-2718.
20. Qian, L. and Sun, G., Durable and regenerable antimicrobial textiles: synthesis and applications of 3-methylol-2, 2, 5, 5-tetramethyl-imidazolidin-4-one (MTMIO). *Journal of Applied Polymer Science*, **2003**, 89(9): 2418-2425.
21. Bundgaard, H. and Johansen, M., Pro-drugs as Drug Delivery Systems VIII. Bioreversible Derivatization of Hydantoins by N-hydroxymethylation. *International Journal of Pharmaceutics*, **1980**, 5(1): 67-77.

Chapter 6

My Contributions

The antimicrobial activity of new water-soluble, anionic polychloramides was evaluated in this research. The antimicrobial polychloramides platform is based on the reaction of maleic anhydrides and primary amines, which could be very water soluble and easily grafted to surfaces.

The major contributions of this thesis are:

1. Water-soluble, anionic polychloramides are demonstrated to be effective biocides. Also, anionic polyamides are easily prepared, and easily grafted to cellulose surfaces without the existence of catalysts and reagents.
2. Polymer-modified Chick-Watson (PCW) was proposed to account for bacterial disinfection kinetics of nonadsorbing polychloramides with polymer solution properties. Modeling results demonstrate that antimicrobial activity is dependent on the polymer properties, such as molecular weight (MW), oxidative chlorine mass fraction (Cl_{mf}), and polymer configuration.
3. The antimicrobial activity of anionic polychloramides exceeds their cationic counterparts, particularly in highly soiled applications. In addition, a separate mechanistic assessment of pure sequestering organic soils and extractive soils is proposed to test their impacts on the biocidal activity of polychloramides, compared to complex soil mixtures.
4. For the first time, imide shuttle adjuvants are proposed to enhance the biocidal activities of polychloramides. In the presence of imide shuttle chemicals in polymer, the produced chlorimides are more effective biocides, compared to the polychloramides alone.